UNIVERSITÀ DEGLI STUDI DI MILANO

SCUOLA DI DOTTORATO DI RICERCA IN SCIENZE BIOCHIMICHE, NUTRIZIONALI E METABOLICHE

DOTTORATO DI RICERCA IN BIOCHIMICA

CICLO XXIII

TESI DI DOTTORATO DI RICERCA

EFFECTS OF HISTONE DEACETYLASE INHIBITORS ON ENERGY METABOLISM

BIO10

ANDREA GALMOZZI
Matr. R07791

TUTOR: **Dott. EMMA DE FABIANI**

COORDINATORE: **Prof. FRANCESCO BONOMI**

ANNO ACCADEMICO 2009/2010

INDEX

Index

INTRODUCTION

Type 2 Diabetes

Type 2 diabetes mellitus (T2DM) is the most common metabolic disease in the world. The westernization of the diet and sedentary lifestyle are the most responsible factors that drive to insulin resistance and T2DM. Maintenance of glucose homeostasis depends on a complex interplay between the insulin responsiveness of skeletal muscle, liver, adipose tissue and glucose-stimulated insulin secretion by pancreatic beta cells. Defects in these organs are responsible for insulin resistance and progression to hyperglycemia.
In addition to the major health consequences to individuals, including higher risk of death, heart disease, stroke, kidney disease, blindness, amputations, neuropathy, and pregnancy-related complications, diabetes and its complications result in a total huge cost in the Public Health. Unfortunately, the incidence of diabetes has more than doubled in the past 25 yr, with 1.6 million new cases diagnosed in adults in 2007[1,2] and a projected increase of 165% from 2000 to 2050[3].
Closely linked with the rise in diabetes prevalence is the rapidly increasing epidemic of obesity around the world, predominantly in developed societies[4]. In 2004, 17% of children in the United States between ages 2 and 19 yr were overweight, and 32% of adults over age 20 were obese[5]. Both obesity and related inactivity are likely to contribute to the pathogenesis of diabetes because the incidence of diabetes can be reduced by modest weight loss and exercise[6-8]. In light of these findings, an important public health goal should be to understand the complex pathophysiology of diabetes and to identify and target specific mechanisms to prevent DM in at-risk individuals.

Risk factors associated with type 2 diabetes

Multiple physiological abnormalities can be found in individuals with established type 2 DM, defined on the basis of elevations in fasting and/or postprandial glucose[2]. These include insulin resistance in muscle and adipose tissue, β-cell dysfunction leading to impaired insulin secretion, increased hepatic glucose production, abnormal secretion and regulation of hormones, and altered balance of central nervous system pathways controlling food intake and energy expenditure. Given all these diverse abnormalities in multiple tissues and the secondary consequences of established hyperglycemia and hyperlipidemia, it is difficult to identify the primary events that lead to the development of diabetes.

Risk factors for the development of and/or progression of type 2 DM include:

1) genetics[9-15], exemplified by the high risk of type 2 DM in particular ethnic groups[16] and the high concordance rates in monozygotic twin pairs[17] and

2) both prenatal and postnatal environmental factors, including suboptimal intrauterine environment[18,19], low birth weight[18,20], obesity[21], inactivity[22], gestational diabetes[23], and advancing age[24].

Several studies have indicated that insulin resistance is common in high-risk individuals years before the onset of type 2 DM[25-27].

Multiple mechanisms have recently emerged as potential causes of insulin resistance and/or diabetes progression, among them impaired mitochondrial capacity and/or function, altered insulin signaling due to cellular lipid accumulation, proinflammatory signals, and endoplasmic reticulum stress and reduced incretin-dependent and -independent β-cell insulin secretion.

The biology of mitochondria

Mitochondria are double-membrane organelles that serve multiple essential cellular functions (Fig. 1) mediated by thousands of mitochondrial-specific proteins encoded by both the nuclear and mitochondrial genomes[28,29]. Although mitochondria are most often recognized for their role in generating the majority of cellular ATP via oxidative phosphorylation (OXPHOS), other essential metabolic functions include the generation by the tricarboxylic acid (TCA) cycle of numerous metabolites that function in cytosolic pathways, oxidative catabolism of amino acids, ketogenesis, ornithine cycle activity ("urea cycle"), the generation of reactive oxygen species (ROS) with important signaling functions[30,31], the control of cytoplasmic calcium[32,33], and the synthesis of all cellular Fe/S clusters, protein cofactors essential for cellular functions such as protein translation and DNA repair[34]. The rate-limiting first step in steroidogenesis also occurs in mitochondria, thus linking mitochondrial function to endocrine homeostasis[35-37]. This multiplicity of organelle functions explains the variability in pathophysiology, severity, and age of onset of the increasing number of diseases recognized to arise from primary or secondary alterations in specific mitochondrial pathways[34,38-40].

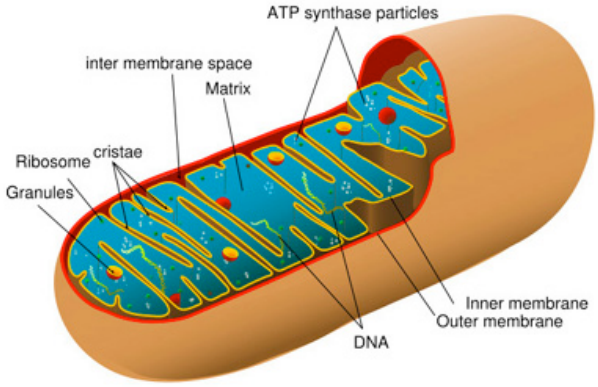

Figure 1. basic structure of the mitochondrion.

The mitochondrial matrix also contains the circular mitochondrial DNA (mtDNA) molecules, normally inherited exclusively from the mother, which encodes for 37 genes (13 of which are subunits of the ETC). Translation of these proteins occurs within the mitochondrial matrix, utilizing mtDNA-encoded rRNA and tRNA (Fig. 2).

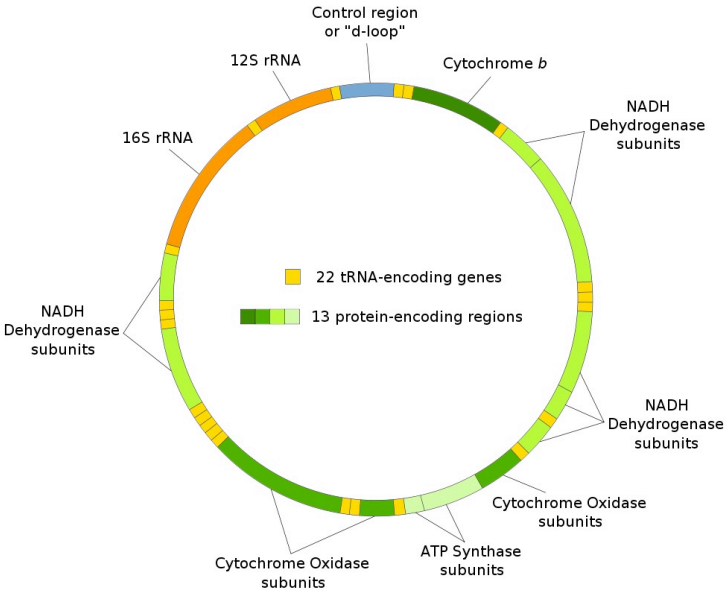

Figure 2. The two strands of mtDNA are differentiated by their nucleotide content with the guanine rich strand referred to as the heavy strand, and the cytosine rich strand referred to as the light strand. The heavy strand encodes 28 genes, and the light strand encodes 9 genes for a total of 37 genes. Of the 37 genes, 13 are for proteins (polypeptides), 22 are for transfer RNA (tRNA) and two are for the small and large subunits of ribosomal RNA (rRNA).

The morphology of mitochondria

In the thin sections observed by electron microscopy, mitochondria appear as discrete, small, double-membrane organelles. However, more recent studies based on light microscopy in live cells have revealed that mitochondria exist as a reticulum that is in continuous communication through dynamic fusion and fission events, moving actively to different regions of the cell through interactions with the cytoskeleton. The mitochondrial reticulum is composed of an outer and an inner membrane, between which is the intermembrane space, and a matrix limited by the inner membrane (Fig. 3). The area of the inner membrane can be greater than that of the outer membrane due to the presence of cristae, inner membrane invaginations that contain all the transmembrane proteins of the electron transport chain (ETC) as well as the mitochondrial ATPase[41-43]. The mitochondrial matrix contains the components of the TCA cycle and of the β-oxidation pathway, which provide reduced nicotinamide adenine dinucleotide (NADH) and reduced flavin adenine dinucleotide ($FADH_2$) to the Electron Transport Chain (ETC).

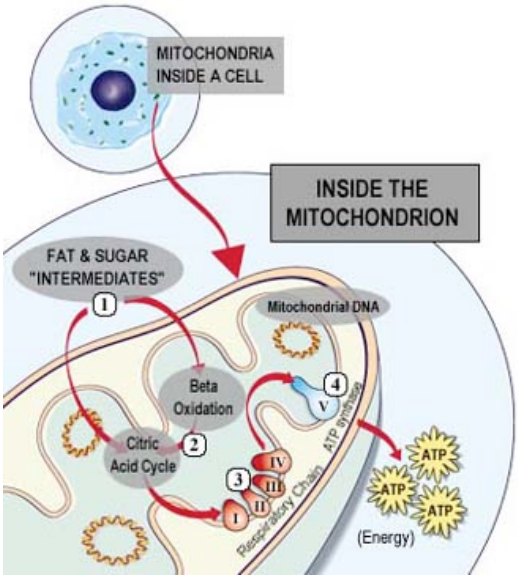

Figure 3. The mitochondrial reticulum is composed of an inner and outer membrane, between which lies the intermembrane space, and a matrix contained within the inner membrane. The surface of the inner membrane is folded into cristae. The organization and distribution of the mitochondrial reticulum is controlled by interactions with cytoskeletal elements such as microtubules. The matrix contains the enzymatic machinery for fatty acid β oxidation, which generates acetyl-CoA from acyl chains, and reducing equivalents in the form of NADH and $FADH_2$.

The electron transfer chain (ETC)

The ETC is composed of five large multisubunit complexes (complexes I to V) with more than 85 individual gene products. The ETC transports electrons from donors (NADH at complex I, $FADH_2$ at complex II) to a final acceptor, molecular oxygen, forming H_2O at complex IV (Fig. 4). The transport of electrons is accompanied by release of large amounts of free energy, most of which is harnessed for the translocation of protons from the matrix to the intermembrane space; the remainder is dissipated as heat (Fig. 5). The energy contained in the proton electrochemical gradient generated by the ETC is then coupled to ATP production as protons flow back into the matrix through the mitochondrial ATPase which constitutes the complex V. Thus, OXPHOS results from electron transport, the generation of a proton gradient, and subsequent proton flux coupled to the mitochondrial ATPase. Each of these steps can vary in efficiency; for example, the exact stoichiometry between electron flow and proton pumping, or between proton pumping and ATP synthesis varies depending on the probability of loss of electrons from the ETC before reaching complex IV and on non-ATPase-coupled proton leak through the inner mitochondrial membrane, for example via uncoupling proteins (UCPs) (Fig. 5).

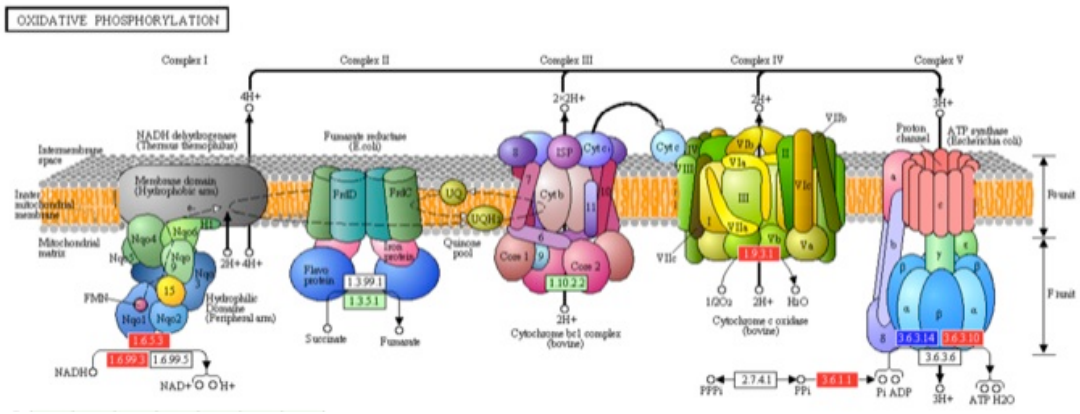

Figure 4. Schematic representation of the Electron Transfer Chain. Electrons derived from reduced donors NADH and $FADH_2$ are transported within the ETC to molecular oxygen, producing water. The flow of electrons within the ETC is coupled to translocation of protons due to the large amount of free energy released during electron transport. The remainder of this free energy is released as heat. The proton gradient thus produced is dissipated through the mitochondrial ATPase, and the consequent decrease in free energy drives ATP synthesis. This process is known as OXPHOS, or coupled respiration.

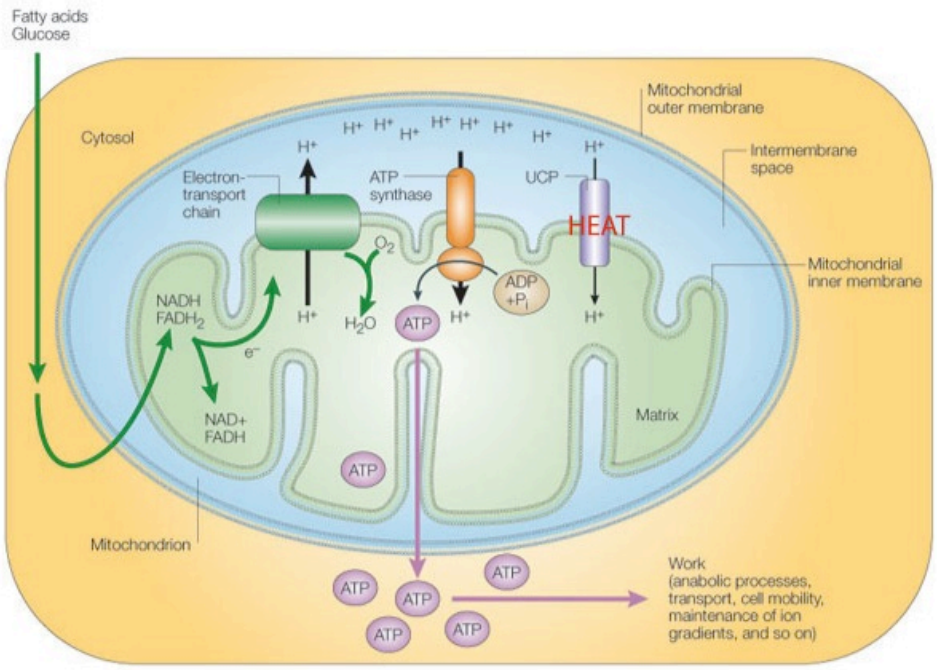

Figure 5. Under circumstances where NADH and $FADH_2$ are available, but movement of electrons down the respiratory chain is slow, some of those electrons will be released from the respiratory chain and reduce molecular oxygen, forming the superoxide anion $O2^-$, hydrogen peroxide, and the hydroxyl radical OH^-. These are the main ROS formed at steady state. Accumulation of ROS activates UCPs, which dissipate the proton gradient without producing ATP, resulting in uncoupled respiration.

Mechanisms regulating mitochondrial density and activity

The term mitochondrial biogenesis is often used to describe the new generation of mitochondria in response to increased energy demands, or the increase of mitochondria necessary for cell growth and division. However, the copy number of specific mitochondrial proteins and the functional capacity of each distinct mitochondrial pathway may be very variable between different tissues and between different physiological conditions. Thus, the term mitochondrial biogenesis can be ambiguous because of multiple parameters, including mtDNA copy number, mitochondrial density, levels of specific mitochondrial proteins, and mitochondrial functional output may vary independently of each other.
For example, the proliferation of mitochondria occurring to sustain hyperplastic growth is probably very different from that occurring to support hypertrophic growth in any given tissue, and the regulatory mechanisms controlling these adaptive changes are likely to be distinct.
Although it is know very little about specific mechanisms that control different modalities of mitochondrial biogenesis, it is clear that these mechanisms require coordination between the nuclear and mitochondrial genomes. Transcription of the mitochondrial genome is under the control of a single transcription factor, *TFAM*, which is encoded by the nuclear genome. In turn, TFAM expression is regulated by the transcription factors NRF (nuclear respiratory factor)-1 and NRF-2, which specifically activate

numerous nuclear-encoded genes involved in mitochondrial respiration[44,45]. Thus, through NRF-stimulated expression of TFAM, the transcription of the mitochondrial genome is stimulated in coordination with that of nuclear-encoded mitochondrial genes. The expression of many other mitochondrial genes is controlled by additional nuclear transcription factors, including peroxisome proliferator-activated receptor (PPAR) α, PPARδ, estrogen-related receptor (ERR) α/γ, and Sp1, which can induce expression of mitochondrial genes in a tissue-dependent and physiological context-dependent manner[46].

A high level of transcriptional coordination is required to ensure coupling of mitochondrial activity to other metabolic activities within the cell. This coordination is accomplished through the action of transcriptional coactivators and corepressors. The best studied coactivators of mitochondrial gene transcription are members of the PPARγ coactivator (PGC) family, including PGC-1α , PGC-1β[47,48], and PPRC, a related serum-responsive coactivator[49]. These cofactors respond to cellular energy-requiring stimuli[46] to activate transcription factors promoting mitochondrial remodeling and/or biogenesis. For example, PCG-1α is highly expressed in muscle, liver, and brown fat, and expression is further increased in these tissues in response to exercise, fasting, and cold exposure, respectively. Although PGC-1α and PGC-1β do not appear to be required for mitochondrial biogenesis during development[50], they are necessary for the expression of the full complement of proteins of mitochondrial OXPHOS and fatty acid β-oxidation pathways in muscle and brown adipose tissue[50-60].

Forced expression studies in adipogenic and myogenic mammalian cell lines demonstrated that PGC-1α markedly induces the expression of NRF-1, NRF-2, and Tfam[47] PGC-1α can also interact directly with and coactivate NRF-1 on the Tfam gene promoter. Studies in primary cardiac myocytes in culture and in the hearts of transgenic mice have demonstrated that overexpression of PGC-1α up-regulates the expression of genes involved in mitochondrial fatty acid oxidation, most of which are PPARα targets, in addition to NRF-1 targets[61]. Cardiac-specific overexpression of PGC-1α in transgenic mice leads to massive mitochondrial proliferation, ultimately resulting in cardiomyopathy and death[61]. Interestingly, in neonatal cardiac myocytes in culture, PGC-1α induces mitochondria that support largely coupled respiration consistent with the known ATP-generating function of this organelle in heart[61]. Lastly, forced expression of PGC-1α in skeletal muscle of transgenic mice triggers mitochondrial proliferation and the formation of mitochondrial-rich type I, oxidative ("slow-twitch") muscle fibers[62]. Collectively, these results indicate that PGC-1α is capable of promoting mitochondrial biogenesis through its coactivating effects on key factors such as NRF-1.

Moreover, PGC-1α and PGC-1β are crucial for the rapid bursts in mitochondrial proliferation that accompany perinatal heart and brown adipose tissue development[50]. These data support the concept that mitochondrial adaptation to specific energy demand is mediated by PGC-1α and PGC-1β; by contrast, mitochondrial expansion during cell proliferation is more likely to depend on serum-responsive coactivators such as PPRC[63].

The role of corepressors in the transcriptional control of energy metabolism genes is less extensively studied. However, evidence in cultured cells and in mouse models points to a critical role of the corepressor RIP140 in controlling important aspects of mitochondrial energy metabolism in both adipose tissue and muscle[63-68].
RIP140 is highly expressed in metabolic tissues[66], and further understanding of its biological role has been greatly improved through the use of loss-of-function mouse model. The RIP140-null animals show that RIP140 is essential for female fertility[69,70] and plays a crucial role in lipid metabolism. In fact, RIP140-null mice are extremely lean and exhibit resistance to obesity and hepatic steatosis as well as enhanced glucose tolerance and enhanced responsiveness to insulin when compared with matched wild-type littermates fed a high-fat diet[66]. Adipogenesis is unaffected in these mice, and expression profiling identified genes involved in catabolism in white adipose tissue as well as in skeletal muscle.
In 3T3-L1 adipocytes, depletion of RIP140 recapitulates the alterations in gene expression, observed in vivo, affecting clusters of genes implicated in glucose uptake, glycolysis, TCA cycle, β-oxidation, mitochondrial biogenesis, oxidative phosphorylation, and mitochondrial uncoupling[71]. The modulation of RIP140 expression may also affect the metabolic properties of skeletal muscle[72,73]. This suggests that RIP140 could serve an important function in terminally differentiated adipocytes and myotubes; in the RIP140-null animals, muscles exhibited a marked increase in mitochondrial activity accompanied by a consequent shift in myofibers towards the more oxidative types. On the other hand, in the transgenic animals, the higher expression of RIP140 resulted in a decrease in both mitochondrial activity and the number of oxidative myofibers. Moreover, RIP140 mRNA levels are higher in glycolytic muscles, extensor digitorum longus (EDL) and gastrocnemius, than in oxidative muscles, soleus and diaphragm, suggesting a role for RIP140 as an inhibitor of oxidative metabolism in skeletal muscle[73].
Finally, RIP140 suppresses UCP1 through interaction with specific enhancer elements and also suppresses expression of genes involved in β-oxidation and respiratory chain assembly. RIP140 also interacts directly with many of the transcription factors and cofactors coactivated by PGC-1α[73].
The mechanisms that control the balance between PGC-1 coactivators and RIP140 and other corepressors are not completely clear yet but probably represent key regulatory mechanisms of energetic adaptation.

Tissue-specific contexts: role of mitochondria

Skeletal Muscle

Mitochondria are particularly important for skeletal muscle function, given the high oxidative requests imposed on this tissue by contraction. Mitochondria play a critical role in giving sufficient levels of ATP needed; this high-level requirement for ATP by sarcomeres has likely contributed to the distinct subsarcolemmal and sarcomere-associated populations of mitochondria in muscle. Moreover, muscle cells must maintain metabolic

flexibility, defined as the ability to rapidly modulate substrate oxidation as a function of ambient hormonal and energetic conditions. For example, healthy muscle tissue predominantly oxidizes lipid in the fasting state, as evidenced by low respiratory quotient (RQ), with subsequent transition to carbohydrate oxidation (increased RQ) during the fed state. Availability of fuels, particularly lipids, and capacity to oxidize them in the mitochondria are also critical for sustained exercise. Thus, mitochondrial functional capacity is likely to directly affect muscle metabolic function and, because of its large contribution to total body mass, to have a significant impact on whole-body metabolism. This possibility is supported by the findings of increased mitochondrial content in skeletal muscle in an individual with hypermetabolism and resistance to weight gain (Luft syndrome)[74].

Skeletal muscle is the largest insulin-sensitive organ in humans, accounting for more than 80% of insulin-stimulated glucose disposal. Thus, insulin resistance in this tissue has a major impact on whole-body glucose homeostasis. Indeed, multiple metabolic defects have been observed in muscle from insulin-resistant but normoglycemic subjects at high risk for diabetes development, including reduced insulin-stimulated glycogen synthesis[25,75,76], alterations in insulin signal transduction[77]; and increased muscle lipid accumulation[78]. Although it remains unclear whether any of these defects play a causal role in insulin resistance, intramuscular lipid excess strongly correlates with the severity of insulin resistance, even after correction for the degree of obesity[78], and has been observed in muscles of multiple fiber types[79]. Moreover, lipid excess has been linked experimentally to induction of insulin resistance[80] and alterations in insulin signal transduction[81-83].

Thus, one possible mechanism by which impaired mitochondrial function might contribute to insulin resistance is through altered metabolism of fatty acids. Increased tissue lipid load, as with obesity, and/or sustained inactivity, may lead to the accumulation of fatty acyl coenzyme A (CoA), diacylglycerols, ceramides, products of incomplete oxidation, and ROS, all of which have been linked experimentally to reduced insulin signaling and action[80-86]. Additional mechanisms potentially linking impaired mitochondrial oxidative function to insulin resistance include reduced ATP synthesis for energy-requiring functions such as insulin-stimulated glucose uptake, abnormalities in calcium homeostasis (necessary for exercise-induced glucose uptake)[87-89] and reduced ATP production during exercise[90], potentially contributing to reduced aerobic capacity, muscle weakness, and decreased voluntary exercise.

Evidences for muscle mitochondrial dysfunction in DM

An important early evidence suggesting that muscle mitochondrial oxidative dysfunction may be associated with insulin resistance in humans was the series of observations by Simoneau and Kelley that obesity is associated with reductions in citrate synthase, malate dehydrogenase, carnitine palmitoylotransferase 1 (CPT1), and cytochrome oxidase (COX) activity in the fasting state[91] and with parallel increases in activity of the glycolytic enzymes hexokinase and phosphofructokinase[92]. Moreover, oxidative activity (e.g., citrate synthase, acyl CoA dehydrogenase) is a robust correlate of insulin sensitivity, even better than either in

triglycerides or long-chain fatty acyl CoA[93]. Impaired metabolic flexibility also correlates with intramyocellular accumulation of lipids[91], and 24-h RQ can predict subsequent weight gain[93,94]. Together, these data suggest that an intrinsic defect in multiple components of oxidative metabolism, or altered regulation, may contribute to the development of both obesity and insulin resistance.

The diminished capacity for appropriate regulation of oxidative metabolism observed in the above studies could be linked to reduced mitochondrial function due to abnormal mitochondrial density and/or in vivo function and/or intrinsic defects in oxidative metabolism of lipids or other substrates. Multiple studies suggest that human insulin resistance is indeed accompanied by impaired *in vivo* mitochondrial oxidative function linked, at least in part, to reduced mitochondrial density. Boushel et al.[95] found modest reductions in ADP and succinate-stimulated oxygen consumption in permeabilized muscle fibers from obese individuals with type 2 DM. In this study, the differences in oxidative capacity did not remain after normalization for mitochondrial mass by citrate synthase activity or mtDNA content, suggesting that reduced mitochondrial mass might be a major contributor.

Nuclear magnetic resonance (NMR) spectroscopy has also been used to assess mitochondrial function in vivo, with studies finding similar reductions in oxidative function in both insulin resistance and type 2 DM. For example, rates of mitochondrial OXPHOS in offspring of type 2 diabetic subjects, as assessed by ^{31}P spectroscopy, are reduced by 30% in the fasting state[96]. The magnitude of this change is strikingly similar to the 38% lower muscle mitochondrial density, assessed by electron microscopy, in this same population, suggesting once again that decreased mitochondrial density might be an important factor in reduced oxidative capacity in subjects with a family history of diabetes.

Alterations in mitochondrial function have also been identified in isolated mitochondria from humans with insulin resistance and DM. Mogensen et al.[97] observed decreases in maximal ADP-stimulated respiration (state 3, malate and pyruvate as substrates) in mitochondria isolated from obese subjects with DM as compared with obesity alone; these differences persisted even after normalization to citrate synthase activity. Thus, these data suggest that in addition to decreased mitochondrial density, there are additional intrinsic defects in TCA cycle, OXPHOS, membrane potential, or adenine nucleotide transporters in mitochondria of individuals with established diabetes.

Analysis of global gene expression patterns has also demonstrated a 20–30% reduction in mRNA expression levels for multiple nuclear-encoded genes of the OXPHOS pathway in humans with type 2 DM[98-100]. Importantly, similar reductions in OXPHOS gene expression have been observed in some, but not all, populations of insulin-resistant, but completely normoglycemic, individuals[99,101].

A recent study of Asian Indian subjects found no correlation between changes in OXPHOS gene expression and insulin resistance[102]. In these individuals, expression of OXPHOS and TCA cycle genes, mtDNA content, and ATP production rates were actually higher in both non diabetic and diabetic individuals compared with Northern European controls, despite lower overall insulin sensitivity. However, circulating triglycerides were significantly elevated in both non diabetic and diabetic individuals of Asian

Indian origin[102]. These observations also raise the question of whether levels of OXPHOS gene expression and function have to be considered relative to the oxidative fuel load in an individual. For example, high OXPHOS expression in the population mentioned above may still be not enough for appropriate and complete oxidation of a chronic high load of circulating lipids, while lower OXPHOS levels may be sufficient under conditions of a low circulating lipid load.
Such data also arise the importance of considering additional aspects of oxidative mitochondrial function beyond OXPHOS expression or capacity. For example, primary myotubes isolated from obese humans with type 2 DM display reduced basal lipid oxidation and insulin-stimulated glucose oxidation with no differences in OXPHOS gene expression[103]. Thus, defects in lipid oxidation in DM can be significant contributors to disfunctional oxidative metabolism even in the absence of detectable alterations in OXPHOS gene expression or function.

Factors affecting OXPHOS gene expression in muscle

Reduced OXPHOS gene expression has been observed in response to genetic and nutritional obesity[104], short-term high-fat feeding (even in humans)[105], lipid infusion[106], and lipid loading of myotubes[104]. However, these responses are not observed in all studies of high-fat feeding; in fact, some studies demonstrate that high-fat feeding is associated with increased numbers of mitochondrial protein and DNA content, potentially mediated by chronic fatty acid activation of PPARs[107-109]. These studies suggest that genetic background[104], age at dietary intervention, specific dietary lipid composition, and duration of diet may be important variables to consider when analyzing the interaction between OXPHOS gene expression and diet. Moreover, alterations in OXPHOS gene expression may be a secondary response to an underlying primary defect in oxidative metabolism, reflecting attempts to compensate the reduction in mitochondrial capacity.
Reduced physical activity could be associated with reduced muscle OXPHOS gene expression. In rats bred for low aerobic capacity over multiple generations, expression of several OXPHOS genes is markedly reduced, even in the absence of obesity[110]. Conversely, OXPHOS expression can be increased with exercise training[111,112], a potent insulin sensitizer.
Finally, genetic and epigenetic modifications may also contribute to reduced expression of OXPHOS genes in type 2 DM. For example, expression of COX7A1, a complex IV gene down-regulated in type 2 DM, is heritable (50–72% heritability, as assessed by analysis in monozygotic and dizygotic twins), indicating a strong genetic or shared familial environmental contribution[113]. Similar patterns are observed for the complex I gene NDUFB6[114] and the ATP synthase component ATP5O[115]. Indeed, expression of nuclear-encoded OXPHOS genes is significantly more concordant between monozygotic twins than expected and is the top-ranking gene set for concordance in pathway analysis of global gene expression. Mediators of mitochondrial biogenesis, including ERRα, may contribute to the strong heritability of OXPHOS components.

Epigenetic mechanisms may also contribute to these patterns because reduced expression parallels increased DNA methylation of both the COX7A1 promoter[113] and NDUFB6[114,116].
As for the other tissues, the expression of OXPHOS genes in muscle is mediated in part by the action of coactivators and corepressors. PGC-1α has been recognized as an important coactivator in skeletal muscle, contributing to fiber type determination, glucose uptake, and oxidative capacity. Moreover, alterations in muscle PGC-1α or β mRNA expression are observed in humans with insulin resistance, being reduced by nearly 50% in muscle from individuals with diabetes[99] and in some populations of normoglycemic insulin-resistant humans[98,101,114]. In turn, PGC-1α expression may also be reduced as a consequence of promoter methylation[117] or caused by insulin itself, obesity, and sustained lipid exposure[103]. For example, saturated fatty acids reduce PGC-1α promoter transcriptional activity and expression in cultured myotubes, in parallel with reduced OXPHOS expression and O_2 consumption[104]. PGC-1 activity can also be modulated at the level of translation and by posttranscriptional changes, including inhibitory acetylation mediated by GCN5[118] and deacetylation by SIRT1 action[119]. These multiple modes of PGC-1α regulation are likely to have evolved from the need to set mitochondrial energy metabolism in response to different inputs.

In summary, insulin resistance has been associated with alterations in skeletal muscle mitochondrial oxidative function and its transcriptional regulatory pathways. However, several lines of evidence suggest that this may not be a causal relationship in all situations. First, oxidative dysfunction is not observed in all insulin resistant individuals[102]. Second, oxidative activity is determined by the need to generate energy in response to cellular demands, such as contraction and ion transport; thus oxidative capacity is not likely to be limiting in the resting state in muscle. Rather, alterations in relative utilization of substrates, an imbalance between fuel load and cellular energy requirements, and/or differential thresholds for generation of or resolution of oxidative stress in this setting may contribute to differential susceptibility to insulin resistance in muscle.

Adipose tissues

The role of mitochondria in adipose tissue is most apparent in brown adipose tissue, where flux through the ETC generates heat in the process of thermogenesis, a potentially important mechanism regulating systemic metabolism even in adult humans[120-123]. In brown fat, electron transport is greatly accelerated due to tissue-specific expression of the mitochondrial UCP1. UCP1 dissipates the proton gradient of sufficient degree to sustain the synthetic activity of the mitochondrial ATPase[121,124-126], thus driving continuous accelerated electron transport. UCP1-mediated uncoupling alone, however, can not fully account for the large thermogenic capacity of brown adipocytes in the absence of mechanisms that ensure continuous substrate delivery to the ETC. Thus, brown adipocyte mitochondria also contain high levels of CPT1b, which is critical for the entry of fatty acids

into the mitochondria. β-Oxidation, in turn, generates large amounts of reducing equivalents for the ETC.
In contrast, white adipocytes have been described to contain less mitochondria compared with brown adipocytes or muscle. However, mitochondrial density increases dramatically, and mitochondrial remodeling occurs during white adipocyte differentiation[127-129], suggesting that mitochondrial functions are required to support the multiple biological roles of mature white adipocytes. Interestingly, a recent compendium of mitochondrial proteins from 14 different mouse tissues indicates that white adipocyte mitochondria contain a more diverse protein repertoire than mitochondria from heart, skeletal muscle, or brain[28]. Thus, white adipocyte mitochondria appear to be equipped for a broader array of functions compared with mitochondria in tissues that must sustain rapid bursts of energy-requiring processes. Among the mitochondrial functions that may be relevant for white adipose tissue function are the anaplerotic generation of metabolic intermediates for fatty acid synthesis and esterification[130], the maintenance of a robust pathway for the folding and secretion of high abundance circulating proteins such as adiponectin[131], and interactions between mitochondrial function and components of the insulin signaling pathway[131].

Adipose tissue mitochondrial activity and insulin resistance

The large capacity of brown adipose tissue mitochondria to oxidize fatty acids results in a considerable impact on whole-body metabolism; increased brown adipose tissue abundance correlates negatively with fuel storage and weight gain in rodents, and vice versa[132].
Recent works have led to reconsideration of the role of brown fat in the balance of energy metabolism, underlining that humans possess adipose tissue depots that are cold-sensitive and hypermetabolic, as assessed by their very high uptake of labeled glucose[123,133]. Such depots appear to be less active as a function of aging and/or obesity[122,134-137]. Thus, impaired mitochondrial capacity in brown adipose tissue might be functionally linked to impaired thermogenesis and energy expenditure, and thus increased susceptibility to obesity-linked insulin resistance.
The relevance of white adipocyte mitochondria to whole-body metabolism and metabolic disease may depend on the extent to which mitochondrial respiratory capacity and/or the total mass of white adipose tissue would be sufficient to impact circulating free fatty acid levels. White adipocytes display a high degree of plasticity[138], and regional differences in metabolic activity can be linked to varying mitochondrial density[139]. Higher mitochondrial density and even UCP1 can be induced in response to pharmacological or genetic alterations of white adipocytes[139-148], suggesting that white adipose tissue could potentially be induced to acquire more oxidative metabolic phenotypes, promoting increased fuel consumption and thus energy expenditure. Whether respiratory chain uncoupling mediated through the induction of UCP1 in white adipocytes alone could reduce free fatty acid release, or whether an additional increase in mitochondrial oxidative capacity would be required, is still an open discussion[149-153].

In addition to the effects on fuel utilization, decreased mitochondrial capacity in adipocytes may also alter adipocyte insulin sensitivity and/or function due to the high energetic requirements for fatty acid storage, adipokine secretion[131], insulin signaling[154], and glucose uptake. Interestingly, in cultured adipocytes, impairment of respiratory chain function through depletion of Tfam during adipocyte differentiation results in impaired insulin-stimulated glucose transport[154].

Evidences for adipose tissue mitochondrial dysfunction in DM

White adipocyte mitochondrial content is decreased in both rodent and human obesity[147,155-158] and correlates with insulin resistance that accompanies obesity. In humans, white adipocyte mtDNA copy number is inversely correlated with age and BMI and directly correlated with basal and insulin-induced lipogenesis[159]. Thus, reduced mtDNA content could reduce adipocyte capacity for lipid storage, promoting ectopic lipid accumulation in peripheral tissues such as muscle and liver. In parallel, the expression of nuclear-encoded OXPHOS genes is down-regulated in visceral adipose tissue of humans with type 2 DM[160]. Administration of thiazolidinediones induces changes in mitochondrial content and remodeling in white adipocytes concomitantly with an improvement in insulin sensitivity[140,143,147,157,161-165]. Mitochondrial levels in white adipocytes are also increased in response to adrenergic stimulation, β-3 agonists, and CB1 blockade in mice[162,166,167] with consequent increased insulin sensitivity.

At the moment it is still unclear if changes in mitochondrial density are a cause or consequence of changes in insulin sensitivity, however, some evidences suggest that lack of insulin signaling does not reduce mitochondrial capacity in adipose tissue. For example, conditional KO mice in the adipose tissue for the insulin receptor (FIRKO mice) display high levels of mitochondrial genes involved in fatty acid oxidation and OXPHOS over the lifespan of the animals[168]. Thus, mechanisms that induce and maintain active mitochondria in adipocytes can bypass defects in insulin signaling, and indeed, insulin signaling may repress mitochondrial gene expression and/or function.

Towards the Brown Fate

The genetic program leading to brown adipose tissue development, and potentially to the high abundance of mitochondria, is initiated by the zinc-finger protein PRDM16[168-171]. Recent articles sustain the hypothesis that brown adipocytes and myocytes share a common cellular lineage; in addition, the transcriptional coactivators PGC-1α and -β[47] play a critical role in the expansion of the mitochondrial reticulum and in the induction of UCP1 and the brown adipose tissue thermogenic program during the perinatal period[50].
Adipocyte mitochondrial density and OXPHOS activity can be regulated in response to factors that affect lipid metabolism. For example, Toh et al.[146] and Nishino[172] et al. find that mice deficient in Fsp27 (also called Cidec) a lipid droplet protein that promotes lipid storage in white and brown adipocytes, have increased whole-body energy expenditure, resistance to diet-induced obesity, and enhanced insulin sensitivity. This apparent paradoxical result (high insulin sensitivity despite deficiency in lipid storage), appears to be due to the increased mitochondrial density and activity in white adipocytes, which are brown-like in their increased capacity to oxidize large quantities of fatty acids. Nitric oxide production by the endothelial nitric oxide synthase has also been linked to enhanced adipose tissue mitochondrial biogenesis and prevention of high-fat diet-induced obesity[167]. Conversely, both genetic and diet-induced obesity result in decreased mitochondrial density and OXPHOS activity in adipose tissue[104,147,156-158], potentially contributing to adipose tissue dysfunction and exacerbation of insulin resistance. The mechanisms by which obesity results in a reduction in adipose mitochondrial density are not known but could be mediated by decreased expression of PGC-1α, as observed in obese humans[173].
Finally, Nedergaard and collegues examining precursors from the purest white adipose tissue depot (epididymal), reported that chronic treatment with the peroxisome proliferator activated receptor γ agonist rosiglitazone promotes not only the expression of PGC-1α and mitochondriogenesis in these cells but also a norepinephrine-augmentable UCP1 gene expression in a significant subset of the cells, providing these cells with a genuine thermogenic capacity. These cells probably constitute a subset of adipocytes (called "brite" adipocytes) with a developmental origin and molecular characteristics distinguishing them as a separate class of cells, since they remain negative for the classical markers of brown adipocytes (Zic1, Lhx8, Meox2, and characteristically PRDM16) or of myocytes (myogenin and myomirs, muscle-specific microRNAs) and retain white fat characteristics such as Hoxc9 expression[148].

Liver

The liver plays a central, unique role in carbohydrate, protein, and fat metabolism. It is critical for maintaining glucose homeostasis during fuel availability, via storage of glucose as glycogen or conversion to lipid for export and storage in adipose tissue, and in the fasting state, via catabolism of glycogen, synthesis of glucose and ketogenesis. In turn,

these responses are regulated by the key hormones insulin and glucagon, which modulate signaling pathways and gene expression, leading to inhibition or stimulation of glucose production, respectively.
Recent human data have highlighted the importance of disordered hepatic metabolism, including inappropriately increased hepatic glucose production, hyperlipidemia, and lipid accumulation, in both obesity and type 2 DM[174]. Similarly, rodent data also support an important role for the liver in diabetes pathogenesis. Liver-specific insulin receptor knockout (LIRKO) mice develop insulin resistance, glucose intolerance, impaired insulin suppression of hepatic glucose production, and altered patterns of hepatic gene expression[175]. Interestingly, these mice are also dyslipidemic and susceptible to atherosclerosis[176]. Given the diverse array of unique metabolic functions centered in the liver, it is not surprising that ultrastructure and function of hepatic mitochondria are distinct from that of muscle. Electron microscopy demonstrates that mitochondrial area is 44% lower in liver than in heart[177] with smaller size, fewer cristae, and lower matrix density. Protein expression of multiple OXPHOS components and Tfam and citrate synthase activity are also lower in liver (e.g., 7% that of cardiac muscle)[178]. Despite lower OXPHOS capacity, state 3 respiration and respiratory control ratio are equivalent in liver and muscle. By contrast, the content of mtDNA is actually higher in the liver than in other tissues.
Impairments in mitochondrial number and/or oxidative function could potentially affect multiple cellular functions within hepatocytes, both directly (e.g., reduced ATP generation, alterations in oxidative stress, reduced capacity for fatty acid oxidation) and indirectly, via effects on energy-requiring processes, including gluconeogenesis, synthesis of urea, bile acids, cholesterol, proteins and detoxification.
Hepatic lipid accumulation may result when adipose lipid storage capacity is exceeded, as in obesity or adipocyte dysfunction (e.g., lipodystrophy)[179]. Alternatively, lipid accumulation may reflect an additional imbalance between *de novo* hepatic lipogenesis and mitochondrial oxidative metabolism. Interestingly, hepatic lipid accumulation is also a robust predictor of not only hepatic, but also muscle and adipose insulin sensitivity[180,181]. Conversely, modest weight loss (about 8 kg) normalizes intrahepatic lipid in subjects with type 2 DM, in parallel with normalization of hepatic insulin sensitivity, even in the absence of changes in intramyocellular lipid accumulation or circulating adipocytokines[182].
Although these data highlight an intimate relationship between obesity, intrahepatic lipid metabolism, and insulin sensitivity in humans, mechanisms responsible for these links remain unclear. One possibility is that excessive hepatic lipid accumulation may play a central, pathogenic role in insulin resistance. This hypothesis comes from experimental lipid loading, which can induce hepatic insulin resistance. Transgenic mice expressing lipoprotein lipase in the liver have a 2-fold increase in hepatic triglyceride content and are insulin resistant[183].
A second possibility is that hepatic insulin resistance itself contributes to alterations in mitochondrial oxidative capacity. Indeed, a recent paper demonstrated that mice with hepatic insulin resistance due to deletions of the major insulin receptor substrates (IRS-1 and IRS-2) have impaired mitochondrial function and biogenesis, as demonstrated by reduced NADH

oxidation, reduced ATP production rates, reduced numbers of mitochondria per cell, reduced fatty acid oxidation, and increased hepatic triglyceride accumulation[184]. Mitochondrial dysfunction was reversed by deletion of Foxo1. These data indicate that normal insulin signaling, which inhibits Foxo1, is required for maintenance of normal mitochondrial function in this model. Finally, these data indicate that hepatic lipid accumulation and insulin resistance are intimately linked with mitochondrial oxidative dysfunction.

In summary, mitochondrial oxidative activity can be considered as a key determinant underlying diabetes risk. In isolation, reductions in mitochondrial activity mediated by genetic factors (family history, ethnicity), epigenetic mechanisms, developmental exposures, and aging may not be sufficient to induce insulin resistance. However, when sustained fuel excess (e.g., resulting from overnutrition or impaired fat storage) exceeds energetic demands and/or oxidative capacity, and/or appropriate compensatory mechanisms are insufficient (e.g., due to inactivity or failure of mitochondria to adapt to higher cellular oxidative demands), a vicious cycle of insulin resistance and impaired insulin secretion can be initiated. Resulting lipid accumulation and oxidative stress can alter transcriptional responses and damage mitochondria, further reducing OXPHOS capacity, compounding the deleterious effects of fuel excess and increasing diabetes risk. Although the importance of the PGC-1 family of coactivators has been stressed thus far, it is likely there are many additional metabolic, transcriptional and epigenetic mechanisms by which mitochondrial function adapts to environmental demands.

The epigenetic concept

Epigenetics can be defined as any inheritable influence on gene activity that does not involve a change in DNA sequence. In all eukaryotic cells, genomic DNA is folded and compacted by histone and non-histone proteins to form nucleosomes and a further structured and dynamic form, generally referred to as chromatin. DNA packaging must be considered as a way to store and retrieve information since it represents a dynamic switch between transcriptional "on-off" states that result in gene activation and gene silencing. The term euchromatin refers to accessible and transcriptionally active nucleosomes, while heteterochromatin is composed by highly condensed genetic material.
In general, the epigenetic control is accomplished by means of two major mechanisms: methylation of cytosine residues in the DNA sequence and modifications of histones and other chromatin-associated proteins. Referring to the latter mechanism, it has long been known that histone tail domains can be covalently modified by acetylation, phosphorylation, methylation at specific amino acid positions (fig. 6) in a way that regulates the contacts with the underlying DNA [185].
More recently, it has become evident that acethylation, phosphorylation, and newly discovered modifications (e.g. ubiquitination and sumoylation) also occur at the level of other chromatin associated proteins, transcription factors, transcriptional coactivators and corepressors, thus modulating their function, and ultimately regulating gene transcription (fig. 6).

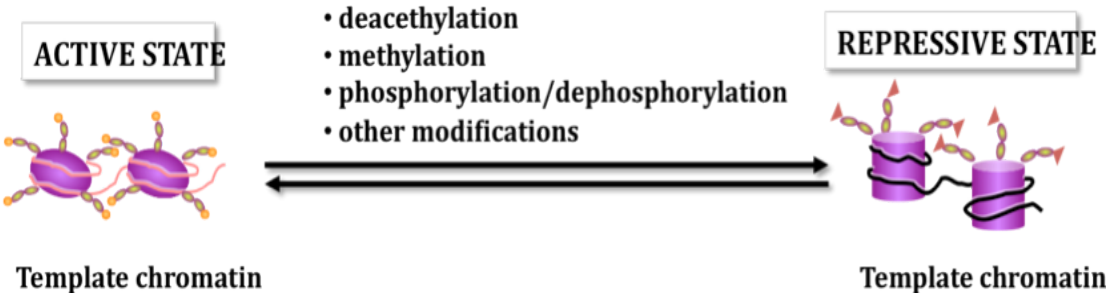

Figure 6. Dynamics of DNA packaging. Post translational modifications of histone and non-histone proteins impose changes in the nucleosomal organization and represent the dynamic switch between transcriptional "on-off" states of chromatin (M_Tablecaption).

The Histone Code

The term "histone code" was proposed in 2001 by Jenuwein and Allis [186] to define a marking system consisting of amino-terminal modifications of histone proteins. These modifications are then read by effector molecules, for example coactivators and corepressors of gene transcription, and translated into biological functions, including chromatin transcription. It has been suggested that these chromatin marks might function in a combinatorial manner, thus increasing their indexing potential or capacity. Altogether, this marking system considerably extends the information potential of the genetic code, and represents an important level of regulation in response to endogenous and exogenous stimuli.

Chromatin Remodeling Enzymes

As mentioned above, histones and chromatin-associated proteins are the targets of multiple post-translational modifications and several enzymes act on chromatin by introducing different post-translational modifications at specific amino acids. These modifications include methylation of arginine (R) residues; methylation, acetylation, ubiquitination, ADP-ribosylation, and sumoylation of lysines (K); and phosphorylation of serines and threonines [187]. A list of the human enzymes involved in the modification of chromatin is reported in table 1.
A single histone protein presents several residues that can undergo post-tranlational modification giving rise to a variety of modified products. An example of this complexity is given by the peptide mass fingerprinting of core histones by mass spectrometric analysis that is able to detect methylation, acetylation, phosphorylation and ubiquitination. This analysis revealed the presence of 13 modification sites in histone H2A, 12 modification sites in histone H2B, 21 modification sites in histone H3, and 14 modification sites in histone H4 [188]. Each site can either be unmodified or modified. In addition, some lysine residue can either be methylated or acetylated and there are three different possibilities for each methylated site (mono, di or tri). Therefore, histone proteins may undergo an extremely large number of possible combinations of modifications.
The post-translational modification state of chromatin is the result of the balanced activity of several enzymes. For instance, the acetylation state of histones is the result of the activity of acetyltransferases and deacetylases.
From the functional point of view, acetylation of histone 3 and histone 4 (H3 and H4) are associated with active transcription and commonly referred as euchromatin modifications. This is most likely due to the fact that acetylation loosens inter- or intra-nucleosomal DNA-histone interactions and, at the same time, affects recognition and protein-protein interactions. On the other side, evidences suggest that methylation of H3 lysine 9 (H3-K9) is a mark for transcriptionally silent chromatin [189]. This modification can be catalyzed by specific enzymes among which histone methyl transferase G9a, which is localized exclusively in euchromatic regions [190].

Type of modification	Class of enzymes	Enzymes	Substrates
acetylation	acetyltransferase	HAT1	H4 (K5, K12)
		GCN5, PCAF	H3 (K9, K14, K18)
		CBP, P300	H3 (K14, K18), H4 (K5, K8), H2AK5, H2B (K12, K15)
		TIP60/PLIP	H4 (K5, K8, K12, K16), H3K14
		HBO1	H4 (K5, K8, K12)
	deacetylases	SirT2-3	H4K16
Lysine methylation	Lysine methyl transferases	SUV39H1-2; G9a:EuHMTase/GLP; ESET/SETDB1: CLL8	H3K9
		MLL1-5; SET1A-B; ASH1	H3K4
		SET2; NSD1; SYMD2	H3K36
		DOT1	H3K79
		Pr-SET7/8	H4K20
	Lysine demethylases	LSD1/BHC110	H3 (K4, K9)
		JHDM1a-b	H3K36
		JHDM2a-b	H3K9
		JMJD2A/JHDM3A, JMJD2B-C	H3 (K9,K36)
		JMJD2D	H3K9
		JARID1A-D	H3K4
		UTX; JMJD3	H3K27
Arginine methylation	Arginine methyl transferases	CARM1	H3 (R2, R17, R26)
		PRMT4	H4R3
		PRMT5	H3R8, H4R3
Phosphorylation	Serine/threonine kinases	Haspin	H3T3
		MSK1-2	H3S28
		CKII	H4S1
		Mst1	H2BS14
		Rsk2	H3S10
Ubiquitination	E3 ligases	Bmi/Ring1a	H2AK119
		RNF20/RNF40	H2BK120

Table 1. Histone-modifying enzymes. Human enzymes and the corresponding substrates (histone protein and amino acid residue) are listed. (M_Tablecaption).

Histone deacetylases

Addition of acetyl groups is one of the most widespread modifications of histones. Acetylation at ε-amino groups of lysine residues at histone tails neutralizes their positive charges, thereby relaxing chromatin structure. Furthermore, acetylated histones also serve as binding sites for bromodomain proteins, often acting as transcriptional coactivators. As shown in table 1, histone acetylation occurs at multiple lysine residues; it is usually carried out by a variety of histone acetyltransferase complexes (HATs) and is reversed through the action of histone deacetylases (HDACs) [186,191].

HDACs do not bind DNA directly, in contrast, through the interaction with transcriptional activators and coactivators, are recruited at target genes and are assembled in large multiprotein transcriptional complexes. Thus, the specific contribution of HDACs to the regulation of gene transcription depends on the cell type and on the availability of interacting proteins.

HDACs represent a large superfamily of proteins whose members are grouped in different classes (Table 2) [192]. Class I HDACs are ubiquitously expressed and found predominantly in the nuclear compartment. They bear a conserved deacetylase domain and are active on histone substrates. The catalytic domain consists of a narrow, tube-like pocket, at the bottom of which a zinc cation is positioned. In cooperation with two His-Asp charge relay systems, the zinc cation facilitates the deacetylation reaction.

Class IIa HDACs carry a large N-terminal with conserved binding sites for the transcription factor myocyte enhancer factor 2 (MEF2) and the chaperone protein 14-3-3. First of all, upon phosphorylation by means of different kinases, the calcium/calmodulin-dependent protein kinase and protein kinase D, class IIa HDACs bind 14-3-3 and translocate from the cytoplasm to the nucleus [193-196]. When interacting with class IIa HDACs, MEF2 acts as transcriptional repressor; in contrast, its dissociation from HDACs promotes the recruitment of the histone acetyltransferase p300 and the conversion of MEF in a transcriptional activator [197-201]. Class IIa HDACs possess only minimal histone deacetylase activity, a behavior that can be explained with the fact that a key tyrosine residue in the catalytic domain is substituted with a histidine in class IIa HDACs [202]. It should be emphasized that the deacetylase activity associated to cell-derived class IIa HDACs is due to the copurification of class I HDACs [203]. At this regard it was shown that HDAC4 (class IIa) recruits preexisting enzimatically active complexes containing HDAC3 (class I) and nuclear co-repressors (NCo-R and SMRT), and that these protein-protein interactions are crucial in the transcriptional repression mechanisms involving histone deacetylation [203]. These evidences suggest that class II HDACs behave as bridging molecules with little enzymatic activity, however at present it cannot be excluded that these enzymes act on other still unknown substrates.

The most characterized member of class IIb HDACs is HDAC6, a cytoplasmic protein that acts on non-histone substrates such as cytoskeletal proteinsebbene and transmembrane proteins [192].

Finally, HDAC11 is the only member of class IV whose functions are still elusive [192].

Class	Protein domains	Members
Class I	Deacetylase catalytic domain Phosphorylation sites (serine residues) at C terminus	HDAC1 HDAC2 HDAC3 HDAC8
Class IIa	Deacetylase catalytic domain Phosphorylation sites (serine residues) at N terminus Myocyte enhancer factor binding sites Binding sites for 14-3-3 chaperone protein	HDAC4 HDAC5 HDAC7 HDAC9
Class IIb	Deacetylase catalytic domain Zinc finger domain or Leucine rich region	HDAC6 HDAC10
Class IV	Deacetylase catalytic domain	HDAC11

Table 2. The mammalian histone deacetylase superfamily. The list does not incluce class III HDACs, a term sometimes used to indicate sirtuins, a distinct group of deacetylases. (M_Tablecaption).

Histone Deacetylase Inhibitors

From the structural point of view, synthetic HDAC inhibitors can be classified in four groups: short-chain fatty acids, hydroxamic acids, benzamide derivatives, and cyclic peptides. We will briefly highlight the main features of each class addressing interested readers to specific reviews on the topic[204].

Short-chain fatty acids such as sodium butyrate, sodium phenylacetate, phenylbutyrate and valproate, are active at millimolar concentrations and can be defined pan-inhibitors although they seem to be less active against class IIb HDACs. The mechanism by which this class of compounds inhibits HDACs has not been fully elucidated.

The first compound bearing a hydroxamic acid moiety to be described as HDAC inhibitor was trichostatin A (TSA), which is produced by Streptomyces hygroscopicus and displays antifungal activities. However, the prototype compound of this class is suberoylanilide hydroxamic acid (SAHA) that was approved by the US FDA in 2006 for cutaneous manifestations of cutaneous T-cell lymphoma. Hydroxamic acids are usually active in the nanomolar range and inhibit HDACs by complexing the zinc cation present in the catalytic pocket of the enzyme with the hydroxamate group.

The cyclic peptide romidepsin (formerly known as FK-228) is produced by Chromobacterium violaceum and shows higher inhibitory activity toward class I HDACs, with IC50 in the nanomolar range. In the cellular reducing environment, this compound is converted into its reduced form that can interact with the enzyme active site. This molecule was very recently approved by US FDA for patients with cutaneous T-cell lymphoma.

Finally, MS-275 is the lead compound of the benzamide derivatives series. This compound is highly active against class I HDACs and almost completely inactive toward class II enzymes.

In addition, several natural compounds have been added to the list of HDAC inhibitors in the last years. The beneficial effects of dietary

isothiocyanates and allyl sulfides on human health, and in particular their cancer chemopreventive effects, have been known for a long time[205] however, only recently their positive actions have been linked with epigenetic mechanism.

A major understanding of HDAC active site structure and of the molecular features required to inhibit HDAC catalytic activity, in particular the presence of a spacer "arm" that allows the entry into the catalytic pocket and of a functional group interacting with the zinc cation, led to the reconsideration of the biological activity of several natural compounds.

Sulforaphane (SFN) is one of the most characterized isothiocyanates found in vegetables. It derives from the glucosinolate glucoraphanin present in cruciferous vegetables, such as broccoli and broccoli sprouts. Like other isothiocyanates, it is metabolized via the mercapturic acid pathway to active metabolites, among which SFN-cysteine displays a good fit for HDAC active site according to computer modeling predictions[206]. Indeed, the effects of SFN in vitro and in vivo systems are associated with increased global histone acetylation[207-209].

Allyl compounds are garlic components comprising diallyl disulfide and S-allyl mercaptocysteine, which are both converted into the active metabolite allyl mercaptane. Docking simulation revealed a good fit between allyl mercaptane and HDAC active site, consistent with accumulation of acetylated histones and growth arrest in cancer cells treated with the active metabolite at micromolar concentrations[210].

Finally, sodium butyrate that we mentioned before as a synthetic HDAC inhibitor, should also be included in the list of naturally occurring inhibitors since it is generated during the fermentation of dietary fibers in the large intestine[211].

Effects of Histone Deacetylase Inhibitors on Energy Metabolism

A recent study provided further evidence supporting the involvement of HDACs in energy expenditure. In fact, Gao et al. reported that sodium butyrate, a dietary component found in cheese and butter and also produced in the large intestine after fermentation of dietary fibers, improves metabolic dysfunction in mice fed a high-fat diet[212]. In particular, supplementation with sodium butyrate prevents diet-induced obesity, increase energy expenditure, and improves insulin sensitivity. These metabolic changes reflect beneficial effects of sodium butyrate on brown adipose tissue and skeletal muscle since treated mice show increased adaptive thermogenesis, and a higher number of oxidative fibers, coupled with enhanced fatty acid oxidation and mitochondrial function, in skeletal muscles.

Beyond Histones

As briefly mentioned above, histones are not the only proteins whose biological activities are modulated by the acetylation state at lysine residues[213]. In particular, acetyltransferases themselves such as the transcriptional coactivators p300 and CBP are heavily acetylated. Acetylation at lysine residues occurs also at the level of other transcription factors and cofactors such as the tumor suppressor p53; nuclear factor κB; members of the O group of the forkhead-box transcription factors; nuclear hormone receptors including androgen, progesterone, estrogen, and liver X receptors; PGC-1α, and receptor interacting protein 140.
In addition, also cytoplasmic proteins present acetylation sites. This is the case for example of metabolic enzymes (acetyl-CoA synthase, glutamate dehydrogenase), of α-tubulin, and heat shock protein 90.

Sirtuins, Transcriptional Coactivators, and Mitochondria

Sirtuins were initially discovered as silencing factors and longevity-linked proteins in lower organisms. The discovery that they act as NAD+-dependent histone deacetylases[214] represented a significant breakthrough that allowed to appreciate the multiple roles played by these enzymes in patho-physiology. Besides histones, sirtuins act on a variety of acetylated substrates with different functions. SIRT1 deacetylates transcription factors and coactivators such as p53, nuclear factor κB, proteins belonging to the forkhead box type O (FOXO) family, PPARγ, PGC-1α; but it also acts on enzymes such as acetyl-CoA synthases, or on structural proteins such as α-tubulin[215].
In mammals, sirtuins regulate a variety of functions, from the control of cellular stress to energy metabolism[216]. The first indication that sirtuins, in particular SIRT1, is involved in the metabolic control in mammals came from the elegant studies of P. Puigserver and coworkers who were investigating the molecular mechanisms responsible for the adaptive metabolic response to fasting. Reduced availability of nutrients, such as that experienced in fasting and calorie restriction, is reflected at the cellular level by a decrease of oxidative pathways and, consequently, by

an increase of NAD+/NADH ratio. Rodgers et al. found that in the fasted state SIRT1 is induced in the liver and deacetylates PGC-1α at specific lysine residues in an NAD+-dependent manner[217]. Deacetylated PGC-1α more actively transactivates the transcription of target genes, particularly those involved in gluconeogenesis[217]. In line with these observations, the knock-down of SIRT1 in the liver leads to reduced glucose production and fatty acid oxidation in the liver, under the fasting condition[218]. These metabolic changes are linked to decreased expression of genes responsible for gluconeogenesis and fatty acid oxidation[218]. These studies clearly demonstrate that SIRT1 is a key regulator of metabolic adaptation to nutrient deprivation and that PGC-1α mediates most of SIRT1 effects.

Effects of SIRT Activators on Energy Metabolism

In 2003 Howitz et al. reported for the first time that small molecules such as the natural polyphenol resveratrol, can extend the lifespan of S. cerevisiae in a Sir2-dependent manner[219].
Subsequent studies in animal models of insulin resistance and high-calorie diet showed that resveratrol administration ameliorates the metabolic derangements observed in these mice[119,220]. In particular, resveratrol attenuates adipogenesis and fat storage in white adipose tissue and, at the same time, improves mitochondrial activity and thermogenesis of brown adipose tissue. Resveratrol also affects insulin and glucose homeostasis since it increases insulin secretion from the pancreas and improves insulin sensitivity in the skeletal muscle, accompanied by enhanced mitochondrial activity and fatty acid oxidation. These metabolic effects are associated to activation of AMP-activated kinase and PGC-1α. In particular, this latter effect is due to SIRT1-dependent deacetylation[119]. Indeed, all these factors are strictly and coordinately linked. In fact, AMP-kinase, a sensor of the cellular energy status that is activated by a rise of AMP/ATP ratio, increases SIRT1 activity by increasing NAD+ cellular levels and consequently causing deacetylation of PGC-1α and FOXO transcription factors[221].
Although the animal studies discussed above clearly indicated that the effects of resveratrol are SIRT1-dependent, the observation that this polyphenol also activates AMP-kinase, makes difficult to establish which is the primary target of resveratrol. In fact, resveratrol increases SIRT1 deacetylating activity toward synthetic substrates containing a fluorescent moiety but appears to have no direct effect on physiological substrates[222,223].

AIM OF THE STUDY

Type 2 diabetes mellitus (T2DM) is the most common metabolic disease in the world. The westernization of the diet and sedentary lifestyle are the most responsible factors that drive to insulin resistance and T2DM. Maintenance of glucose homeostasis depends on a complex interplay between the insulin responsiveness of skeletal muscle, liver, adipose tissue and glucose-stimulated insulin secretion by pancreatic beta cells. Defects in these organs are responsible for insulin resistance and progression to hyperglycemia.

Understanding the integrated pathophysiology initiating the development of insulin resistance should extend our capacity to identify novel therapeutic targets for the prevention and/or treatment of T2DM. This biology remains incompletely characterized, in part, due to the interaction of multiple organ systems and numerous intracellular perturbations within these organs (including disrupted signaling and metabolic alterations) governing the development of insulin resistance. The complexity of this biology is further underscored by the progressive changes in the systemic milieu including the onset of hyperinsulinemia, elevated circulating free fatty acids and triglycerides, hyperglycemia, and the activation of systemic immune system during the development of T2DM.

Skeletal muscle is integral to the development of insulin resistance and is a major reservoir for postprandial glucose storage. In skeletal muscle, loss of mitochondrial function is evident in some insulin-resistant subjects years before they develop diabetes. Mitochondria are particularly important for skeletal muscle function, given the high oxidative demands imposed on this tissue by intermittent contraction, in fact they ensure adequate levels of ATP needed for contraction by the muscle sarcomere. Moreover, muscle cells must maintain metabolic flexibility, defined as the ability to rapidly modulate substrate oxidation as a function of hormonal and energetic conditions.

The molecular mechanisms that control mitochondrial number and function remain poorly understood, and only a few transcription factors or coactivators (e.g., PGC-1α, NRF1, Tfam) have been associated with this process. Notably, skeletal muscle differentiation and remodelling are also controlled at the epigenetic level, via transcriptional modulation of key genes in mitochondrial biogenesis and oxidative metabolism, involving enzymes, such as members of the histone deacetylase (HDAC) family, in particular those belonging to class I and class II, which modulate post-translational modifications on target proteins. The current knowledge on HDACs is that they function in general as transcriptional repressors, however their role *in vivo* is likely more complex. Sirtuins (SIRT), members of class III HDACs, represent an example of this complexity

since they may act either as activators of gene transcription by increasing the PGC-1α coactivating activity, or as transcriptional repressors by targeting p53. A number of recent studies have demonstrated that direct or indirect sirtuin activators promote mitochondrial function in vivo ameliorating the metabolic profile in animal models of insulin resistance/diabetes[119,215,221].

Less is known on the effects of HDACs modulators on energy metabolism, however a recent study reported that supplementation with sodium butyrate, a dietary component active as HDAC inhibitor, promotes energy expenditure and mitochondrial function in mice fed with a high fat diet[212].

Given the importance of skeletal muscle metabolism in insulin resistance/diabetes, and given the role of HDACs in skeletal muscle biology, it is reasonable to speculate that modulation of these enzymes would play a role in this pathology that deserves to be investigated more deeply.

Based on the evidences that mitochondrial dysfunction is often associated to whole body metabolic dysregulation, aim of this study is to better understand the role of histone deacetylases in the regulation of mitochondrial biogenesis and in the modulation of all these mechanisms underlying the pathophisiology of insulin resistance.

To this end we treated a cellular model of skeletal muscle (C2C12 cell line) with pan- and class selective HDAC inhibitors (HDACi), in particular with SAHA (pan-inhibitor), MS275 (Class I HDAC inhibitor) and MC1568 (Class II HDAC inhibitor), to evaluate the effects of these compounds on mitochondrial density, activity and on the whole transcriptome.

Moreover, the *in vivo* study has been performed in a genetic model of insulin resistance (*Db/Db* mice) to characterize the effects of the biochemical inhibition of HDACs in the main tissues involved in the homeostasis of energy metabolism, such as skeletal muscle, white and brown adipose tissues and liver.

MATERIALS AND METHODS

Reagents and Plasmids

Valproic Acid (VPA) and Trichostatin A (TSA) were from Sigma Aldrich (Milano, Italy), Suberoyl anilide hydroxamic acid (SAHA) were from Cayman Chemical (Ann Arbor, MI). MS275, MC1568 were sinthetized by the laboratory of Prof. Antonello Mai (Roma, Italy). 8Br-cAMP and KT5720 were from Sgma Aldrich (Milano, Italy).
MitoTracker Green FM and MitoTracker Red CM-H_2XRos were from Molecular Probes, Invitrogen (Carlsbad, CA), Hoechst 33258 were from Sigma Aldrich (Milano, Italy). The primary antibody anti Acetyl-H3, anti CREB, anti Phospho-CREB, the secondary antibody anti rabbit IgG were from Cell Signaling Technology (Danvers, MA). The primary antibody anti Acetyl Tubulin, anti alpha tubulin, anti beta actin and the secondary antibody anti mouse IgG were from Sigma Aldrich (Milano, Italy).
The plasmid pTKmTFALuc was provided by Dr. Enrique Saez (The Scripps Research Institute, La Jolla, CA).
The plasmids PGC-1 alpha promoter 2kb luciferase (Addgene plasmid 8887) and PGC-1 alpha promoter luciferase delta CRE (Addgene plasmid 8888) were from Addgene (Cambridge, MA).
The plasmid pCDNA3HDAC1 was provided by Dr. Eric Olson (University of Texas Southwestern Medical Center, Dallas, TX).

Cell cultures and transfections

C2C12 myoblast

C2C12 myoblast are a subclone (produced by H. Blau, et al) of the mouse myoblast cell line established by D. Yaffe and O. Saxel.
The C2C12 cell line differentiates rapidly, forming contractile myotubes and producing characteristic muscle proteins. Treatment with bone morphogenic protein 2 (BMP-2) cause a shift in the differentiation pathway from myoblastic to osteoblastic.
Manteinance medium: Dulbecco's Modified Eagle's Medium. To make the complete growth medium, add fetal bovine serum to a final concentration of 10%, L-Glutamine and Pen/Strep.
Differentiation medium: Dulbecco's Modified Eagle's Medium. To make the complete growth medium, add horse serum to a final concentration of 2%, L-Glutamine and Pen/Strep.
Temperature: 37.0°C
Subculturing protocol:
Cultures must not be allowed to become confluent as this will deplete the

myoblastic population in the culture.

1. Remove and discard culture medium.
2. Briefly rinse the cell layer with 0.25% (w/v) Trypsin- 0.53 mM EDTA solution to remove all traces of serum which contains trypsin inhibitor.
3. Add 3.0 ml of Trypsin-EDTA solution to flask and observe cells under an inverted microscope until cell layer is dispersed (usually within 5-7 minutes).

Note: To avoid clumping do not agitate the cells by hitting or shaking the flask while waiting for the cells to detach. Cells that are difficult to detach may be placed at 37°C to facilitate dispersal.

4. Add 7.0 ml of complete growth medium and aspirate cells by gently pipetting.
5. Add appropriate aliquots of the cell suspension to new culture vessels.

Inoculate at a cell concentration between 1.5 X 10 exp5 and 1.0 X 10 exp6 viable cells/75 cm2.

6. Incubate cultures at 37°C.

Medium Renewal: Every two days.

Differentiation protocol:

Plate cells at the final concentration of 70000 cells/ml in 24-, 12- or 6-well plates. Two days after plating, cells become confluent. Switch the medium with the differentiation medium and renew it every two days for 4 days.
At the fifth day cells are completely differentiated.

Transfection protocol:

Prepare the mix DNA/Lipofectamine 2000 ratio 1:2.5 (200ng of total DNA per well) in DMEM medium without serum and antibiotics. Mix formation time: 30 min.
Meantime split the cells and use 8000 cells/ well.
Prepare a mix with culture media, the cells and add to this mix the DNA/Lipofectamine2000 mix (usually the DNA/cells mix is 1/10 of the total volume of the mix with cells). Incubate cells with the DNA/Lipofectamine mix up to 45 min. Plate the cells with DNA mix and after an overnight remove the medium a treat the cells.
C2C12 cells were treated with VPA 5mM, TSA 50nM, SAHA 5μM, MS275 5μM, MC1568 5μM, 8Br-cAMP 1mM or KT5720for different times.
Cells were lysed using britelite™ plus (Perkin Elmer, Monza, Italy) and RLU were detected with EnVision (Perkin Elmer Waltham, MA).

Generation of clones stably transfected:
Cells were transfected as above descripted. The following day, media were replaced with media containing G418 in order to select cells that have stably incorporated the plasmid into their genomic DNA. The media were renew every two days for 15 days increasing G418 concentration to avoid the generation of resistant cells and splitting them when needed.

Real Time quantitative RT-PCR

Total RNA from C2C12 myotubes was double extracted with TRIzol Reagent® (Invitrogen) and purified with commercial kit (Macherey-Nagel, Milano, Italia) and quantitated with Nanodrop (Thermo Scientific, Wilmington, DE). Specific mRNA was amplified and quantitated by real time PCR, using Sybr Green kit (Bio-Rad, Milano, Italia) as previously described (De Fabiani et al., 2003) or iScript^{TM} One Step RT-PCR for Probes (Bio-Rad, Milano, Italia), following the manufacturer's instructions. Primer sequences are available on request. Data were normalized to 18S rRNA or 36B4 mRNA and quantitated setting up a standard curve.
We monitored the specificity of the amplified products by melting curve analysis, when PCR was run with SybrGreen kit. Experiments were performed in triplicate and repeated at least twice with different cell preparations. Primers for real-time PCRs were designed with Primer Express software (Applied Biosystems, Monza-Milan, Italy) or IDT software avilable on line and optimized to work in a two-step protocol (40 cycles of amplifications each consisting of a denaturation step at 95° C for 15 s and an annealing/extension step at 60° C for 60 s) or one-step protocol (10 min at 50°C for reverse transcription, 40 cycles of amplifications each consisting of a denaturation step at 95° C for 10 s and an annealing/extension step at 60° C for 30 s). The oligonucleotides used for real-time PCR were synthesized by Primm (Milano, Italy) or Eurofin MWG Operon (Ebersberg, Germany).
For mitochondrial DNA cotent QPCR was performed on 12S mtDNA sequence and cyp7a1 promoter DNA sequence.

Immunocytochemistry

C2C12 cells were cultured in 4-well plate. After incubation with the compounds at the appropriate concentration, cells were stained with MitoTracker Green 200 nM and MitoTracker Red CM-H_2Xros 400 nM. Cells

were incubated for 30 minutes at 37°C. After incubation dyes were removed and cells were washed three times with PBS. After that, cells were incubated 30 seconds with Hoechst 33258 in order to mark the nuclei, washed three times with PBS and pictures were taken using a fluorescence microscope Axiovert 200 (Zeiss).

Mitochondrial density and activity

C2C12 cells were cultured in 96-well plate. After incubation with the compounds at the appropriate concentration, cells were stained with MitoTracker Green and MitoTracker Red CM-H_2Xros as described above. Cells were incubated for 30 minutes at 37°C. After incubation with Hoechst 33258, cells were washed three times with PBS and fluorescence intensity were measured using EnVision (Perkin Elmer, Waltham, MA).

Protein extraction and Western Blot analysis

C2C12 myotubes were lysed using SDS sample buffer (62.5 mM Tris- HCl pH 6.8, 2% w/v SDS, 10% glycerol, 50 mM DTT, 0.01% w/v bromophenol blue or phenol red).

A. Solutions and Reagents

Transfer Buffer: 25 mM Tris base, 0.2 M glycine, 20% methanol (pH 8.5).
10X Tris Buffered Saline (TBS): To prepare 1 liter of 10X TBS: 24.2 g Tris base, 80 g NaCl; adjust pH to 7.6 with HCl (use at 1X).
Blocking Buffer: 1X TBS, 0.1% Tween-20 with 5% w/v nonfat dry milk; for 150 ml, add 15 ml 10X TBS to 135 ml water, mix. Add 7.5 g nonfat dry milk and mix well. While stirring, add 0.15 ml Tween-20 (100%).
Wash Buffer: 1X TBS, 0.1% Tween-20 (TBS/T).
Primary Antibody Dilution Buffer: 1X TBS, 0.1% Tween-20 with 5% nonfat dry milk as indicated on primary antibody datasheet

B. Protein Blotting

Lyse cells by adding 1X SDS sample buffer (100 µl per well of 6-well plate). Immediately scrape the cells off the plate and transfer the extract to a microcentrifuge tube. Keep on ice.
Sonicate for 10–15 seconds for complete cell lysis and to shear DNA (to reduce sample viscosity).
Microcentrifuge for 5 minutes.
Load 20 µl onto SDS-PAGE gel (10 cm x 10 cm).
Electrotransfer to nitrocellulose membrane.

C. Membrane Blocking and Antibody Incubations

I. Membrane Blocking

Incubate membrane in 25 ml of blocking buffer for one hour at room temperature.

Wash three times for 5 minutes each with 15 ml of TBS/T.

II. Primary Antibody Incubation

Proceed to one of the following specific set of steps depending on the primary antibody used.

Incubate membrane and primary antibody (at the appropriate dilution as recommended in the product datasheet) in 10 ml primary antibody dilution buffer with gentle agitation overnight at 4°C.

Wash three times for 5 minutes each with 15 ml of TBS/T.

Incubate membrane with the species appropriate HRP-conjugated secondary antibody for 1h at room Temperature with gentle agitation.

Wash three times for 5 minutes each with 15 ml of TBS/T.

D. Detection of Proteins

Incubate membrane with appropriate volume of SuperSignal West Pico Chemiluminescent Substrate (Pierce Thermo Scientific) for 5 minutes.

Drain membrane of excess developing solution (do not let dry), wrap in plastic wrap and expose to x-ray film.

Antibody dilutions used for western blot:

1. Anti Acetyl Histon H3: 1:1000
2. Anti Acetyl Tubulin: 1:1000
3. Anti Tubulin: 1:1000
4. Anti beta-actin: 1:2000

5. Anti rabbit IgG: 1:5000
6. Anti mouse IgG: 1:5000

Microarray analysis

Microarray analysis were performed by Genopolis.Arrays and conditions used in the experiments are reported in Tables 1-6. Data handling was mainly done using Bioconductor 2.4. The Robust Multichip Average (RMA) method was employed to calculate probe set intensity. RMA is a robust multi-chip average expression method that estimates the probe-level data from a set of chips: the perfect-match (PM) values are background-corrected, normalized and finally summarized resulting in a set of expression measures. To filter out noisy data before the selection of

differentially expressed genes a filter is applied based on a Inter Quantile Range (IQR). The identification of differentially expressed genes was addressed using Linear Models for Mi- croarray Data (LIMMA). The identification of differentially expressed genes (DEGs) was addressed using linear modeling approach and empirical Bayes methods together with false discovery rate correction of the p-value (Benjamini-Hochberg).

Table 1

Title	C2C12 project
Date	January 11, 2010
Chip	mogene10sttranscriptcluster.db
Samples number	15
Condition number	5
Normalization Method	RMA
Prefiltering Method	IQR
Filtered Probesets	17168
Remaining Probesets	18344
DEG Selection Method	Limma
DEG Selection Threshold	0.001
Experimental Design	commonBaseline
Total DEG number	2355

Table 2

Title	Gastrocnemius
Date	April 14, 2010
Chip	mogene10sttranscriptcluster.db
Samples number	12
Condition number	3
Normalization Method	RMA
Prefiltering Method	IQR
Filtered Probesets	9380
Remaining Probesets	19435
DEG Selection Method	Limma
DEG Selection Threshold	0.01
Experimental Design	commonBaseline
Total DEG number	2778

Table 3

Title	Vastus Lateralis
Date	April 8, 2010
Chip	mogene10sttranscriptcluster.db
Samples number	12
Condition number	3
Normalization Method	RMA
Prefiltering Method	IQR
Filtered Probesets	10757
Remaining Probesets	18058
DEG Selection Method	Limma
DEG Selection Threshold	0.01
Experimental Design	commonBaseline
Total DEG number	2624

Table 4

Title	Liver
Date	April 15, 2010
Chip	mogene10sttranscriptcluster.db
Samples number	12
Condition number	3
Normalization Method	RMA
Prefiltering Method	IQR
Filtered Probesets	9096
Remaining Probesets	19719
DEG Selection Method	Limma
DEG Selection Threshold	0.05
Experimental Design	commonBaseline
Total DEG number	911

Table 5

Title	BAT
Date	July 19, 2010
Chip	mogene10sttranscriptcluster.db
Number of Samples	12
Number of Conditions	3
Normalization Method	RMA
Prefiltering Method	IQR
Filtered Probesets	9657

Remaining Probesets	19158
DEG Selection Method	Limma
DEG Selection Threshold	0.005
FoldChange Threshold	1
Experimental Design	commonBaseline
Total number of DEGs	1057

Table 6

Title	WAT
Date	July 22, 2010
Chip	mogene10sttranscriptcluster.db
Number of Samples	9
Number of Conditions	3
Normalization Method	RMA
Prefiltering Method	IQR
Filtered Probesets	1016
Remaining Probesets	27799
DEG Selection Method	Limma
DEG Selection Threshold	0.03
FoldChange Threshold	1
Experimental Design	commonBaseline
Total number of DEGs	1024

Table 1-6: conditions used for microarray analysis in C2C12 myotubes, gastrocnemius, vastus lateralis, liver, brown adipose tissue and white adipose tissue of *Db/Db* mice.

Animal Studies

C57BLKS/J-Lepr$^{db/db}$ mice were purchased from The Jackson Laboratory. Nine-week-old male *db/db* mice were randomized into four groups according to glucose levels and body weight and treated with intraperitoneal (i.p.) injection of SAHA (25mpk), MS275 (10mpk), MC1568 (6.5 mpk) or with vehicle (DMSO) every other day.
All the compounds were dissolved in DMSO and stored at +4°C. Prior to use, the solutions were warmed in a 42°C water bath with agitation. For blood analysis, *db/db* mice were fasted for 16 hr and blood was collected from the tail vein. Glucose levels were determined using an Accu-Chek Active glucometer (Roche). Triglyceride levels were determined by the

Plasma Triglyceride Kit (Sentinel). Free fatty acid levels were determined by the NEFA-HR kit (Wako). Insulin levels were determined using an AlphaLISA® Human Insulin Research Immunoassay Kit (Perkin Elmer). Cholesterol levels were determined using ABX Diagnostic Cholesterol kit (ABX Pentra). Cholesterol distribution in plasma lipoprotein fractions was determined by FPLC using a Superose 6 column (Amersham, Milano, Italia). One-ml fractions were collected and assayed for cholesterol using an enzymatic kit (ABX Pentra)and triglycerides (Sentinel). ALT and AST levels were determined using ALT or AST Reagent Set (Teco Diagnostic).
For glucose tolerance tests, mice were fasted for 16 hr, and glucose levels from tail-vein blood were determined before and 30, 60, 90, and 120 min after i.p. injection of glucose (2 g/kg). For insulin tolerance tests, random fed mice were injected i.p. with insulin (Humulin R, Eli Lilly) (2 U/kg). Glucose levels were determined before and 30, 60, 120, 180, and 210 min after injection. At the end of treatments, gastrocnemius, vastus lateralis, soleus, brown and white fat, liver and blood samples were collected from individual animals.
Animal studies were conducted strictly following regulations of European Community (EEC Directive n. 609/86) and local regulations for animal care (Italian Legislative Decree n. 116, 27/01/1992).

Indirect Calorimetry

Oxygen consumption, heat production, and activity were measured over 3 days using the Oxymax Lab Animal Monitoring System (Columbus Instruments). Mice (five 10-week-old *db/db* males per group) were individually housed and allowed to acclimate in the experimental cages with free access to food and water. Animals were maintained on a 12 hr light/dark cycle and were treated with vehicle or compounds for 15 days prior to the start of the experiment. During the experiment, mice were dosed as described above. Data was analyzed using the OxymaxWin v3.32 software package. Statistical comparisons of repeated measurements were made using ANOVA.

Histological Analysis

Muscle
8 µm thick sections from gastrocnemius muscle of treated mice, embedded in paraffin, were deparaffinized with xylene and rehydrated

through graded ethanol and stained using the following protocols:

SUCCINATE DEHYDROGENASE
1. Phosphate buffer (100mM, pH 7.6)
Solution A (1.36g KH_2PO_4 /100ml) 12ml
Solution B (1.42g Na_2HPO_4/100ml) 88ml
2. NBT Stock
Phosphate buffer as above 100ml
KCN 6.5mg
EDTA 185mg
Nitroblue tetrazolium (NBT) 100mg
3. Succinate stock (500 mM sodium succinate)
Sodium succinate 2.7g
Distilled water 20ml
Freeze in 5ml amounts
4. Incubation medium
NBT stock 2.0ml
Succinate stock 0.2ml
Phenazine methosulphate 0.7mg (one small crystal)
Mix just before use, keep out of strong light.

Incubation for 30 minutes at 37°C
Wash in distilled water, clear and mount.

GOMORI TRICHROME

Harris's Hematoxylin for 10 min
Wash for 10 min
Gomori Trichrome for 10 min
Wash in acetic acid 0,2 % twice
Dehydrate, clear and mount in Biomount.

PAS
Reagents:
Carnoy fixative
Periodic acid acqueous solution 0.5 %
Schiff reactive
Sodium metabisulfite 0.5 %

Protocol:

Put slices in Carnoy fixative at 4°C for 5 min
Rinse Carny fixative and incubate in periodic acid 0.5% for 10 min
Put slices in Schiff reactive, protect from light for 20 min
Wash in sodium metabisulfite 0.5 % for 10 min
Wash in distilled water rapidly
Counterstain in Mayer's hematoxylin for 5 min
Wash in water for 5 min
Dehydrate, clear and mount.

ESTERASE
Reagentis
Phosphate buffer 0.2 M pH 7.27
a-naphthyl acetate 1% in acetone
pararosaniline stock solution
Sodium notrite 4% in H_20

Solutions:
pararosaniline stock solution:

Pararosaniline	4 g
Distilled Water	80 ml
HCl	20 ml

Warm the solution gently shaking.
Cool, filter and store for 15 days at RT

Incubation solution:

Phosphate buffer 0.2 M pH 7.27	10 ml
a-naphthyl acetate 1%	10 drops
Pararosaniline stock solution	9 drops
Sodium nitrite 4 %	8 drops

Mix first pararosaniline and sodium nitrite, shake and add all the other reagents.

Protocol:
Incubation in Esterase solution at 37 °C for 1 hour
Wash in H_2O for 10 min.
Dehydrate starting from alcohol 90%
Clear and mount.

ALCALINE PHOSPHATASE:
Reagents:
Boric acid

Borax
Water
a-naphthyl phosphate
Fast blue RR
Magnesium sulfate 0,1 M

Solutions:

1.Borate buffer pH 8,8
Boric acid 0,2 M
Borax 0,05 M
2. Alcaline phosphatase solution pH a 8,6

Borate buffer pH 8,8	90 ml
a-naphtyl phosphate	150 mg
Fast blue RR	200 mg
Magnesium sulfate 0,1 M	10 ml

Protocol:

Incubation with Alcaline phosphatase solution at 37°C for 1 hour
Wash with water 3 times
Fix with formalin 10% for 10 min.
Wash with water for 5 min.
Mount in glycerine.

Immunohistochemistry

White adipose tissue was fixed with Carnoy solution/Clorophorm, dehydrated, and embedded in paraffin, and 8 µm thick sections were subjected to hematoxylin-and-eosin staining. For immunohistochemistry, slides containing 8 µm sections were deparaffinized with xylene and rehydrated through graded ethanol. Antigen retrieval was performed with NH_4Cl 0.05 M for 30 min at RT. Endogenous peroxidase activity was blocked with 1% hydrogen peroxide in PBS for 20 min. Blocking step was performed incubating the slices in 1% BSA in PBS-Triton 0.1% for 1 hour at RT. Purified rat anti-mouse Mac1 antibody (AbD Serotec, Oxford, UK) or rabbit anti-mouse UCP1 antibody (Abcam, Cambridge, MA) was applied at 1:300 concentration in BSA 1% PBS overnight at 4°C. Slices were subsequently incubated with anti-rat (Vector Laboratories, Burlingame,

CA)or anti-rabbit (Perkin Elmer, Waltham, MA) biotinylated secondary antibodies at 1:3000 concentration. Histochemical reactions were performed using diaminobenzidine (DAB), and the slices were counterstained with hematoxylin.

Cell size measurement

Images at 20X magnification of H&E stained sections of WAT and BAT were analysed using Photoshop CS3 software (Palo Alto, CA), converting pixel number in surface dimensions and adjusted for the magnification factor.

Statistical Analyses

Statistical analyses were performed with Student's *t* test or one-way ANOVA followed by Dunnett's Post Test when needed using GraphPad InStat version 5.0 for Macintosh (GraphPad, San Diego, California).
All the statisctical analysis are compared against control group, except where indicated.

RESULTS

HDAC inhibitors promote mitochondrial biogenesis in C2C12 myotubes.

Because histone deacetylases (HDACs) are involved in the development and in the physiology of skeletal muscle, we treated differentiated C2C12 with different HDAC inhibitors and we checked their effects on mitochondrial biogenesis.

First, we validated the specificity of each compound to inhibit all the classes of HDACs or a specific one of them. To this end, we treated C2C12 myotubes for 24 hours with SAHA, a pan-inhibitor of HDACs, and with two Class selective HDAC inhibitors: MS275 (Class I selective inhibitor) and the MC1568 (class II selective inhibitor) and we checked the acetylation status of two different targets of HDACs: the Histone H3 as Class I HDAC target and the α-tubulin as Class II HDAC target.

As expected, even using different concentration of the compound, the treatment with SAHA increases the acetylation status of both targets, while the Class I selective HDAC inhibitor MS275 increases the acetylation status only of the Histone H3. Vice versa, the Class II HDAC selective inhibitor MC1568 increases only the acetyl-α-tubulin levels (fig.1).

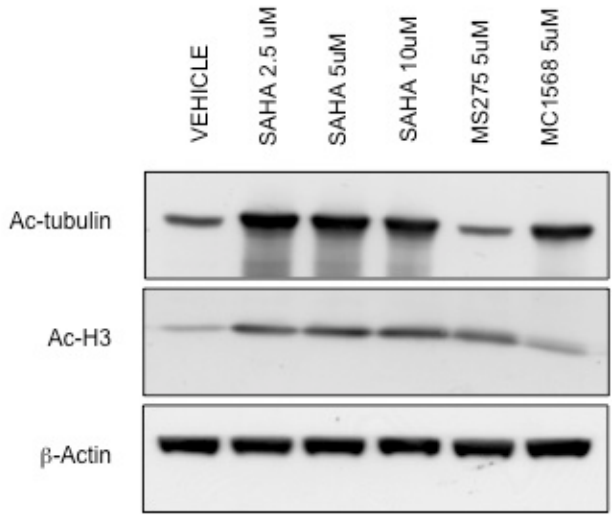

Figure 1: Acetylation levels of HDAC targets. Histone H3 is a target of Class I HDACs, while α-tubulin is the Class II HDAC target.

Once demonstrated the specificity of the different treatments on HDAC activity, using specific stainings for mitochondrial density and activity showed that only SAHA and MS275 treatments were able to increase both mitochondrial density and activity, while MC1568 was ineffective (fig. 2).

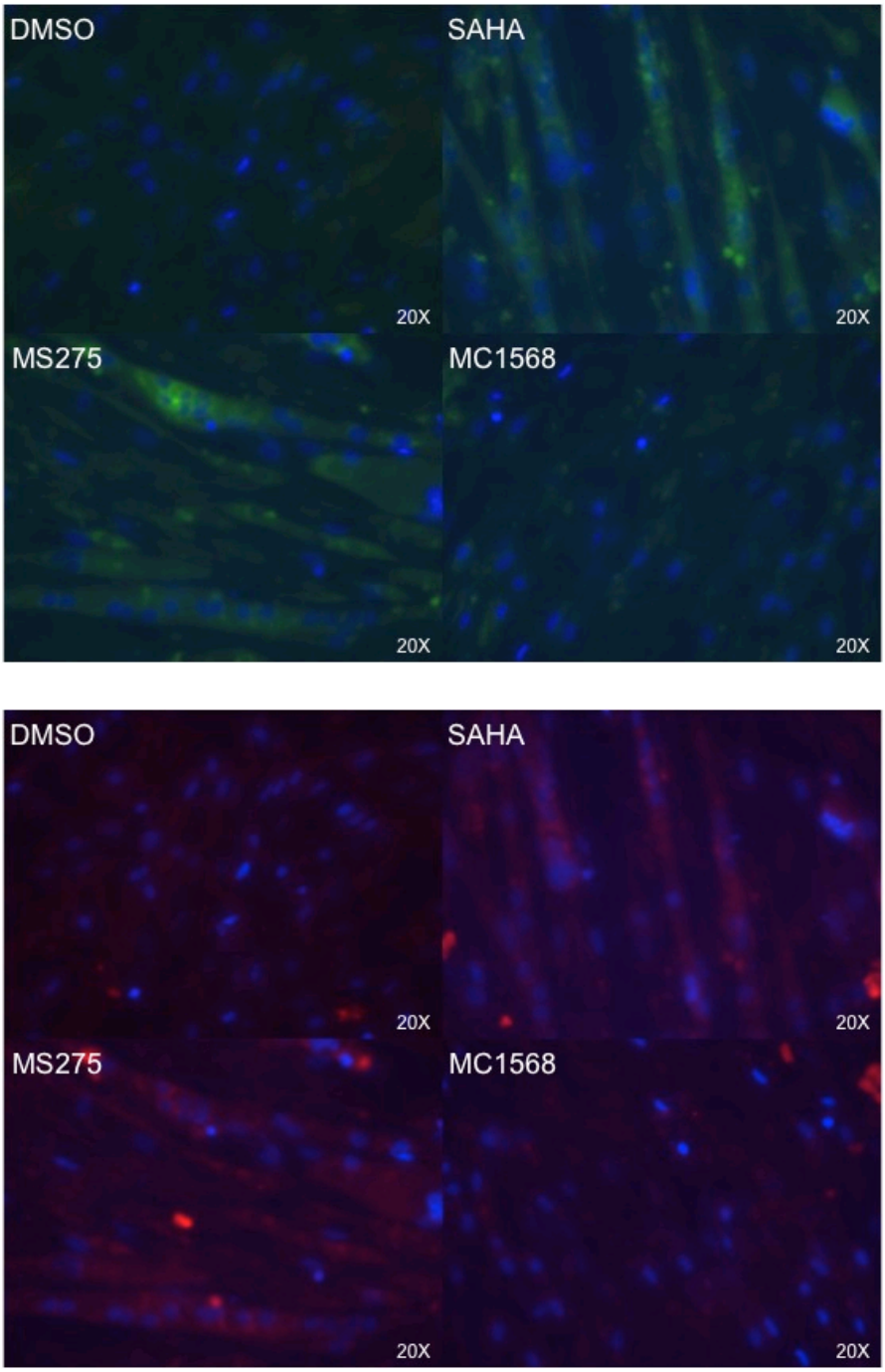

Figure 2: Fluorescence microscopy showing C2C12 myotube treated for 60 hours with vehicle, SAHA 5μM, MS275 5μM and MC1568 5μM. Cells have been labelled with MitoTracker Green 200 nM and MitoTracker Red CM-H_2XRos 400 nM.

In order to quantify the effects observed, we set up a method to measure fluorescence intensity in 96 well plates using Hoechst staining as relative paramenter to normalize the data.
As in the case of fluorescence microscopy, we observed a significant increase of mitochondrial density and activity after treatment with SAHA and MS275, while we do not observe any differences with MC1568 (fig.3).

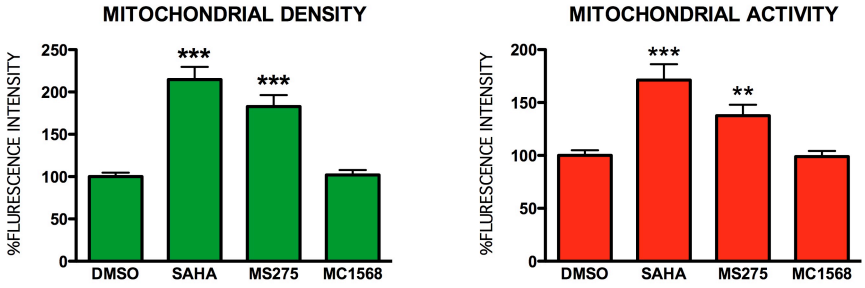

Figure 3: Fluorescence intensity quantifications of mitochondrial density and activity in C2C12 treated for 60 hours with with vehicle, SAHA 5μM, MS275 5μM and MC1568 5μM. Cells have been labelled with MitoTracker Green 200 nM and MitoTracker Red CM-H_2XRos 400 nM. (**p<0.01, ***p<0.001)

To definitely demonstrate that inhibition of Class I HDACs induces mitochondrial biogenesis, we measured mitochondrial DNA (mtDNA) content in C2C12 myotubes after HDACi treatments. Consistently with the previous results, we founded that SAHA and MS275 significantly increase mtDNA content (fig.4).

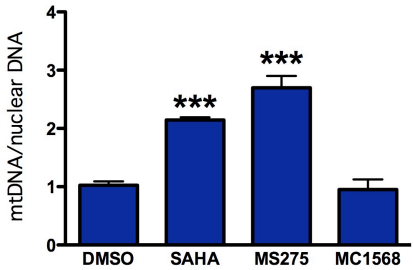

Figure 4: mitochondrial DNA content in C2C12 cells treated for 60 hours with vehicle, SAHA 5μM, MS275 5μM and MC1568 5μM. Real Time QPCR was performed using NADH Dehydrogenase 1 as mtDNA template, and Cyp7a1 promoter region as nuclear DNA. (***p<0.001)

Class I HDACs induce a transcriptional reprogramming towards a more oxidative phenotype in C2C12 myotubes.

In order to understand how class selective HDAC inhibitors affect oxidative metabolism, we performed a microarray analysis in differentiated C2C12 cells. The myotubes were exposed to the pan inhibitor SAHA, the Class I HDAC selective inhibitor MS275 and the Class II HDAC selective inhibitor MC1568.
The whole genome wide analyses revealed that SAHA regulates 1574 genes, MS275 1152 genes, and MC1568 only 155 genes (fig.5).

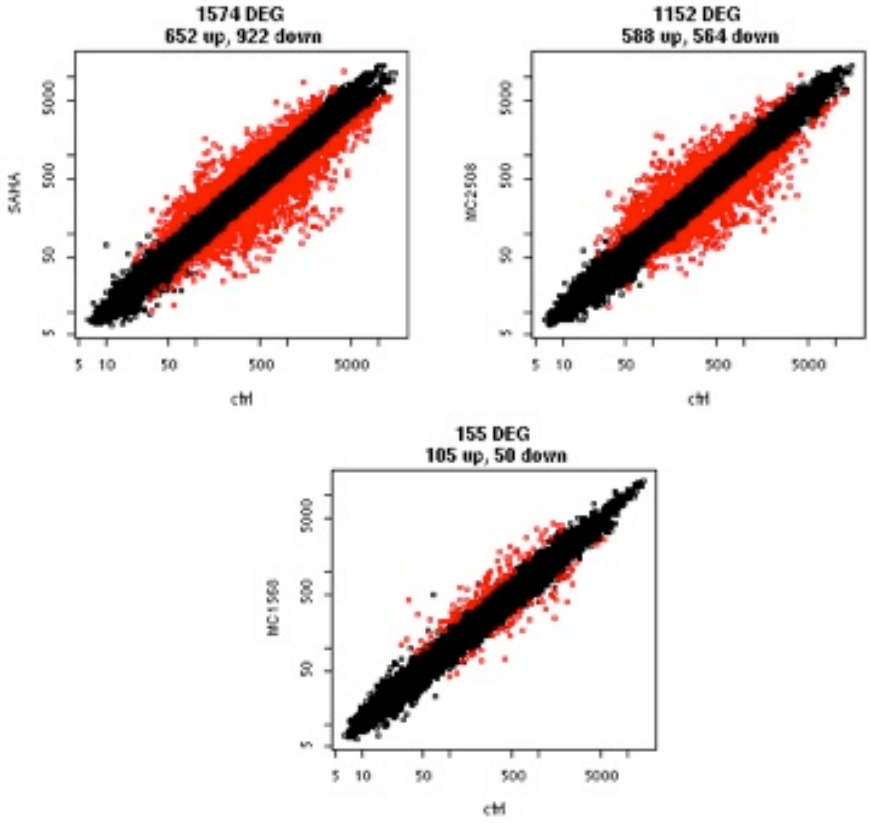

Figure 5: differentially expressed genes in C2C12 myotubes after treatment with SAHA, MS275 and MC1568.

Among all the pathways analyzed, we observed that SAHA and MS275 treatments significantly regulate more than 10% of the genes belonging to metabolic pathway. On the other hand, MC1568 affect only 7 metabolic genes. Interestingly, SAHA and MS275 shared 61 genes. About this subset, we defined different biological processes and we founded that

more than 50% of these genes belong to carbohydrate and lipid metabolism (fig. 6).

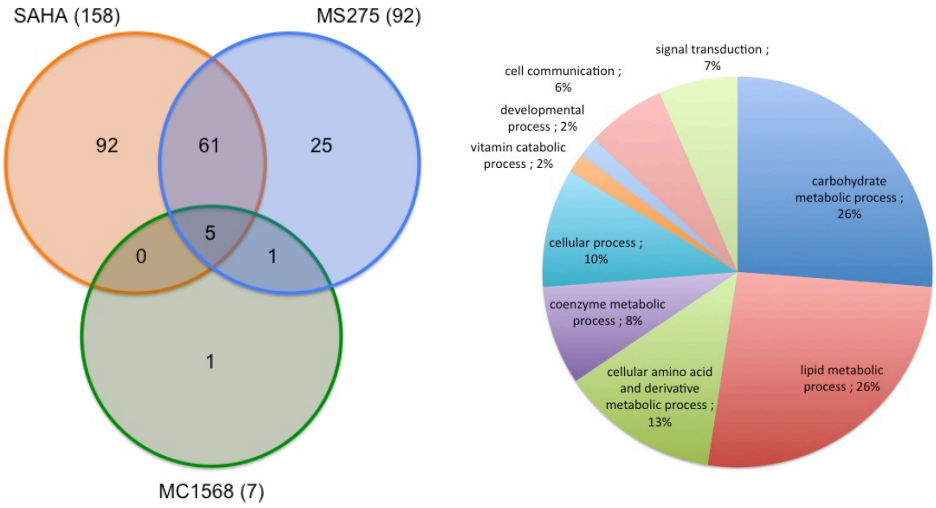

Figure 6: left. Venn Diagram of the differentially expressed genes belonging to the KKEGG pathway "Metabolic genes" of SAHA, MS275 and MC1568 groups.
Right. Cake presenting the biological processes of the 61 genes shared by SAHA and MS275.

We validated the microarray data by QPCR and we found that different transcription factors, such as PGC-1α, the master regulator of mitochondrial biogenesis, Tfam and Tfb1m, the two main transcription factors of mitochondrial DNA, were upregulated. In addition we founded that several OXPHOS genes (Cox7a1, Cox5a, Cox6a1 and ETFDH), but also different genes involved in glucose (Glut4, Glut1, Pdk4, Pkm2), lipid (Lcad and Hadh) and TCA cycle (Idh3α, Mdh2, Suclg1 and Bckdhb) were similarly regulated by SAHA and MS275 treatments, while MC1568 was ineffective (fig.7).

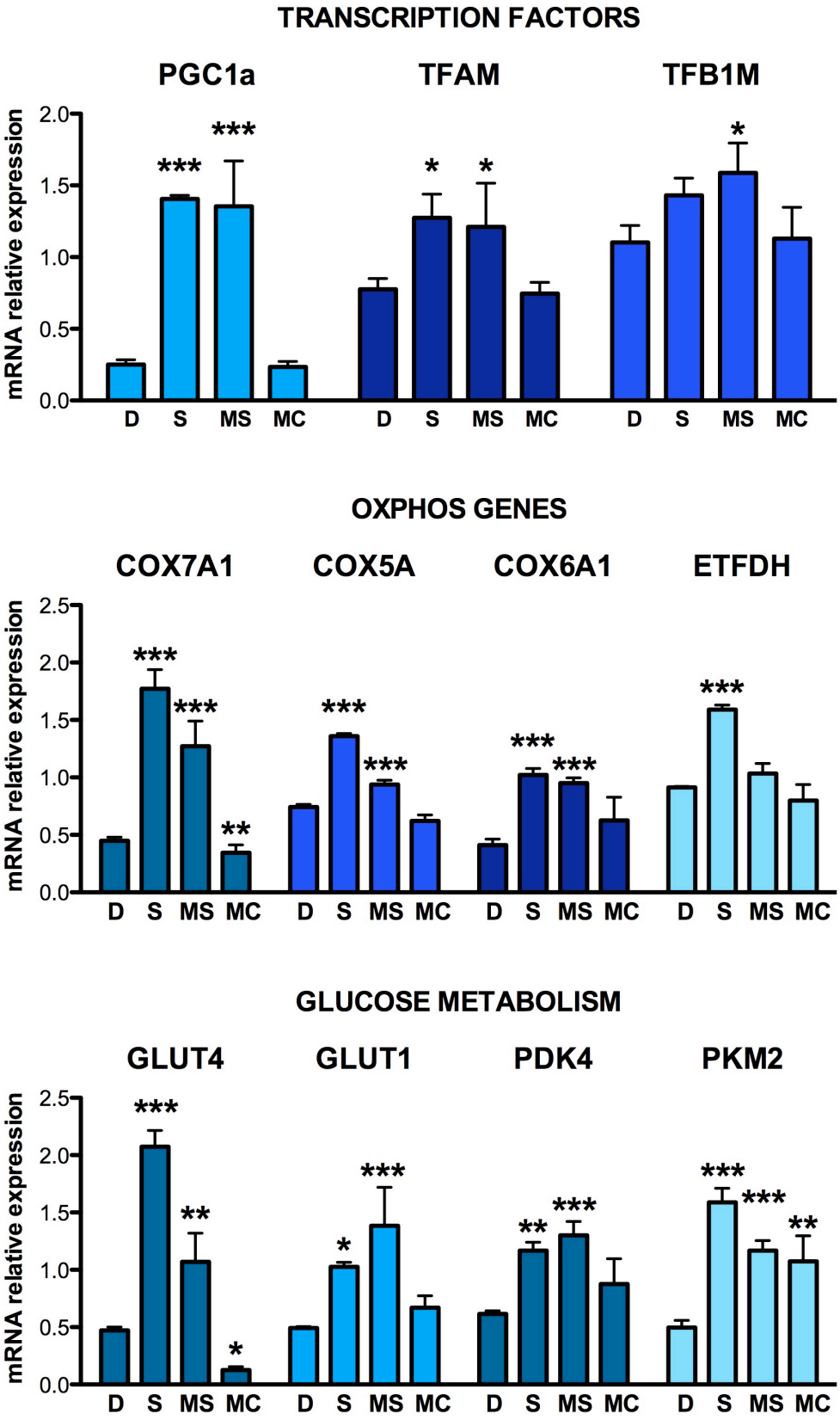
TRANSCRIPTION FACTORS
PGC1a
TFAM
TFB1M
mRNA relative expression
2.0
1.5
1.0
0.5
0.0
D S MS MC
OXPHOS GENES
COX7A1
COX5A
COX6A1
ETFDH
2.5
GLUCOSE METABOLISM
GLUT4
GLUT1
PDK4
PKM2

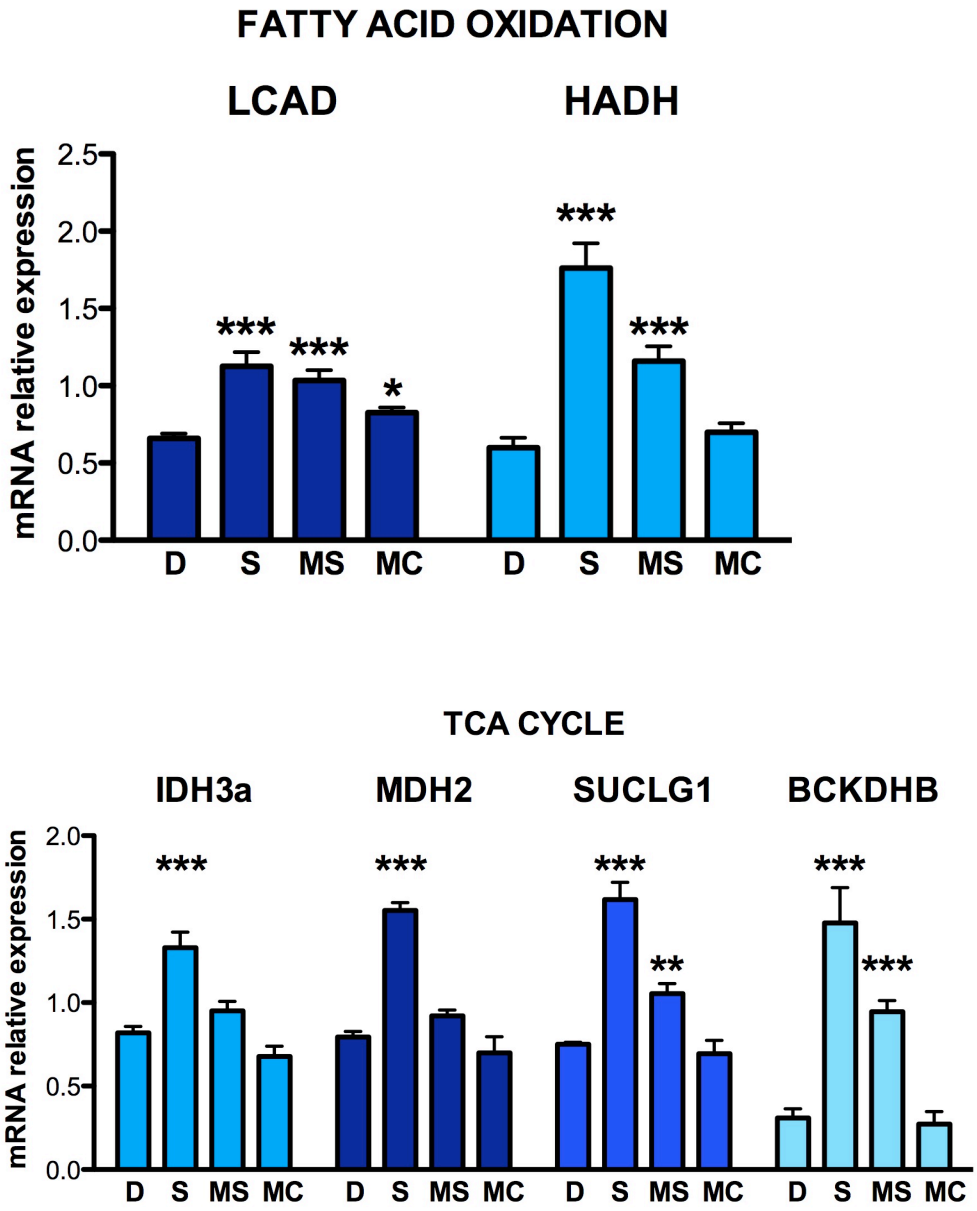

Figure 7: gene expression profile of transcription factors and coregulators, OXPHOS genes, glucose, lipid, TCA cycle in C2C12 myotubes after treatment with SAHA, MS275 or MC1568. Statistical comparison of these totals was made using ANOVA. *p<0.05, **p<0.01,***p<0.001.

Notably, most of the genes analyzed are related to mitchondrial function and activity, such as PGC-1a, Tfam, TFB1M, and others. In order to test if these compounds could affect mitchondrial function we generated stable C2C12 cell line expressing luciferase gene under the control of a PGC-1α responsive region of the Tfam promoter. As shown in figure 8, in stable

engineered C2C12 myotubes, SAHA and MS275 increased PGC-1α driven luciferase activity. As expected, MC1568 treatment did not increase luciferase activity indicating that it does not influence PGC-1α expression and consequently mitochondrial function (fig.8)

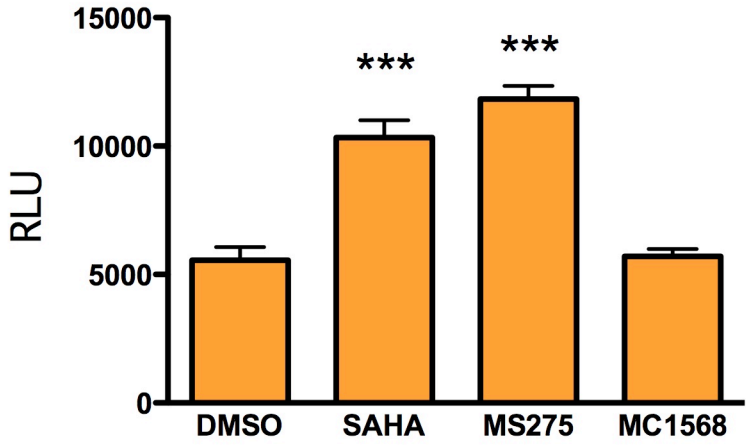

Figure 8: Stable C2C12 transcfected with TfampromLuc reporter plasmid and treated with HDACi for 24 hours. Statistical comparison of these totals was made using ANOVA. ***p<0.001.

Class I selective HDACi reduce glycemia, insulin levels and glucose clearence in *Db/Db* mice.

To substantiate our in vitro results, we further test the effects of HDACi in a genetic mouse model of metabolic disorder, such as the diabetic mice Db/Db. Mice were treated every other day with the indicated compounds for a total of 20 days. As reported in figure 9, mice receaving MS275 at the end of the experiment showed a significant reduction in body weight, while other treatment did not affect this paramenter, despite a comparable food consumption (fig. 9).

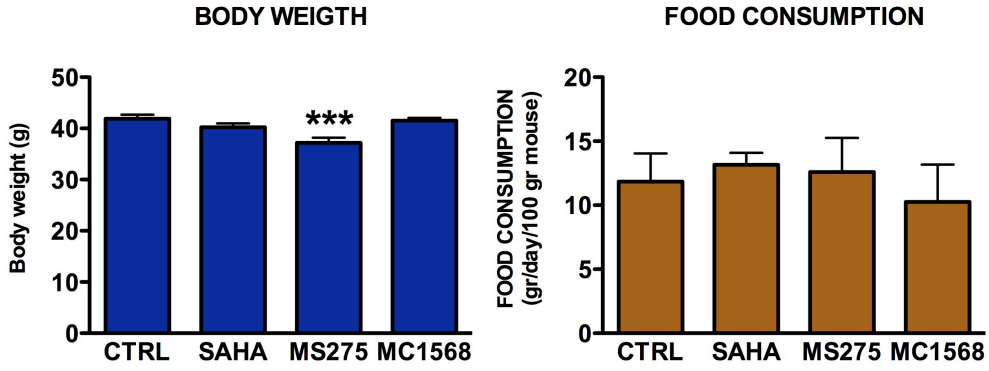

Figure 9: DbDb mice treated for 23 days with different HDACi. Left. Body weight measured in fasted mice before sacrifice. (N=10)
Right. Food consumption measurement was repeated 3 times for a period of 3 days every time for every cage. (N= 3 cages / treatment). Statistical comparison of these totals was made using ANOVA. ***p < 0.001.

Interestingly, we observed a dramatic reduction in fasted glycemia in animals treated with SAHA and MS275, but not with MC1568. In parallel with the reduced plasma glucose levels we observed a reduction in the insulin plasma levels and in the homeostatic model assessment (HOMA-IR) in the MS275 treated gruop. We detected similar effects in the HOMA-IR of the SAHA treated group, even if plasma insulin did not change significantly (fig.10).

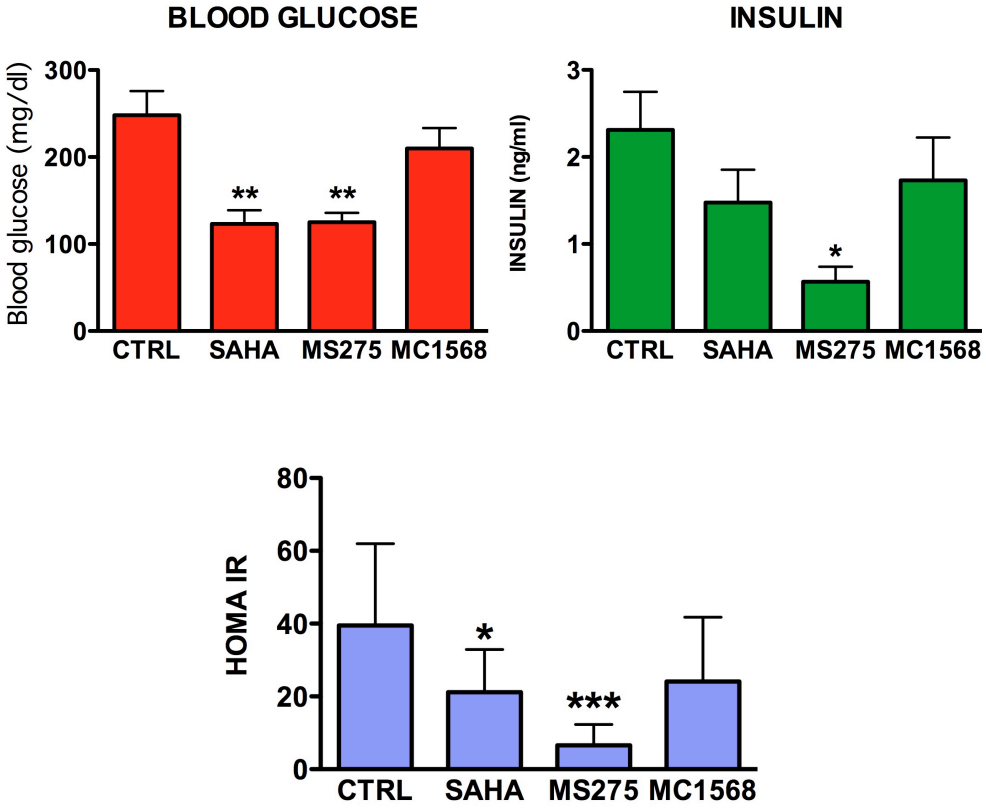

Figure 10: Blood glucose, insulin levels and HOMA index in *DbDb* mice treated with HDACi. Glucose was measured in fasted mice before sacrifice. The HOMA index, or homeostatic model assessment, is a method used to quantify insulin resistance (HOMA-IR= (fasted glucose (mg/dl) x fasted insulin (mU/L)) / 405). statistical comparison of these totals was made using ANOVA. *p < 0.05, **p<0.01, ***p<0.001.

We also performed a glucose tolerance test and an insulin tolerance test which demonstrate the increased glucose clearence and insulin sensitivityin mice treated with SAHA and MS275, but again MC1568 fails (fig.11)

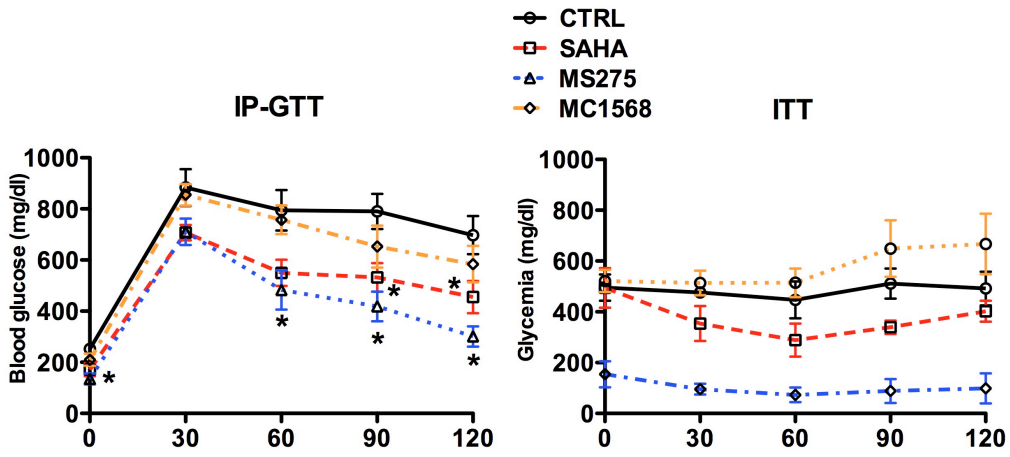

Figure 11: intraperitoneal Glucose Tolerance Test in *DbDb* mice treated with HDACi. Mice were fasted for 16 hr, and glucose levels from tail-vein blood were determined before and 30, 60, 90, and 120 min after i.p. injection of glucose (2 g/kg). For ITT, random fed mice were injected i.p. with insulin (2 U/kg). Glucose levels were determined before and 30, 60, 120, 180, and 210 min after injection. Statistical comparison of these totals was made using ANOVA. *p < 0.05.

We did not detect any changes in total cholesterol and plasma bile acids levels. Surprisingly FPLC profile reveals an important reduction in VLDL pick in SAHA and MS275 treated groups, due to a decrease in associated triglycerides, as confirmed by triglycerides quantification in FPLC fractions (FIG.12).

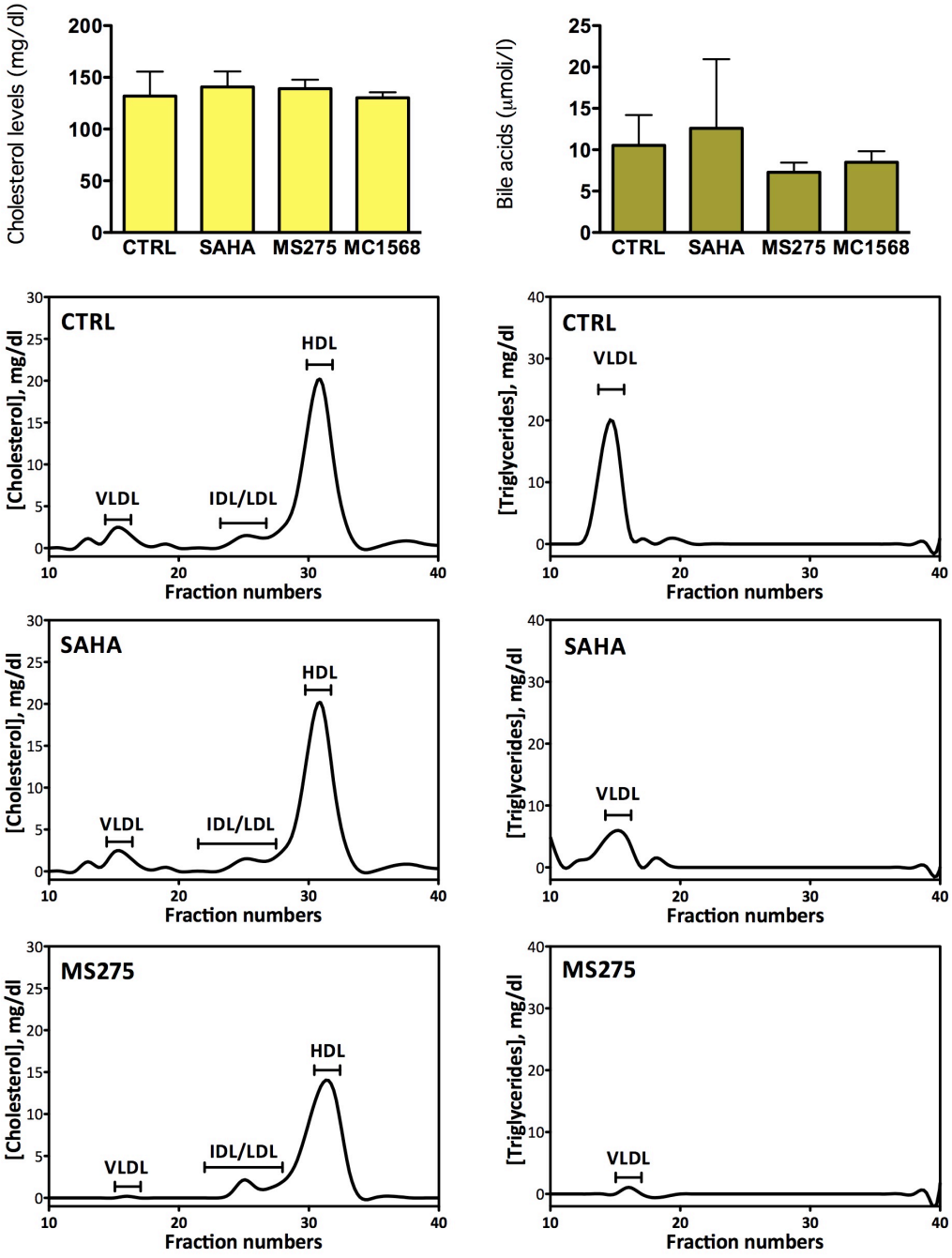

Figure 12: Plasma cholesterol and plasma bile acids quantifications. Cholesterol and triglycerides distribution in plasma lipoprotein fractions determined by FPLC. One-ml fractions were collected and assayed for cholesterol using an enzymatic kit. (N= 10)

Finally to exclude liver dysfunction we performed histological analysis of the liver in mice treated with SAHA and MS275 and we observed a strong reduction in lipid accumulation after MS275 treatment improving liver phenotype. SAHA treatment also showed a reduction in lipid droplet size, even if lipid accumulation in the liver is not completly reverted (fig.13).
Consistent with this observation, we mesured the plasma transaminases levels and we founded that none of the compounds raise ALT and AST levels, actually MS275 treatment reduce significantly their levels (fig.13).

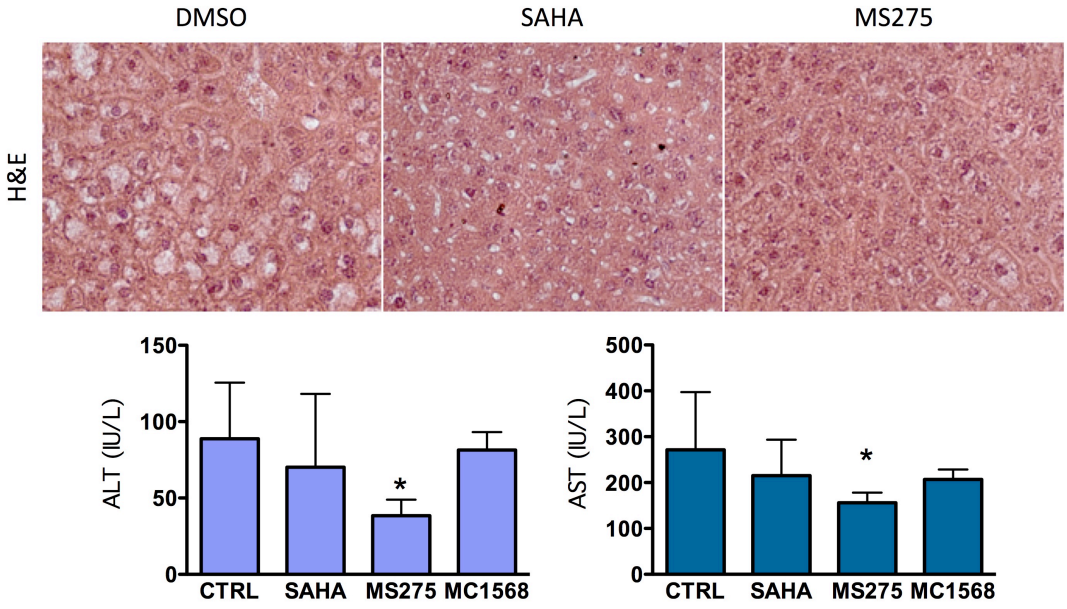

Figure 13: Hematoxylin and eosin staining reveals an improvement in liver phenotype in the MS275 treated group and, in a lesser degree, in the SAHA treated group. As consequence of the improvement of liver functionality, ALT and AST were reduced in the mice treated with MS275; statistical comparison of these totals was made using ANOVA. *$p < 0.05$.

Class I HDAC inhibitors increase energy expenditure in *Db/Db* mice.

Based on the results previously described, we performed metabolic cage analysis on animals treated with vehicle, SAHA and MS275 in order to verify which metabolic parameters were affected by the compounds directly in the living animals. Mice were individually housed and allowed to acclimate in the experimental cages with free access to food and water. Animals were maintained on 12 hr light/dark cycles. After acclimatation we started recording oxygen consumption, CO_2 production, heat production and activity.
Although SAHA treatment did not affect any of the parameters recorded, we found that MS275 treated mice significantly consume more oxygen and produce more CO_2 during the dark cycle. No changes were detected in the activity of the mice (fig.14).

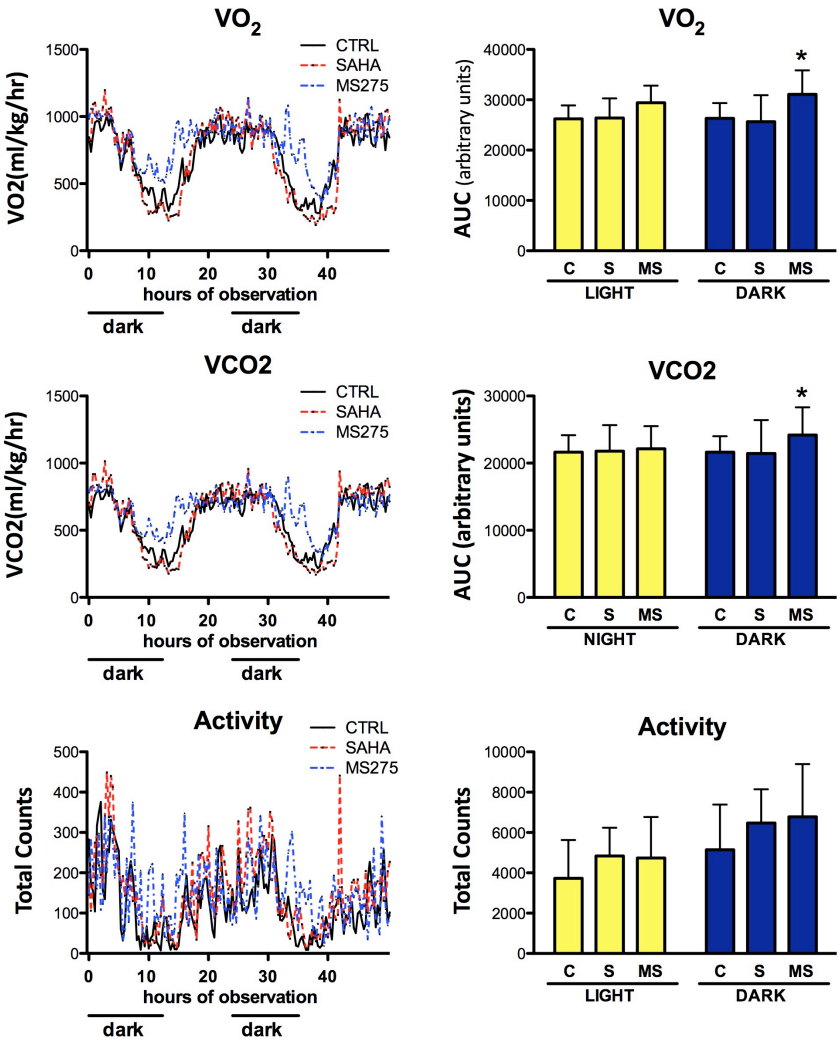

Figure 14: Effect of HDACi on Energy Expenditure in Diabetic Mice. Oxygen consumption, CO_2 production, and activity were measured over 3 days by indirect calorimetry. Data on heat production (calculated from gas exchange data; kcal/mass/time), VO_2 (volume of oxygen consumed; ml/mass/time), VCO_2 (volume of CO_2 produced; ml/mass/time) and activity (XYZ coverage; total activity counts) were analyzed using the OxymaxWin v3.01 software package. Statistical comparisons of repeated measurements were made using ANOVA. In the graphs data are expressed as area under the curve (AUC) calculated for the light and the dark period over the 3 recording days; statistical comparison of these totals was made using ANOVA. *p < 0.05.

These changes reflect a reduction in the respiratory exchange ratio (VCO_2/VO_2) indicating that mice preferentially use fat as fuel source (fig.15).

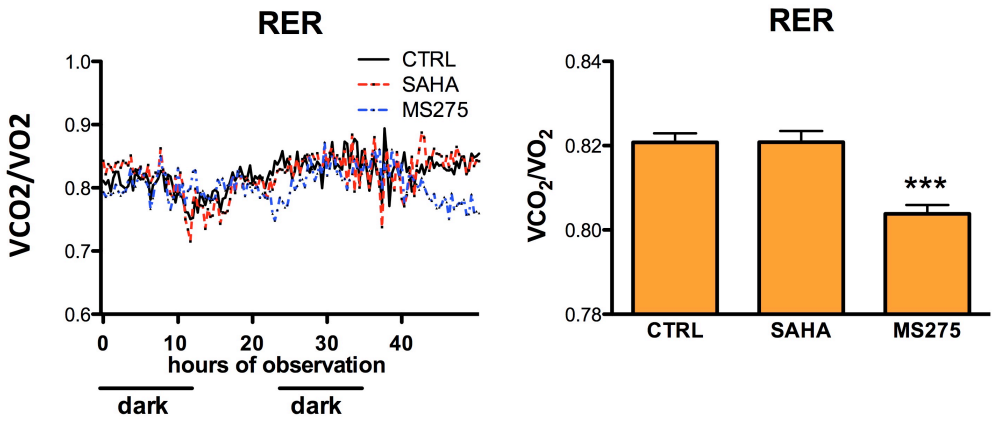

Figure 15: Effect of HDACi on Respiratory Exchange Ratio in Diabetic Mice. In the graphs data are expressed as area under the curve (AUC) over the 3 recording days; statistical comparison of these totals was made using ANOVA. ***p < 0.001.

Finally we observed that in mice treated with MS275 the heat production was increased. Since the heat production is an indirect measurement, we confirm this result evaluating the rectal temperature of the different groups of animals. Indeed we found an increased body temperature in

fasted mice treated with MS275, suggesting a possible role of brown fat (fig.16).

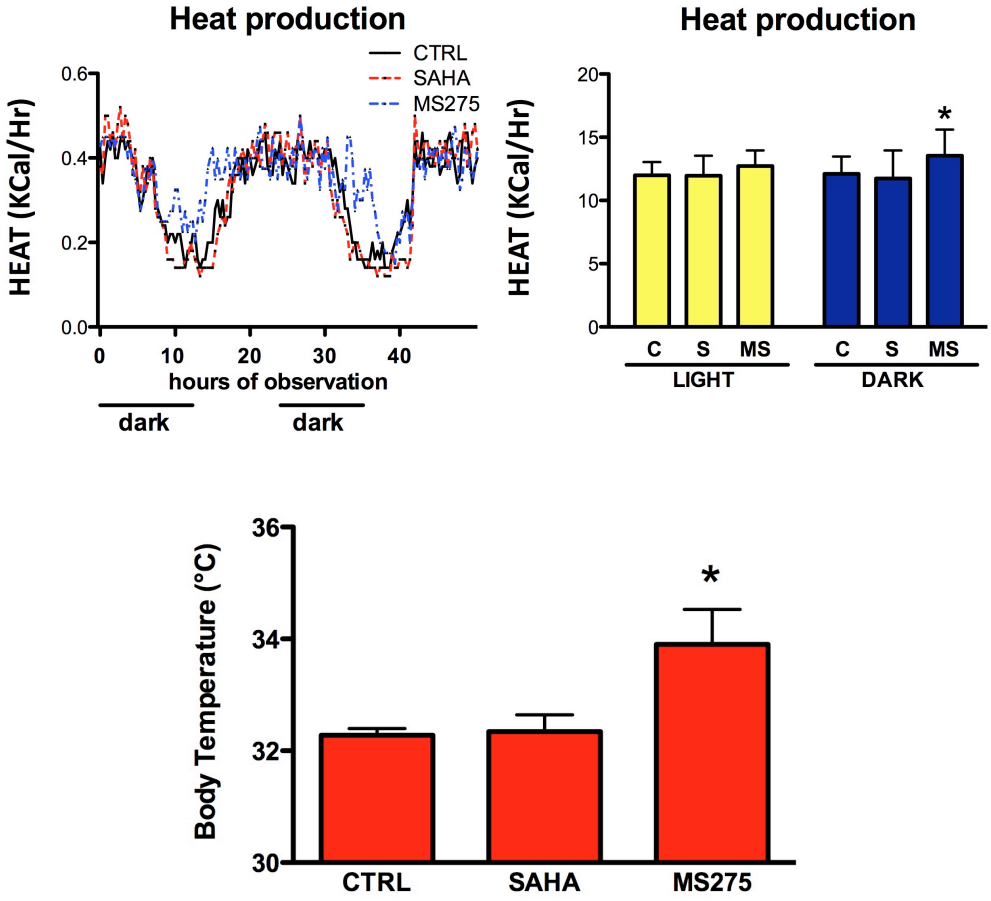

Figure 16: Effect of HDACi Heat production in Diabetic Mice. Data on heat production (calculated from gas exchange data; kcal/mass/time) were analyzed using the OxymaxWin v3.01 software package. Statistical comparisons of repeated measurements were made using ANOVA. In the graph data are expressed as area under the curve (AUC) calculated for the light and the dark period over the 3 recording days; statistical comparison of these totals was made using ANOVA. *p < 0.05.

Effects of HDAC inhibitors in target tissues of *Db/Db* mice

Skeletal muscle

In order to understand the effects of SAHA and MS275 in different metabolic tissues we performed genome-wide analyses in two different muscle types, gastrocnemuis, a mixed fiber, and vastus lateralis, a classical white fiber, in the liver and in white and brown adipose tissues.
Subsequently, we validated all the microarray analyses by QPCR. In all tissues analyzes we found a reprogramming of the gene expression profile of relevant genes involved in metabolism and its regulation.
In particular, in gastrocnemius muscle, we first checked that HDACi reached the tissue and inhibit thei targets (fig.17), next we observed an increased expression of general transcription factors associated to mitochondria (PGC-1α and β, ERRα, Tfam and TFB1M) and genes in the glicolysis (PKM2), fatty acid oxidation (LCAD), TCA cycle (IDH3α, SUCLG1) and oxidative phosphorylation (CYT C, COX6A1 and ETFDH) (fig.18).

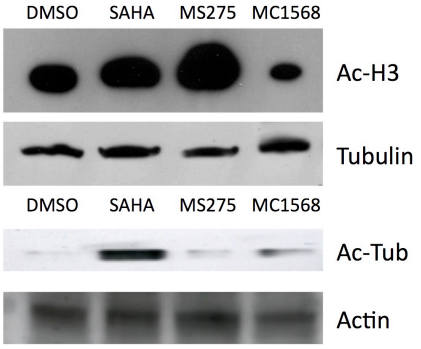

Figure 17: Western Blot analyses of acetyl-Tubulin and Acetyl-Histone H3

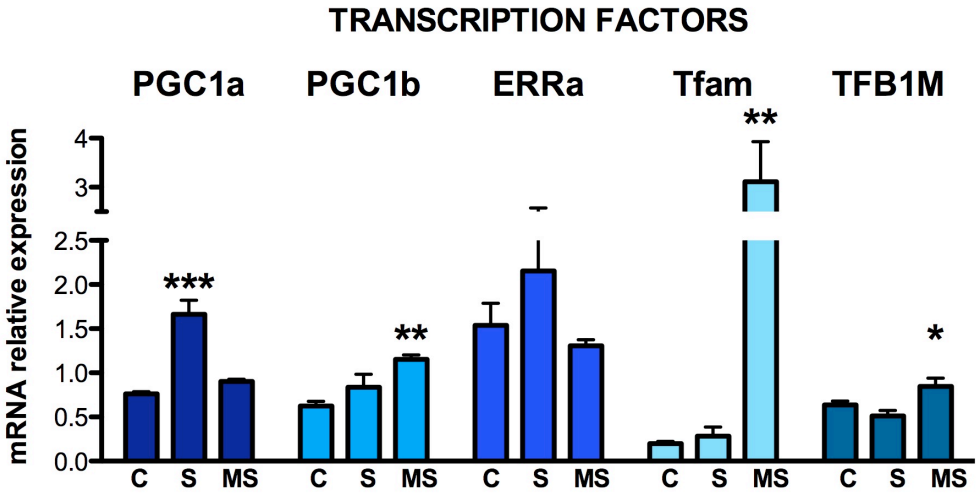

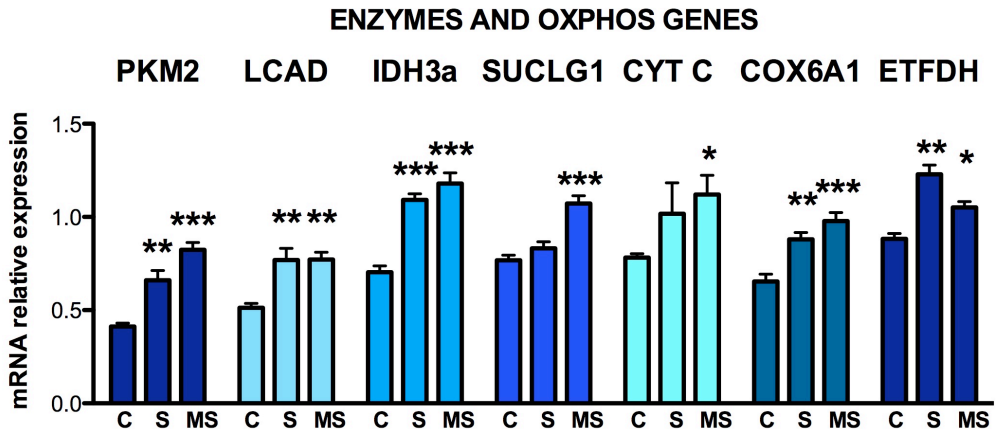

Figure 18: effects of HDACi on gene expression profile in gastrocnemius muscle. Statistical comparison of these totals was made using ANOVA. *p<0.05, **p<0.01,***p<0.001.

Similar effects in gene expression profile were also observed in two other muscle fibers, such as vastus lateralis and soleus, respectively a white fiber and a red one.

Even in these cases we observed an increase in genes involved in mitochondrial biogenesis andan increase of classical mitochondrial markers, such as Cyt C or COX6A1. Finally, even in these muscle we found an increase in metabolic genes, like LCAD or PKM2. (fig.19).

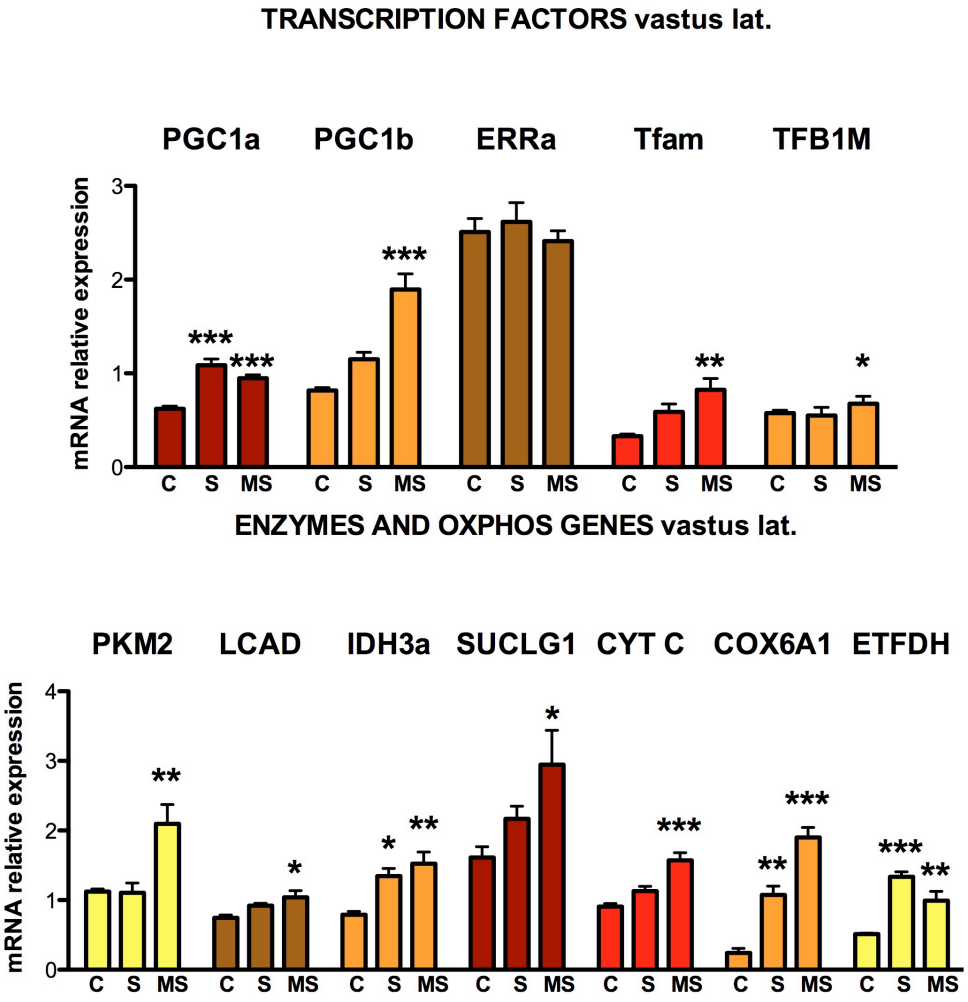
TRANSCRIPTION FACTORS vastus lat.
PGC1a
PGC1b
ERRa
Tfam
TFB1M
mRNA relative expression
0
1
2
3
***
***
***
**
*
C S MS C S MS C S MS C S MS C S MS
ENZYMES AND OXPHOS GENES vastus lat.
PKM2
LCAD
IDH3a
SUCLG1
CYT C
COX6A1
ETFDH
mRNA relative expression
0
1
2
3
4
**
*
*
**
*
***
**
***
***
**
C S MS C S MS C S MS C S MS C S MS C S MS C S MS

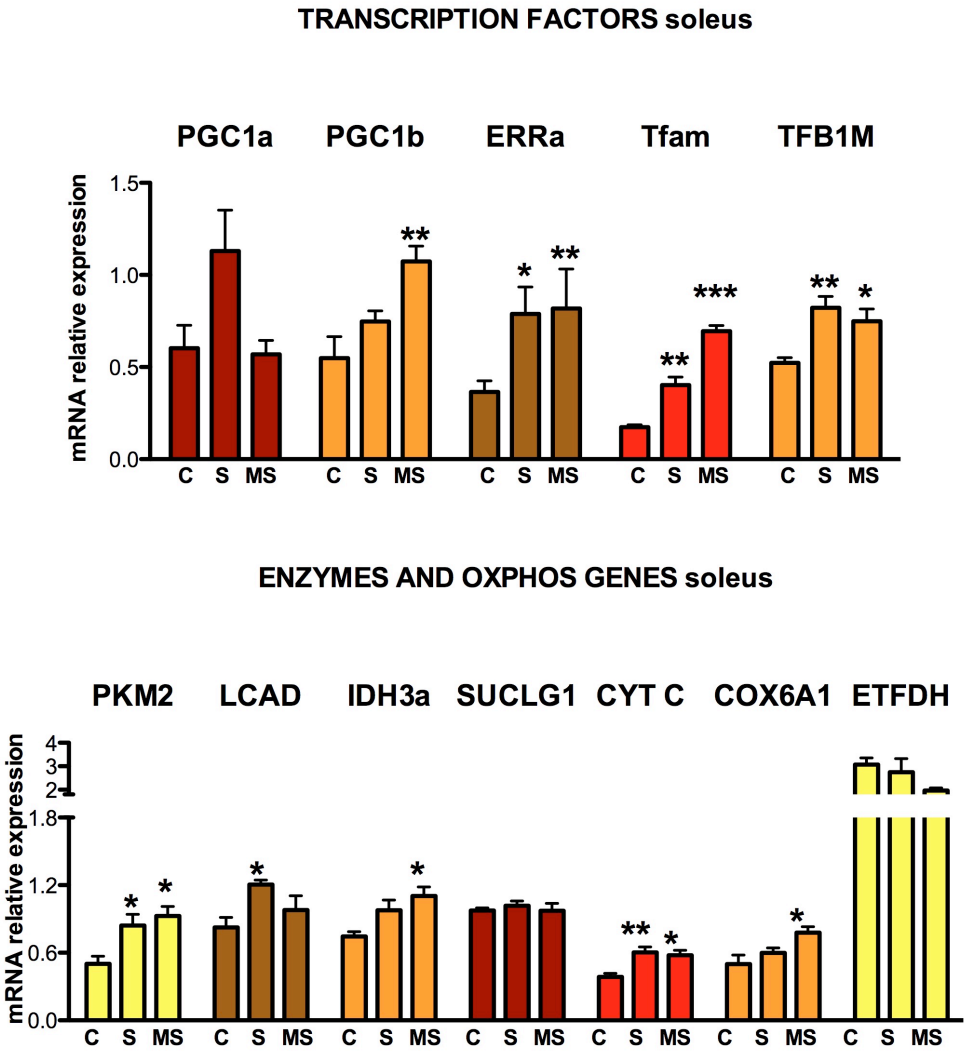

Figure 19: effects of HDACi on transcription factors and cofactors, metabolic and OXPHOS genes in vastus lateralis and soleus. Statistical comparison of these totals was made using ANOVA. *p<0.05, **p<0.01,***p<0.001.

All these data suggest an improved oxidative metabolism and to confirm these observation we analyzed the muscle oxidative capacity trough succinate dehydrogenase (SDH) staining of gastrocnemius fibers(fig.20).
As shown in figure 20 MS275, and SAHA to a lesser degree, increase the proportion of dark brown fibers, indicating an increased oxidative capacity of gastrconemius muscle. The shift toward more oxidative fibers occurred without any changes in typical markers of type I an II fibers (fig.21).

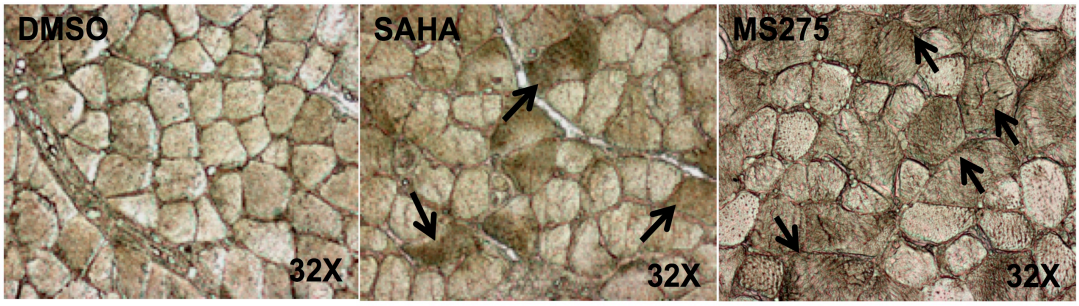

Figure 20: succinate dehydrogenase staining in gastrocnemius muscle of *DbDb* mice treated with SAHA or MS275 comare to the vehicle group. Arrows indicate darker fibers, indicating more oxidative capacity.

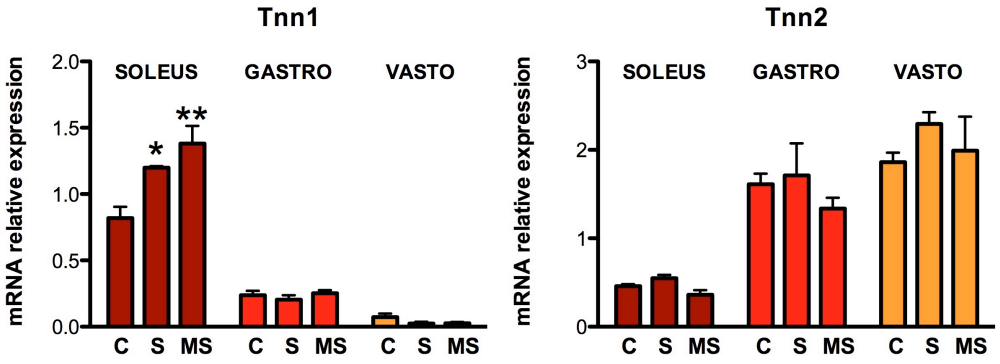

Figure 21: QPCR analysis on Troponin 1 and 2 expression, markers of type I and II fibers. Statistical comparison of these totals was made using ANOVA. *p<0.05, **p<0.01.

Furthermore, we also used Periodic acid-Schiff stain (PAS) to detect glycogen in gastrocnemius muscle. Interestingly we observed different behaviors between SAHA and MS275 groups; in particular, SAHA treatment reduced glycogen accumulation, while MS275 treated mice showed more glycogen storage compare to the vehicle treated group (fig.22). In addition, Gomori trichrome staining highlighted ragged red fibers in control group indicating mitochondrial myopathy which appear to be reduced by SAHA and MS275 treatments (fig.22).

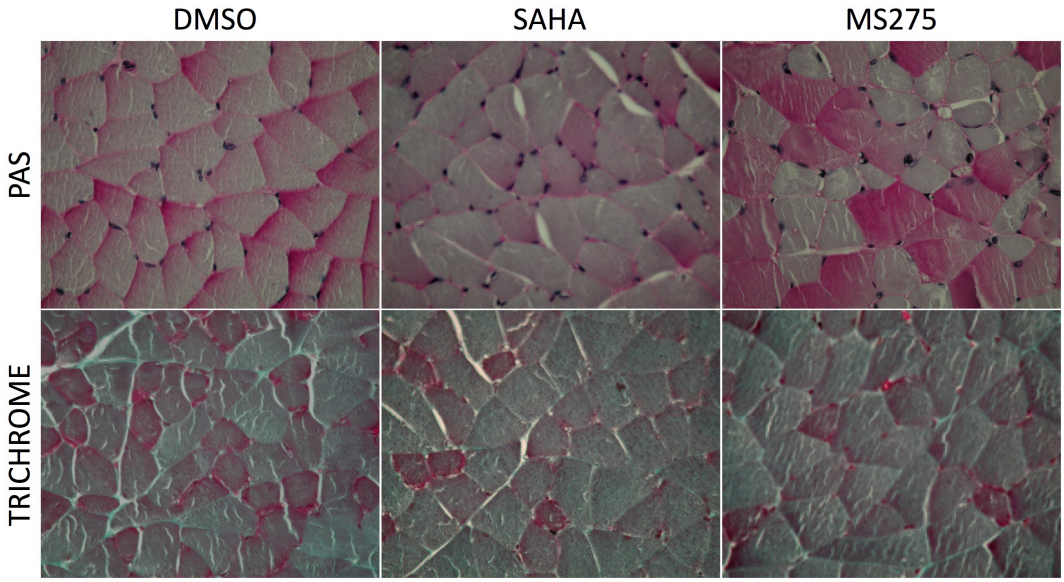

Figue 22: PAS and Gomori Trichrome stainings in gastrocnemius muscle of *DbDb* mice treated with HDACi.

Finally, we did not observe any toxicity of the treatments in the gastrocnemuis muscle, as showed by alkaline phosphatase (ALP) and esterase stainings where we did not found any difference among the three different groups. (fig.23)

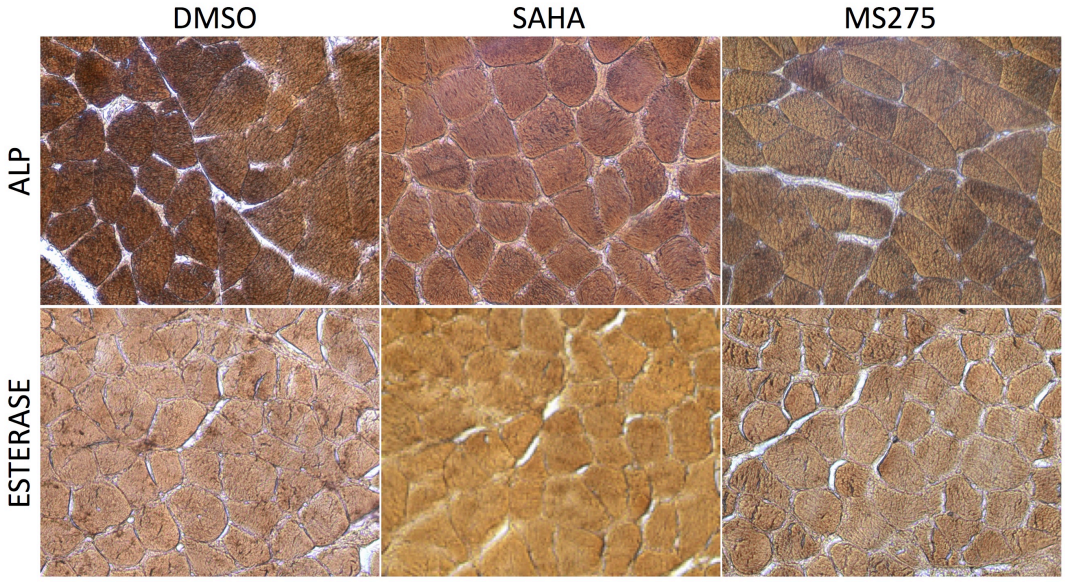

Figure 23: esterase ad alkaline phosphatase stainings in gastrocnemius muscle of *DbDb* mice treated with HDACi.

Brown Adipose Tissue (BAT)

In order to explain the increased body temperature in MS275 treated group, we performed gene expression profile in brown adipose tissue and we found that class I selective inhibition significantly increases the expression of classical markers of brown fat, such as UCP1, ELOVL3, DIO2, CIDEA and PRDM16(fig.24). Interestingly we observed also an increased expression of the β3 subunit of the adrenergic receptor, suggesting an increase of the brown fat functionality.

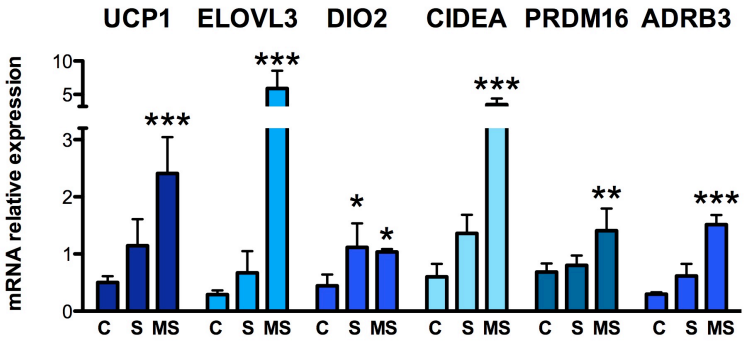

Figure 24: gene expression profile in brown adipose tissue of *DbDb* mice treated with HDACi or vehicle. Statistical comparison of these totals was made using ANOVA. *p<0.05, **p<0.01,***p<0.001.

Moreover, as for the muscle tissues, in the MS275 group we detected a significant increased expression of PGC-1a, PGC-1b and of typical markers of mitochondrial biogenesis, as Tfam, TFB1M and Cyt C (fig.25).

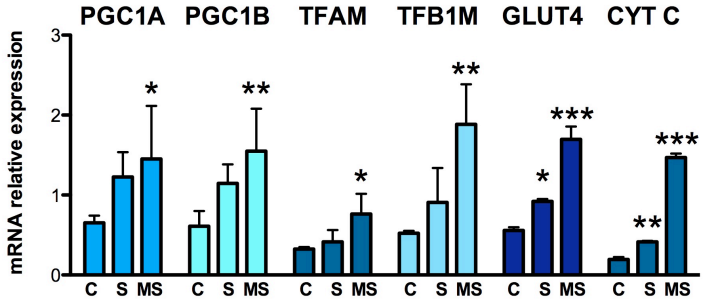

Figure 25: gene expression of transcription factors, cofactors and metabolism related genes in brown adipose tissue of *DbDb* mice treated

with HDACi or vehicle. Statistical comparison of these totals was made using ANOVA. *p<0.05, **p<0.01,***p<0.001.

SAHA treatment seems to be less effective, even if it shows a tendence to increase the gene expression of classical markers of brown fat (fig.24).
In addition, hematoxylin and eosin staining reveals a reduced cell size after SAHA and MS275 treatments (fig.26). These data, considering the increased expression of the adrenergic receptor, suggest an improved brown fat phenotype.

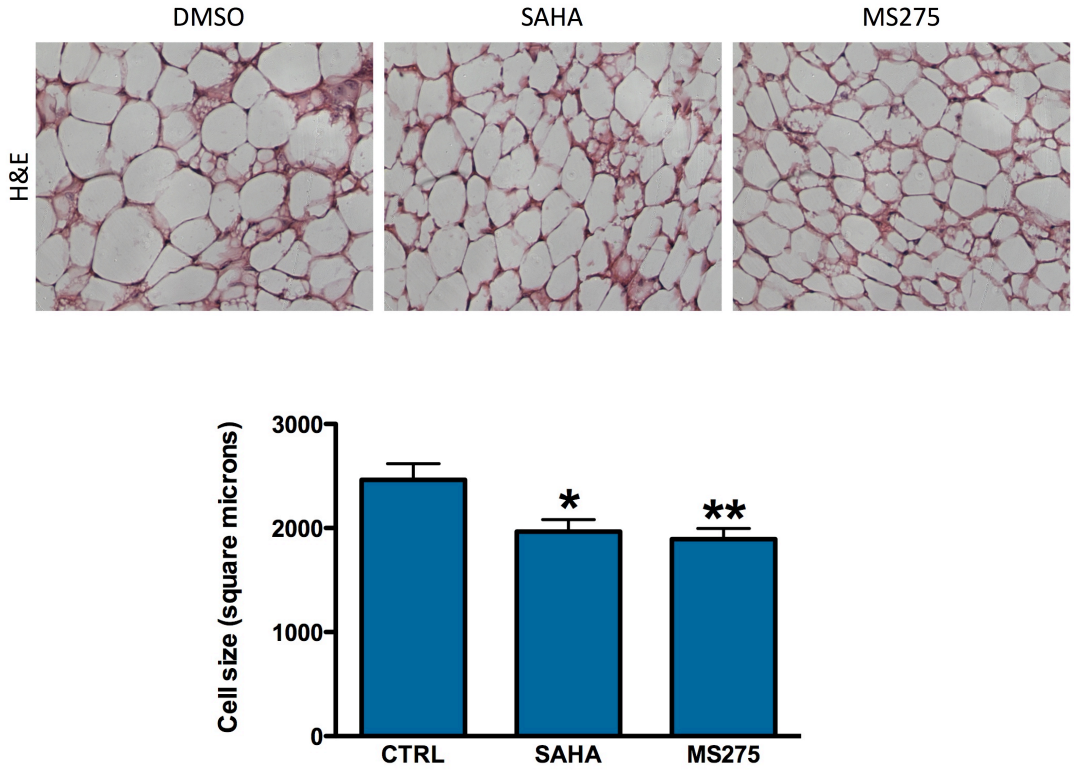

Figure 26: Upper panel. Hematoxylin and Eosin staining of brown adipose tissue in *DbDb* mice treated with HDACi or vehicle. Lower panel. Measurement of the adipocyte cell size in brown fat.Statistical comparison of these totals was made using ANOVA. *p<0.05, **p<0.01.

White Adipose Tissue (WAT)

White fat is another tissue playng a key role in energy balance. In order to understand if HDACi treatments affected metabolic parameters and transcription also in this district, we performer QPCR and histological analysis.
As for the trascriptional expression profile in muscle tissues and brown fat, even int the WAT we observed an upregulation of genes involved in mitochondrial biogenesis, such as PGC1α, Tfam and Cyt C.

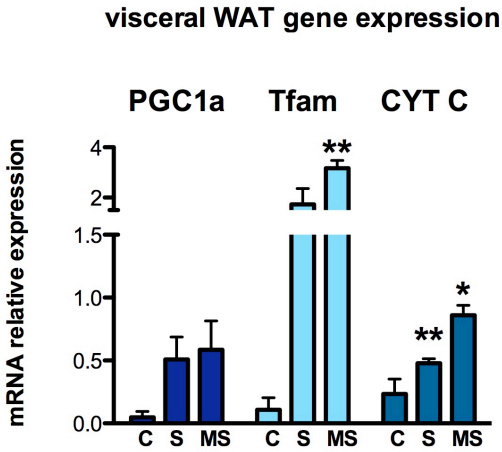

Figure 27: QPCR expression of mitochondrial regulators and markers in white adipocyte from *DbDb* mice treated with HDACi or vehicle. Statistical comparison of these totals was made using ANOVA. *p<0.05, **p<0.01.

Consistent with the results reported above, we also observed that several genes involved in lipid metabolism were upregulated, such as the lipid fatty acid transporters CD36 and CPT1b, the long chain acyl-CoA dehydrogenase LCAD, the hormone-sensitive lipase HSL and the uncoupling protein 3 (fig.28).

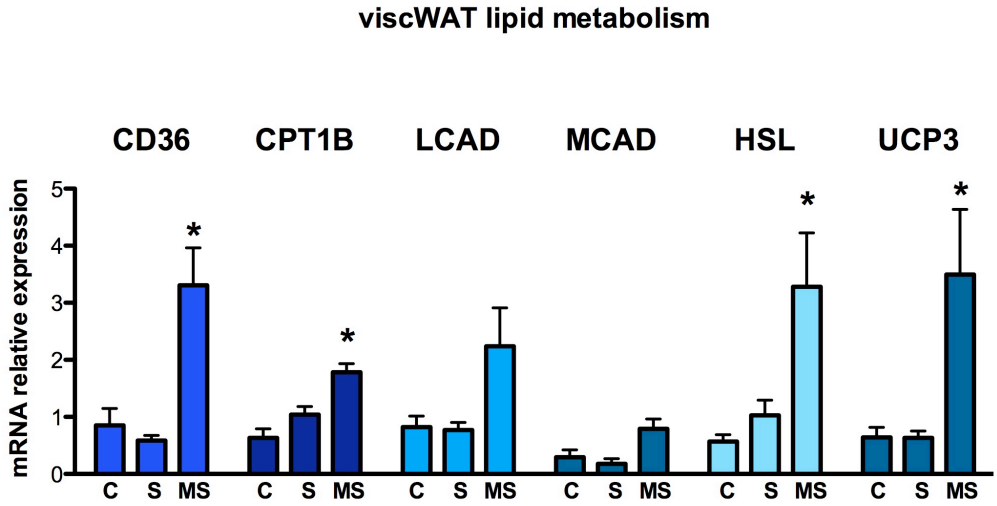

Figure 28: Lipid metabolism gene expression profile in white adipocyte from *DbDb* mice treated with HDACi or vehicle. Statistical comparison of these totals was made using ANOVA. *p<0.05.

We also checked the classical markers of adipose tissue and we observed that all of these were upregulated after treatment with MS275, indicating a more physiological profile. In order to substantiate the improved fat phenotype, we analyzed the expression of typical markers of inlammation and we saw that the expression of the iNOS was dramatically reduced, confirmig the hyothesis of the improved fat functionality. Also PTGS2 was reduced, even if not significantly, while TNFα did not change (fig.29).

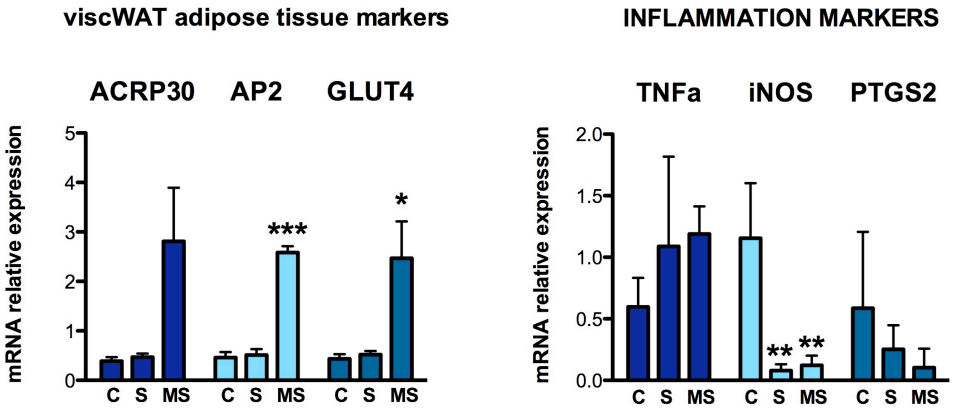

Figure 29: adipose tissue markers and inflammation markers expression levels in white adipocyte from *DbDb* mice treated with HDACi or vehicle. Statistical comparison of these totals was made using ANOVA. *p<0.05.

Finally hystological analysis confirmed the gene expression profile results. In fact hematoxylin and eosin staining revealed a lower cells size of adipocytes in the MS275 group, probably due to the increase in lipid catabolism and the immunohistochemistry assay against MAC1, a typical marker of macrophage recruitment, in the peripheral district appeared strongly reduced in mice treated with MS275 and, in a lesser degree, also in the SAHA treated group (fig.30).

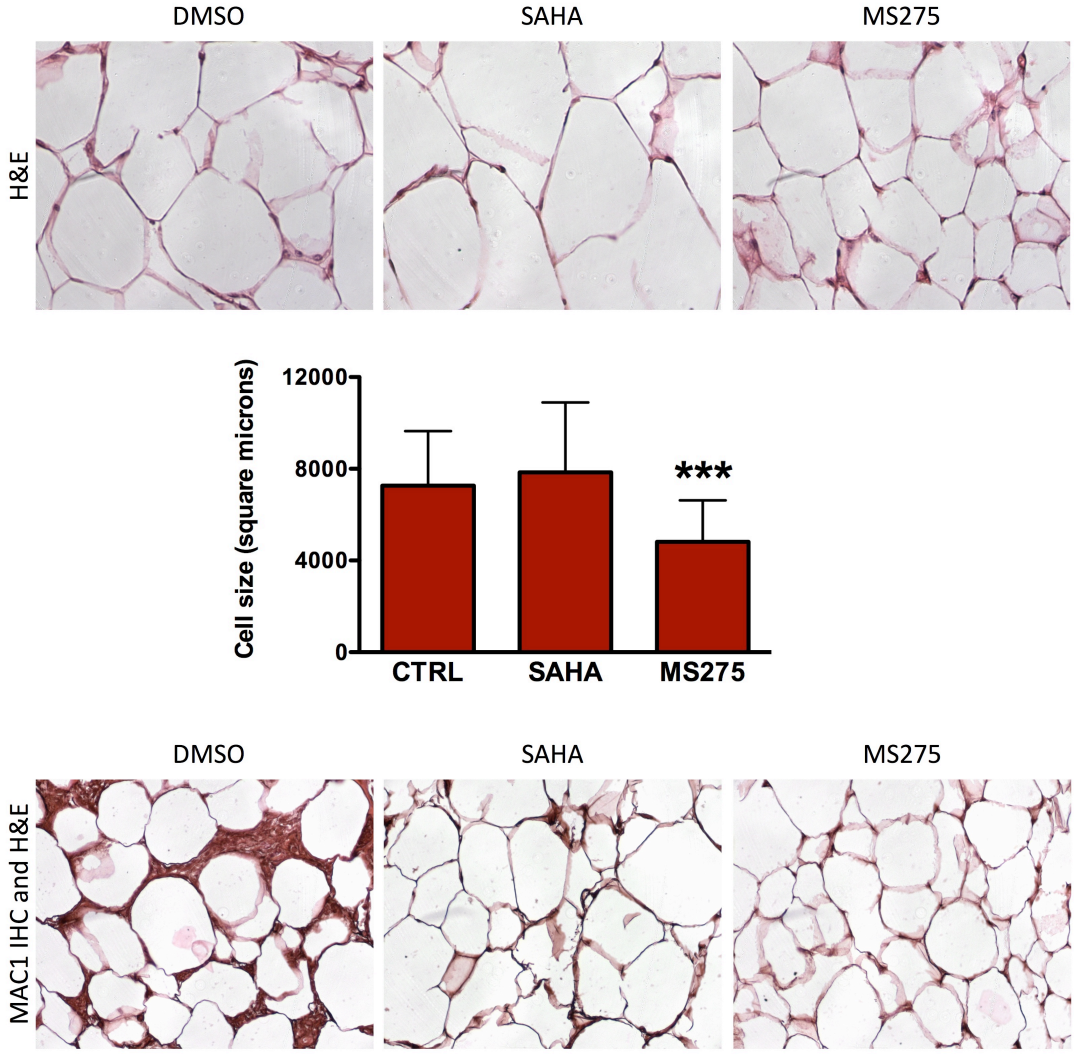

Figure 30: top. Hematoxylin and eosin staining od white adipose tissue in *DbDb* mice treated with vehicle, SAHA or MS275 (magnification 20X). Center. Adipocyte cell size measurement of adipocytes. Bottom. Immunohistochemistry of white adipocytes against MAC1 (Magnification 10X). Statistical comparison of these totals was made using ANOVA. ***p<0.001.

Treatment with Class I HDAC inhibitor induce Brown-like phenotype in white adipocyte

Transcriptome analysis in visceral fat showed that treatment with Class I selective HDAC inhibitor MS275 promotes the expression of classical markers of brown adipocyte differentiation. The heatmap in figure 31 shows that more than 90% of the genes belonging to the GO Biological process Brown fat cell differentiation is upregulated after treatment with MS275. In contrast, very small differences can be observed after treatment with SAHA. (Fig. 31)

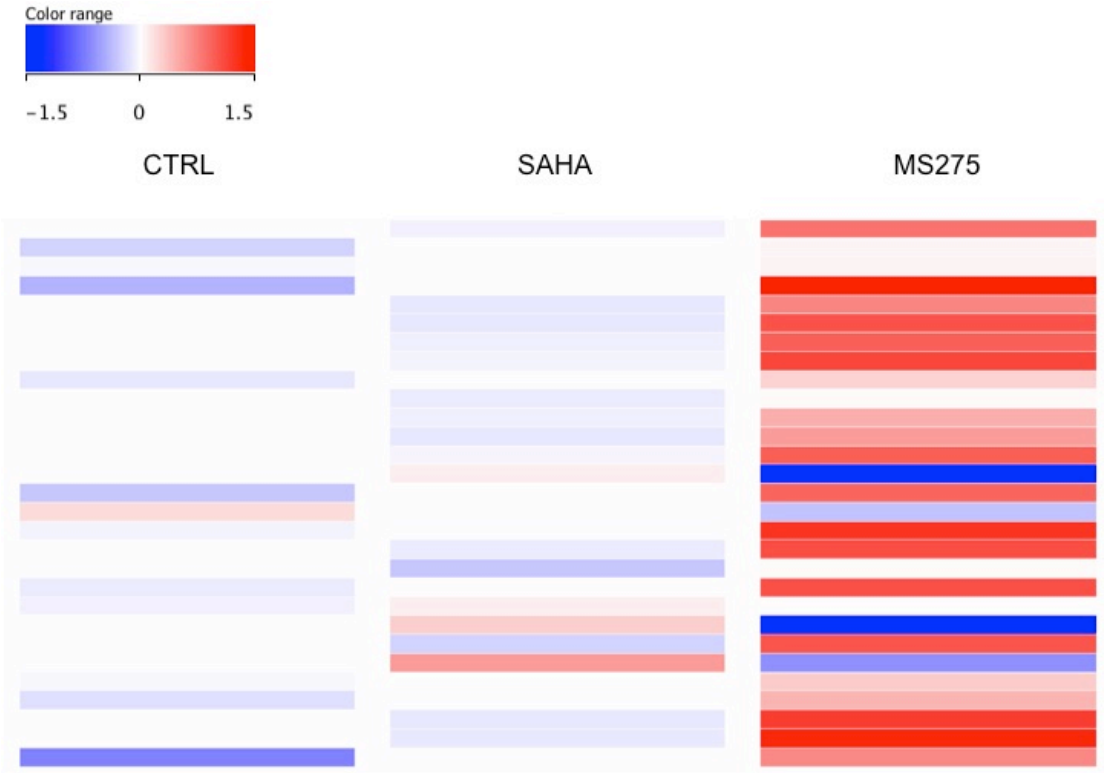

Figure 31: Heatmap of the biological process Brown fat cell differentiation. MS275 seems to promote the expression of the entire pathway, suggesting a brown like phenotype in white adipocyte.

In order to confirm the microarray analysis we performed QPCR assays on visceral WAT and we observed that the most typical markers of BAT, such as Dio2, Elovl3, Cidea, the uncoupling protein UCP1 and the Adrenergic Receptor subunit beta 3. MS275 treated adipocytes remained negative for PRDM16: this suggest a brown like phenotype, or a "brite adipocyte" phenotype as described by Nedergaard and colleagues (Fig. 32).

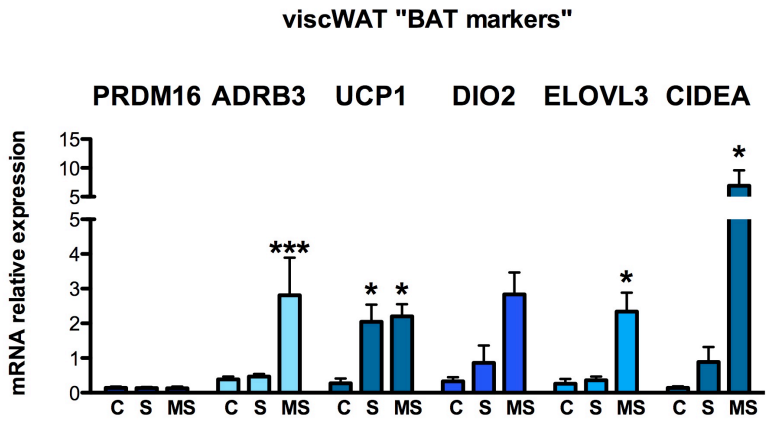

Figure 32: gene expression of brown fat cell markers in white adipose tissue of *DbDb* mice treated with HDACi or vehicle. Statistical comparison of these totals was made using ANOVA. *p<0.05,***p<0.001.

We also checked the presence of the UCP1 in the visceral WAT by immunohistochemistry and we founded that in the MS275 treated group UCP1 appears to be strongly increased. Also the white adipose tissue of the SAHA treated group is positive for the uncoupling protein UCP1, even if in a lesser degree compare to the MS275 treated group. (Fig. 33)

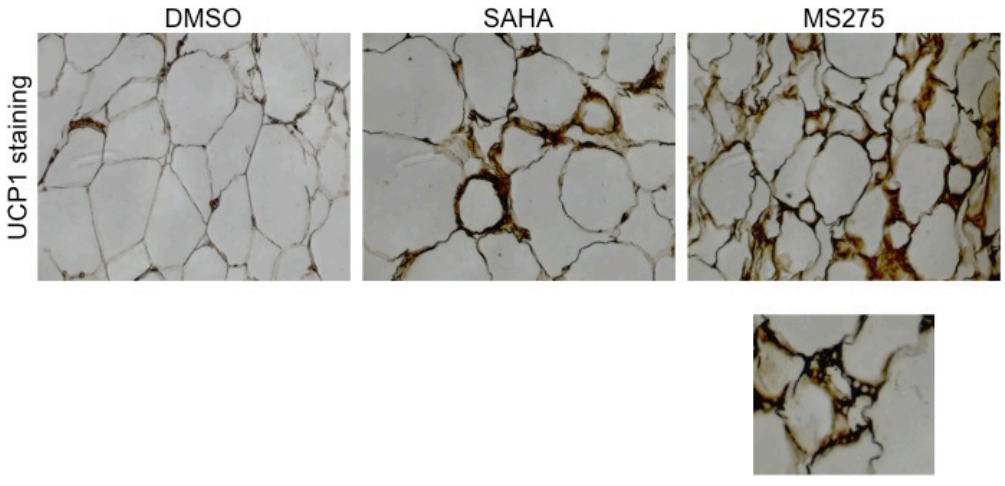

Figure 33: Top. UCP1 staining in paraffin embedded sections of visceral WAT of *Db/Db* mice treated with HDACi or vehicle. Bottom. Multilocular adipocyte founded in the UCP1 stained section of the MS275 treated mouse (Brown like or "Brite adipocyte").

DISCUSSION

Recent experimental evidences reported in the literature have revealed that the control of metabolic pathways occurs at the transcriptional level also by means of epigenetic mechanisms, and particularly through chromatin remodeling[224]. This discovery has relevant implications and may lead to a more comprehensive understanding of physiologic situations as well as of metabolic diseases such as obesity, diabetes and metabolic syndrome. At this regard, liver, skeletal muscle, brown and white fat represent the main target tissues subjected to metabolic control.
Chromatin acetylation is undoubtedly the main epigenetic mechanism through which gene expression can be regulated, therefore, histone acetyl transferases (HATs) and especially histone deacetylases (HDACs) most likely play a major role in chromatin remodeling. For example, it has been demonstrated that HDACs play a central role in the development and remodelling of skeletal muscle myofiber[225,226]. In addition, Gao and coworkers recently published that sodium butyrate, a HDAC inhibitor, improves insulin sensitivity and increases energy expenditure in mice fed with a high fat diet[212].
Although the involvment of these enzymes in the regulation of these processes has been clearly demonstrated, it is still unclear which class of HDACs is mainly involved and how HDACs can affect the metabolic profile of different tissues.
To address these questions, in this study we examined the effects on energy metabolism of different histone deacetylase inhibitors (HDACi). In particular we used the well known pan inhibitor SAHA, the Class I HDAC inhibitor MS275 and the MC1568, a Class II HDAC inhibitor, using in vitro and in vivo approaches.

HDACi promote mitochondrial biogenesis in C2C12 myotubes.

In a cellular model of skeletal muscle we observed that the treatments with the pan-inhibitor SAHA or with the Class I selective inhibitor MS275, but not with the Class II HDAC inhibitor, were able to promote mitochondrial biogenesis, probably through a PGC-1α-dependent mechanism. In fact, after treatment with SAHA and MS275, the expression of PGC-1α was strongly upregulated and this led to increase mitochondrial density, activity and mitochonadrial DNA content.
In addition, experiments using clones stably expressing the luciferase gene under the transcriptional control of the PGC-1α responsive region of the Tfam promoter, indicated that the treatment with the pan inhibitor or with the Class I HDAC inhibitor increases the trancriptional activity of the

Tfam promoter, sustaining the hypothesis that HDACi act through a PGC-1α dependent mechanism.

We also characterized the effects of these compounds in C2C12 performing a genome-wide analysis: we found that SAHA and MS275 increase, respectively, the expression of 128 and 92 genes belonging to the KEGG pathway of metabolic processes and among these genes, more than 50% are involved in glucose and lipid metabolism, such as GLUT4, LCAD, IDH3α and the ETC proteins COX7A1, COX5A or COX6A1.

In contrast, MC1568 affected only 7 genes in the KEGG pathway of the metabolic processes, indicating that probably Class II HDAC activity is not directly involved in the regulation of the energy metabolism and mitochondrial biogenesis. Class IIa HDACs possess only minimal histone deacetylase activity[202], and this can contribute to explain the very small effects that we observed in cells treated with class II selective inhibitor. In addition, class IIb HDACs act on extranuclear targets that are probably less involved in metabolic regulation; therefore it is not surprising that their inhibition in C2C12 cells minimally affects gene transcription. Different results were obtained by using a genetic approach, as in the case of the work by Potthoff and coworkers[225]. The knock-out allows to completely delete the expression of the proteins; in that case, the repressive complex in which HDACs are recruited, are totally disrupted. Instead, using a biochemical inhibition, it is possible to modulate the activity of the enzymes, thus HDACs are still present in the cells and can still interact with factors and cofactors.

Collectively, these results reveal that HDACs, and in particular Class I HDACs, can affect mitochondrial biogenesis and that the inhibition of its activity may drive the cells towards a more oxidative phenotype.

HDACi reduce glycemia in diabetic obese mice.

In order to understand whether HDACi can promote mitochondrial biogenesis *in vivo*, we treated insulin resistant obese mice (*Db/Db*), an animal model of diabetes, with SAHA, MS275 and MC1568.

After SAHA and MS275 treatments, but not after MC1568 treatment, mice showed a reduced glycemia (-50%); moreover, only MS275 induced a reduction of obesity (-8% of total body weight) and of the plasma insulin levels (-75%) in treated mice. In addition, SAHA and MS275 improved the glucose tolerance, suggesting an increase in insulin sensitivity. Based on these results, we performed CLAMS analysis on SAHA and MS275 groups and we demonstrated that mice treated with Class I HDAC selective

inhibitor increase energy expenditure and oxygen consumption. This may be due to the improved ability to burn substrates, such as glucose or fatty acids. In fact, MS275 group showed also a significant reduction in the respiratory exchange ratio, suggesting that these mice use preferentially fat as energy source. Since the locomotor activity is comparable among the groups, these data indicate that MS275 treated mice have an increased basal metabolism, and this correlates with increased heat production following MS275 administration, suggesting an effect of this compound on brown adipose tissue.

The ability of MS275 treated mice to better use and store substrates is also suggested by the reduced body weight and the increased glycogen storage in muscle. Moreover, skeletal muscle is one of the main tissues which can use fatty acids as energy source. Notably, in diabetic subjects, intracellular lipid accumulation causes reduced mitochondrial oxidative capacity in skeletal muscle[227,228]. The reduction of respiratory exchange ratio in diabetic mice treated with MS275 could indicate an increased mitochondrial function in skeletal muscle (see below), which uses fatty acids to produce ATP and stores glucose in the form of glycogen. In agreement with this, MS275, and SAHA in a lesser degree, reduced not only glucose but also plasma triglycerides.

HDACi treatments did not reduce food intake or locomotor activity, indicating that there was no toxicity from these compounds; this is corroborated by the plasma transaminases levels which appeared even lower after treatment with MS275. These results indicate an improvement in liver function, in which lipid accumulation resulted dramatically reduced after treatment with MS275 and SAHA, even if to a lesser degree.

In summary, in a diabetic mouse model, treatments with HDAC pan-inhibitor or Class I inhibitor reduce glycemia, plasma triglycerides and hepatic lipid accumulation; in addition, Class I HDAC inhibitor administration reduces obesity, increases energy expenditure and heat production.

Class I HDAC inhibition promotes mitochondrial biogenesis in skeletal muslce.

Skeletal muscle constitutes the 40% of the total body weight and, for this reason, it plays a central role in fatty acid utilisation and glucose homeostasis. At this regard, mitochondria are particularly important for skeletal muscle function, given also the high oxidative requests imposed on this tissue by contraction.

In order to explain the changes in blood chemistry and in metabolic parameters observed in mice, we performed gene expression analysis in three different muscle fibers; in particular we focused our attention on *gastrocnemius*, a muscle in which both type I and type II myofibers are present, on *soleus*, where type I fibers are predominant, and on *vastus lateralis* that, in contrast, is mainly constituted by type II fibers.

Collectively, in all the muscles analyzed, we found that, in mice treated with the Class I HDAC selective inhibitor, mitochondrial markers were upregulated as well as central enzymes belonging to glucose and fatty acid metabolism. These results support the hypothesis that the inhibition of Class I histone deacetylase promote oxidative metabolism and can contribute to explain the reduced glycemia, the reduction in plasma triglycerides and the increased oxygen consumption observed in these mice.

Skeletal muscle is the largest insulin-sensitive organ in humans, accounting for more than 80% of insulin-stimulated glucose disposal. Thus, insulin resistance in this tissue has a major impact on whole-body glucose homeostasis; one possible mechanism by which impaired mitochondrial function might contribute to insulin resistance is through an altered metabolism of fatty acids. The increased expression of OXPHOS genes following treatment with MS275 and SAHA, even if to a lesser degree, could improve fatty acid metabolism and mitochondrial function, increasing insulin sensitivity in muslce.

Succinate dehydrogenase (SDH) staining of sections of gastrocnemius corroborates the previuosly described results; in fact in mice treated with MS275, but also in the SAHA treated group to a lower extent, SDH staining revealed darker myofibers compared to the control group, indicating a more oxidative capacity of the myofibers. This switch towards fat utilisation, besides increasing insulin sensitivity, leads to increased glucose uptake and storage in the form of glycogen.

Moreover, mitochondrial dysfunction and morphological alterations highlighted by trichrome staining appeared strongly reduced after MS275 treatment, indicating again that inhibiting Class I HDAC it is possible to modulate mitochondrial biogenesis and function.

Interestingly, we did not observe any change in the expression of type I or type II troponins, indicating that the metabolic switch does not correlate with a reprogramming in muscle fiber types, as observed in previously published works[212,221,225]. This suggests that HDACi act at the level of the metabolic adaptation of mature skeletal muscle, without interfering with the myofiber differentiation.

Collectively, these data indicate a role of Class I HDACs in modulating

mitochondrial biogenesis and oxidative metabolism in skeletal muscle.

Class I HDAC inhibition reduces brown adipocyte size and improves brown fat functionality.

The role of mitochondria in adipose tissue is most apparent in brown adipose tissue, where flux through the ETC generates heat in the process of thermogenesis, a potentially important mechanism regulating systemic metabolism[120-123].

After MS275 administration, in brown adipose tissue we found an increase in the expression of PGC-1α, Tfam and mitochondrial markers, indicating an induction of mitochondrial biogenesis. In addition, in parallel with the induction of mitochondrial biogenesis, we observed that HDACi significantly increased expression of the insulin dependent glucose transporter; even in this case, these data suggest an increased insulin sensitivity and can contribute to explain the reduced glycemia observed in SAHA and MS275 treated groups.

Moreover, brown adipocytes appeared smaller and showed an increase in the expression of the typical markers of brown fat, such as UCP1, DIO2, ELOVL3 and CIDEA. The increased expression of the beta 3 subunit of the adrenergic receptor (ADRB3), after MS275 treatment, leads to hypothesize that brown fat, which is totally dysregulated in *Db/Db* mice, besides being more differentiated, can be also more functional; this increase in brown fat functionality could be responsible for the increase in the heat production and the increased body temperature detected in these mice.

In this tissue, the treatment with SAHA appeared to be less effective than MS275 in promoting mitochondrial biogenesis; nevertheless, brown adipocytes from SAHA treated mice resulted significantly smaller with respect to the vehicle treated mice and typical brown fat markers also showed a tendency to increase.

Taken together these results indicate that brown fat morphology and functionality are affected by HDACi and, in particular, that inhibitinig Class I HDACs it is possible to promote thermogenesis and energy expenditure.

Inhibition of class I HDAC promotes mitochondrial biogenesis and energy expenditure in white adipocytes.

Mitochondrial content in white adipocytes is decreased in both rodent and human obesity[147,155-158] and correlates with insulin resistance that accompanies obesity. In mice treated with MS275 we found an increased expression of PGC-1α and a consequent increase in Tfam expression. This suggests that, even in the white adipose tissue, by inhibiting class I HDACs it is possible to induce mitochondrial biogenesis. In addition, we also observed a general increased expression of genes involved in lipid metabolism, such as the fatty acid transporters CD36 and CPT1b or the hormone-sensitive lipase HSL.

Moreover, it has been demonstrated that adipocyte hypertrophy is associated with insulin resistance[229]; following MS275 treatment, mice showed a significant reduction in white adipocyte size and, in addition, a reduced macrophage recruitment into the tissue, followed by a decreased expression of some inflammatory markers. These data indicate that the inflammatory status of white fat is probably reduced and this could lead to an improvement in insulin signaling and adipokine expression in white fat.

White adipocytes display a high degree of plasticity[138], and regional differences in metabolic activity can be linked to varying mitochondrial density[139]. Higher mitochondrial density and even UCP1 expression can be induced in response to pharmacological or genetic alterations of white adipocytes[139-148], suggesting that white adipose tissue could potentially be induced to acquire more oxidative metabolic phenotypes, promoting increased fuel consumption and, thus, energy expenditure.

In mice treated with MS275, microarray analysis revealed a general induction of the genes belonging to the brown fat differentiation pathway, which includes 29 genes such as the adrenergic receptor beta subunit 1, 2 and 3, the transcriptional factor C/EBPα, β and PRDM16, the nuclear receptor PPARγ, the fatty acid binding protein 4 (FABP4 or AP2), the glucose transporter GLUT4 and the uncpoupling protein 1 (UCP1). In agreement with this observation, we found that white adipocytes, following MS275 treatment, were positive to the uncoupling protein 1 and to classical markers of brown fat, such as DIO2, ELOVL3 and ADRB3. Nevertheless these cells remained negative for PRDM16, the main transcription factor regulating brown adipocyte differentiation, suggesting that they did not transdifferentiate to brown adipocytes. Thus, it is possible that the inhibition of class I histone deacetylases induced a brown-like phenotype, or "brite phenotype", as observed for example after chronic somministration of rosiglitazone in primary cultures of white

adipocytes[148].
In summary, in white adipose tissue, Class I HDAC inhibition regulates lipid accumulation, reduces inflammation and promotes energy expenditure by increasing mitochondrial biogenesis and UCP1 expression.

Conclusions.

These results confirmed a role of mitochondrial dysfunctions in metabolic disorders; by promoting oxidative metabilsm *in vivo* it is possible to increase energy expenditure and ameliorate the obese and diabetic phenotype.
For the first time we demonstrated a mitochondrial signature assignable to class I HDACs. Class I histone deacetylases participate in the regulatory network of mitochondrial biongenesis and their biochemical inhibition can promote oxidative metabolism *in vitro* and *in vivo* in different tissues.
HDAC inhibitors could be valuable tools to understand dysregulated mechanisms at the basis of metabolic dysfunctions, and histone deacetylases may have potential application in the prevention and treatment of metabolic syndrome.

REFERENCES

1 ADA, A. D. A. Diabetes statistics. *http://www.diabetes.org/diabetes-basics/diabetes-statistics/* (2008).

2 Centers for Disease Control and Prevention, U. D. o. H. a. H. S. National diabetes fact sheet. *http://www.cdc.gov/diabetes/pubs/factsheet07.htm* (2007).

3 Boyle, J. P. *et al.* Projection of Diabetes Burden Through 2050. *Diabetes Care* **24**, 1936-1940, doi:10.2337/diacare.24.11.1936 (2001).

4 Roglic, G. *et al.* The Burden of Mortality Attributable to Diabetes. *Diabetes Care* **28**, 2130-2135, doi:10.2337/diacare.28.9.2130 (2005).

5 Ogden, C. L. *et al.* Prevalence of Overweight and Obesity in the United States, 1999-2004. *JAMA* **295**, 1549-1555, doi:10.1001/jama.295.13.1549 (2006).

6 Hu, F. B. *et al.* Diet, Lifestyle, and the Risk of Type 2 Diabetes Mellitus in Women. *New England Journal of Medicine* **345**, 790-797, doi:doi:10.1056/NEJMoa010492 (2001).

7 Tuomilehto, J. *et al.* Prevention of Type 2 Diabetes Mellitus by Changes in Lifestyle among Subjects with Impaired Glucose Tolerance. *New England Journal of Medicine* **344**, 1343-1350, doi:doi:10.1056/NEJM200105033441801 (2001).

8 Knowler, W. C. *et al.* Reduction in the incidence of type 2 diabetes with lifestyle intervention or metformin. *N Engl J Med* **346**, 393-403, doi:10.1056/NEJMoa012512 346/6/393 [pii] (2002).

9 Barroso, I. *et al.* Dominant negative mutations in human PPAR[gamma] associated with severe insulin resistance, diabetes mellitus and hypertension. *Nature* **402**, 880-883 (1999).

10 Fajans, S. S., Bell, G. I. & Polonsky, K. S. Molecular Mechanisms and Clinical Pathophysiology of Maturity-Onset Diabetes of the Young. *New England Journal of Medicine* **345**, 971-980, doi:doi:10.1056/NEJMra002168 (2001).

11 Florez, J. C. *et al.* TCF7L2 Polymorphisms and Progression to Diabetes in the Diabetes Prevention Program. *New England Journal of Medicine* **355**, 241-250, doi:doi:10.1056/NEJMoa062418 (2006).

12 Grant, S. F. A. *et al.* Variant of transcription factor 7-like 2 (TCF7L2) gene confers risk of type 2 diabetes. *Nat Genet* **38**, 320-323, doi:http://www.nature.com/ng/journal/v38/n3/suppinfo/ng1732_S1.html (2006).

13 Horikawa, Y. *et al.* Genetic variation in the gene encoding calpain-10 is associated with type 2 diabetes mellitus. *Nat Genet* **26**, 163-175, doi:http://www.nature.com/ng/journal/v26/n2/suppinfo/ng1000_163_S1.html (2000).

14 O'Rahilly, S., Barroso, I. & Wareham, N. J. Genetic Factors in Type 2 Diabetes: The End of the Beginning? *Science* **307**, 370-373, doi:10.1126/science.1104346 (2005).

15 Owen, K. R. & McCarthy, M. I. Genetics of type 2 diabetes. *Current Opinion in Genetics & Development* **17**, 239-244 (2007).

16 Knowler, W. C., Pettitt, D. J., Saad, M. F. & Bennett, P. H. Diabetes mellitus in the pima indians: Incidence, risk factors and pathogenesis. *Diabetes/Metabolism Reviews* **6**, 1-27, doi:10.1002/dmr.5610060101 (1990).

17 Poulsen, P., Ohm Kyvik, K., Vaag, A. & Beck-Nielsen, H. Heritability of Type II (non-insulin-dependent) diabetes mellitus and abnormal glucose tolerance – a population-based twin study. *Diabetologia* **42**, 139-145, doi:10.1007/s001250051131 (1999).

18 Barker, D. J. P. *et al.* Type 2 (non-insulin-dependent) diabetes mellitus, hypertension and hyperlipidaemia (syndrome X): relation to reduced fetal growth. *Diabetologia* **36**, 62-67, doi:10.1007/bf00399095 (1993).

19 Dabelea, D. *et al.* Intrauterine exposure to diabetes conveys risks for type 2 diabetes and obesity: a study of discordant sibships. *Diabetes* **49**, 2208-2211, doi:10.2337/diabetes.49.12.2208 (2000).

20 Rich-Edwards, J. W. *et al.* Birthweight and the Risk for Type 2 Diabetes Mellitus in Adult Women. *Annals of Internal Medicine* **130**, 278-284 (1999).

21 Lazar, M. A. How Obesity Causes Diabetes: Not a Tall Tale. *Science* **307**, 373-375, doi:10.1126/science.1104342 (2005).

22 Manson, J. E. *et al.* Physical activity and incidence of non-insulin-dependent diabetes mellitus in women. *The Lancet* **338**, 774-778 (1991).

23 Buchanan, T. A. & Xiang, A. H. Gestational diabetes mellitus. *The Journal of Clinical Investigation* **115**, 485-491 (2005).

24 LONNROTH, P. & SMITH, U. Aging Enhances the Insulin Resistance in Obesity through both Receptor and Postreceptor Alterations. *J Clin Endocrinol Metab* **62**, 433-437, doi:10.1210/jcem-62-2-433 (1986).

25 Eriksson, J. *et al.* Early Metabolic Defects in Persons at Increased Risk for Non-Insulin-Dependent Diabetes Mellitus. *New England Journal of Medicine* **321**, 337-343, doi:doi:10.1056/NEJM198908103210601 (1989).

26 Martin, B. C. *et al.* Role of glucose and insulin resistance in development of type 2 diabetes mellitus: results of a 25-year follow-up study. *The Lancet* **340**, 925-929 (1992).

27 Matthews, D. R. & Levy, J. C. Impending type 2 diabetes. *The Lancet* **373**, 2178-2179 (2009).

28 Pagliarini, D. J. *et al.* A Mitochondrial Protein Compendium Elucidates Complex I Disease Biology. *Cell* **134**, 112-123 (2008).

29 Mootha, V. K. *et al.* Integrated Analysis of Protein Composition, Tissue Diversity, and Gene Regulation in Mouse Mitochondria. *Cell* **115**, 629-640 (2003).

30 Starkov, A. A. The Role of Mitochondria in Reactive Oxygen Species Metabolism and Signaling. *Annals of the New York Academy of Sciences* **1147**, 37-52, doi:10.1196/annals.1427.015 (2008).

31 Murphy, M. P. How mitochondria produce reactive oxygen species. *Biochem J* **417**, 1-13, doi:10.1042/bj20081386 (2009).

32 Murgia, M., Giorgi, C., Pinton, P. & Rizzuto, R. Controlling metabolism and cell death: At the heart of mitochondrial calcium signalling. *Journal of Molecular and Cellular Cardiology* **46**, 781-788 (2009).

33 Rimessi, A., Giorgi, C., Pinton, P. & Rizzuto, R. The versatility of mitochondrial calcium signals: From stimulation of cell metabolism to induction of cell death. *Biochimica et Biophysica Acta (BBA) - Bioenergetics* **1777**, 808-816.

34 Lill, R. & Muhlenhoff, U. Maturation of iron-sulfur proteins in eukaryotes: mechanisms, connected processes, and diseases. *Annu Rev Biochem* **77**, 669-700, doi:10.1146/annurev.biochem.76.052705.162653 (2008).

35 Miller, W. L. Steroidogenic acute regulatory protein (StAR), a novel mitochondrial cholesterol transporter. *Biochimica et Biophysica Acta (BBA) - Molecular and Cell Biology of Lipids* **1771**, 663-676 (2007).

36 Miller, W. L. Minireview: Regulation of Steroidogenesis by Electron Transfer. *Endocrinology* **146**, 2544-2550, doi:10.1210/en.2005-0096 (2005).

37 Gonzalez, I. L. Barth syndrome: TAZ gene mutations, mRNAs, and evolution. *American Journal of Medical Genetics Part A* **134A**, 409-414, doi:10.1002/ajmg.a.30661 (2005).

38 Muravchick, S. Clinical implications of mitochondrial disease. *Advanced Drug Delivery Reviews* **60**, 1553-1560.

39 Gargus, J. J. Genetic Calcium Signaling Abnormalities in the Central Nervous System: Seizures, Migraine, and Autism. *Annals of the New York Academy of Sciences* **1151**, 133-156, doi:10.1111/j.1749-6632.2008.03572.x (2009).

40 Gandhi, S. *et al.* PINK1-Associated Parkinson's Disease Is Caused by Neuronal Vulnerability to Calcium-Induced Cell Death. *Molecular Cell* **33**, 627-638 (2009).

41 Benard, G. & Rossignol, R. Ultrastructure of the Mitochondrion and Its Bearing on Function and Bioenergetics. *Antioxidants & Redox Signaling* **10**, 1313-1342, doi:doi:10.1089/ars.2007.2000 (2008).

42 Stuart, R. Supercomplex organization of the oxidative phosphorylation enzymes in yeast mitochondria. *Journal of Bioenergetics and Biomembranes* **40**, 411-417, doi:10.1007/s10863-008-9168-4 (2008).

43 Vonck, J. & Sch‰fer, E. Supramolecular organization of protein complexes in the mitochondrial inner membrane. *Biochimica et Biophysica Acta (BBA) - Molecular Cell Research* **1793**, 117-124 (2009).

44 Scarpulla, R. C. Nuclear Control of Respiratory Chain Expression in Mammalian Cells. *Journal of Bioenergetics and Biomembranes* **29**, 109-119, doi:10.1023/a:1022681828846 (1997).

45 Virbasius, J. V. & Scarpulla, R. C. Activation of the human mitochondrial transcription factor A gene by nuclear respiratory factors: a potential regulatory link between nuclear and mitochondrial gene expression in organelle biogenesis. *Proceedings of the National Academy of Sciences of the United States of America* **91**, 1309-1313 (1994).

46 Scarpulla, R. C. Transcriptional Paradigms in Mammalian Mitochondrial Biogenesis and Function. *Physiol. Rev.* **88**, 611-638, doi:10.1152/physrev.00025.2007 (2008).

47 Wu, Z. *et al.* Mechanisms Controlling Mitochondrial Biogenesis and Respiration through the Thermogenic Coactivator PGC-1. *Cell* **98**, 115-124 (1999).

48 Lin, J., Puigserver, P., Donovan, J., Tarr, P. & Spiegelman, B. M. Peroxisome Proliferator-activated Receptor gamma Coactivator 1beta (PGC-1beta), A Novel PGC-1-related Transcription Coactivator Associated with Host Cell Factor. *Journal of Biological Chemistry* **277**, 1645-1648, doi:10.1074/jbc.C100631200 (2002).

49 Andersson, U. & Scarpulla, R. C. PGC-1-Related Coactivator, a Novel, Serum-Inducible Coactivator of Nuclear Respiratory Factor 1-Dependent Transcription in Mammalian Cells. *Mol. Cell. Biol.* **21**, 3738-3749, doi:10.1128/mcb.21.11.3738-3749.2001 (2001).

50 Sonoda, J., Mehl, I. R., Chong, L.-W., Nofsinger, R. R. & Evans, R. M. PGC-1beta controls mitochondrial metabolism to modulate circadian activity, adaptive thermogenesis, and hepatic steatosis. *Proceedings of the National Academy of Sciences* **104**, 5223-5228 (2007).

51 Arany, Z. *et al.* Transcriptional coactivator PGC-1[alpha] controls the energy state and contractile function of cardiac muscle. *Cell Metabolism* **1**, 259-271 (2005).

52 Handschin, C. *et al.* Skeletal Muscle Fiber-type Switching, Exercise Intolerance, and Myopathy in PGC-1Œ± Muscle-specific Knock-out Animals. *Journal of Biological Chemistry* **282**, 30014-30021, doi:10.1074/jbc.M704817200 (2007).

53 Handschin, C. *et al.* Abnormal glucose homeostasis in skeletal muscle‚Äìspecific PGC-1Œ± knockout mice reveals skeletal muscle‚Äìpancreatic Œ≤ cell crosstalk. *The Journal of Clinical Investigation* **117**, 3463-3474 (2007).

54 Lai, L. *et al.* Transcriptional coactivators PGC-1Œ± and PGC-lŒ≤ control overlapping programs required for perinatal maturation of the heart. *Genes & Development* **22**, 1948-1961 (2008).

55 Lehman, J. J. *et al.* The transcriptional coactivator PGC-1{alpha} is essential for maximal and efficient cardiac mitochondrial fatty acid oxidation and lipid homeostasis. *Am J Physiol Heart Circ Physiol* **295**, H185-196, doi:10.1152/ajpheart.00081.2008 (2008).

56 Leick, L. *et al.* PGC-1{alpha} is not mandatory for exercise- and training-induced adaptive gene responses in mouse skeletal muscle. *Am J Physiol Endocrinol Metab* **294**, E463-474, doi:10.1152/ajpendo.00666.2007 (2008).

57 Lelliott, C. J. *et al.* Ablation of PGC-1Œ≤ Results in Defective Mitochondrial Activity, Thermogenesis, Hepatic Function, and Cardiac Performance. *PLoS Biol* **4**, e369 (2006).

58 Leone, T. C. *et al.* PGC-1Œ± Deficiency Causes Multi-System Energy Metabolic Derangements: Muscle Dysfunction, Abnormal Weight Control and Hepatic Steatosis. *PLoS Biol* **3**, e101 (2005).

59 Lin, J. *et al.* Defects in Adaptive Energy Metabolism with CNS-Linked Hyperactivity in PGC-1[alpha] Null Mice. *Cell* **119**, 121-135 (2004).

60 Vianna, C. R. *et al.* Hypomorphic mutation of PGC-1[beta] causes mitochondrial dysfunction and liver insulin resistance. *Cell Metabolism* **4**, 453-464 (2006).

61 Lehman, J. J. *et al.* Peroxisome proliferator-activated receptor gamma coactivator-1 promotes cardiac mitochondrial biogenesis. *J Clin Invest* **106**, 847-856, doi:10.1172/JCI10268 (2000).

62 Lin, J. *et al.* Transcriptional co-activator PGC-1 alpha drives the formation of slow-twitch muscle fibres. *Nature* **418**, 797-801, doi:10.1038/nature00904 nature00904 [pii] (2002).

63 Vercauteren, K., Gleyzer, N. & Scarpulla, R. C. Short Hairpin RNA-mediated Silencing of PRC (PGC-1-related Coactivator) Results in a Severe Respiratory Chain Deficiency Associated with the Proliferation of Aberrant Mitochondria. *Journal of Biological Chemistry* **284**, 2307-2319, doi:10.1074/jbc.M806434200 (2009).

64 Christian, M., White, R. & Parker, M. G. Metabolic regulation by the nuclear receptor corepressor RIP140. *Trends in Endocrinology & Metabolism* **17**, 243-250 (2006).

65 Debevec, D. *et al.* Receptor Interacting Protein 140 Regulates Expression of Uncoupling Protein 1 in Adipocytes through Specific Peroxisome Proliferator Activated Receptor Isoforms and Estrogen-Related Receptor {alpha}. *Mol Endocrinol* **21**, 1581-1592, doi:10.1210/me.2007-0103 (2007).

66 Leonardsson, G. r. *et al.* Nuclear receptor corepressor RIP140 regulates fat accumulation. *Proceedings of the National Academy of Sciences of the United States of America* **101**, 8437-8442 (2004).

67 Parker, M. G., Christian, M. & White, R. The nuclear receptor co-repressor RIP140 controls the expression of metabolic gene networks. *Biochem. Soc. Trans.* **34**, 1103-1106, doi:10.1042/bst0341103 (2006).

68 Powelka, A. M. *et al.* Suppression of oxidative metabolism and mitochondrial biogenesis by the transcriptional corepressor RIP140 in mouse adipocytes. *The Journal of Clinical Investigation* **116**, 125-136 (2006).

69 Steel, J. H., White, R. & Parker, M. G. Role of the RIP140 corepressor in ovulation and adipose biology. *J Endocrinol* **185**, 1-9, doi:185/1/1 [pii] 10.1677/joe.1.05896 (2005).

70 Tullet, J. M. *et al.* Multiple signaling defects in the absence of RIP140 impair both cumulus expansion and follicle rupture. *Endocrinology* **146**, 4127-4137, doi:en.2005-0348 [pii] 10.1210/en.2005-0348 (2005).

71 Christian, M. *et al.* RIP140-targeted repression of gene expression in adipocytes. *Mol Cell Biol* **25**, 9383-9391, doi:25/21/9383 [pii] 10.1128/MCB.25.21.9383-9391.2005 (2005).

72 Herzog, B. *et al.* The nuclear receptor cofactor, receptor-interacting protein 140, is required for the regulation of hepatic lipid and glucose metabolism by liver X receptor. *Mol Endocrinol* **21**, 2687-2697, doi:me.2007-0213 [pii] 10.1210/me.2007-0213 (2007).

73 Seth, A. *et al.* The Transcriptional Corepressor RIP140 Regulates Oxidative Metabolism in Skeletal Muscle. *Cell Metabolism* **6**, 236-245 (2007).

74 Luft, R., Ikkos, D., Palmieri, G., Ernster, L. & Afzelius, B. r. A CASE OF SEVERE HYPERMETABOLISM OF NONTHYROID ORIGIN WITH A DEFECT IN THE MAINTENANCE OF MITOCHONDRIAL RESPIRATORY CONTROL: A CORRELATED CLINICAL, BIOCHEMICAL, AND MORPHOLOGICAL STUDY. *The Journal of Clinical Investigation* **41**, 1776-1804 (1962).

75 Ducluzeau, P.-H. *et al.* Regulation by Insulin of Gene Expression in Human Skeletal Muscle and Adipose Tissue. *Diabetes* **50**, 1134-1142, doi:10.2337/diabetes.50.5.1134 (2001).

76 Vaag, A., Henriksen, J. E. & Beck-Nielsen, H. Decreased insulin activation of glycogen synthase in skeletal muscles in young nonobese Caucasian first-degree relatives of patients with non-insulin-dependent diabetes mellitus. *The Journal of Clinical Investigation* **89**, 782-788 (1992).

77 Pratipanawatr, W. *et al.* Skeletal Muscle Insulin Resistance in Normoglycemic Subjects With a Strong Family History of Type 2 Diabetes Is Associated With Decreased Insulin-Stimulated Insulin Receptor Substrate-1 Tyrosine Phosphorylation. *Diabetes* **50**, 2572-2578, doi:10.2337/diabetes.50.11.2572 (2001).

78 Jacob, S. *et al.* Association of increased intramyocellular lipid content with insulin resistance in lean nondiabetic offspring of type 2 diabetic subjects. *Diabetes* **48**, 1113-1119, doi:10.2337/diabetes.48.5.1113 (1999).

79 Malenfant, P. *et al.* Fat content in individual muscle fibers of lean and obese subjects. *Int J Obes Relat Metab Disord* **25**, 1316-1321, doi:10.1038/sj.ijo.0801733 (2001).

80 Dresner, A. *et al.* Effects of free fatty acids on glucose transport and IRS-1,Äìassociated phosphatidylinositol 3-kinase activity. *The Journal of Clinical Investigation* **103**, 253-259 (1999).

81 Holland, W. L. *et al.* Inhibition of Ceramide Synthesis Ameliorates Glucocorticoid-, Saturated-Fat-, and Obesity-Induced Insulin Resistance. *Cell Metabolism* **5**, 167-179 (2007).

82 Koves, T. R. *et al.* Mitochondrial Overload and Incomplete Fatty Acid Oxidation Contribute to Skeletal Muscle Insulin Resistance. *Cell Metabolism* **7**, 45-56 (2008).

83 Savage, D. B., Petersen, K. F. & Shulman, G. I. Disordered Lipid Metabolism and the Pathogenesis of Insulin Resistance. *Physiol. Rev.* **87**, 507-520, doi:10.1152/physrev.00024.2006 (2007).

84 Chibalin, A. V. *et al.* Downregulation of Diacylglycerol Kinase Delta Contributes to Hyperglycemia-Induced Insulin Resistance. *Cell* **132**, 375-386 (2008).

85 Houstis, N., Rosen, E. D. & Lander, E. S. Reactive oxygen species have a causal role in multiple forms of insulin resistance. *Nature* **440**, 944-948, doi:http://www.nature.com/nature/journal/v440/n7086/suppinfo/nature04634_S1.html (2006).

86 Yu, C. *et al.* Mechanism by Which Fatty Acids Inhibit Insulin Activation of Insulin Receptor Substrate-1 (IRS-1)-associated Phosphatidylinositol 3-Kinase Activity in Muscle. *Journal of Biological Chemistry* **277**, 50230-50236, doi:10.1074/jbc.M200958200 (2002).

87 Lanner, J. T., Bruton, J. D., Katz, A. & Westerblad, H. Ca2+ and insulin-mediated glucose uptake. *Current Opinion in Pharmacology* **8**, 339-345 (2008).

88 Lebeche, D., Davidoff, A. J. & Hajjar, R. J. Interplay between impaired calcium regulation and insulin signaling abnormalities in diabetic cardiomyopathy. *Nat Clin Pract Cardiovasc Med* **5**, 715-724 (2008).

89 Park, S. *et al.* Chronic elevated calcium blocks AMPK-induced GLUT-4 expression in skeletal muscle. *Am J Physiol Cell Physiol* **296**, C106-115, doi:10.1152/ajpcell.00114.2008 (2009).

90 Kacerovsky-Bielesz, G. *et al.* Short-Term Exercise Training Does Not Stimulate Skeletal Muscle ATP Synthesis in Relatives of Humans With Type 2 Diabetes. *Diabetes* **58**, 1333-1341, doi:10.2337/db08-1240 (2009).

91 Simoneau, J., Colberg, S., Thaete, F. & Kelley, D. Skeletal muscle glycolytic and oxidative enzyme capacities are determinants of insulin sensitivity and muscle composition in obese women. *FASEB J.* **9**, 273-278 (1995).

92 Simoneau, J.-A. & Kelley, D. E. Altered glycolytic and oxidative capacities of skeletal muscle contribute to insulin resistance in NIDDM. *J Appl Physiol* **83**, 166-171 (1997).

93 Bruce, C. R. *et al.* Muscle Oxidative Capacity Is a Better Predictor of Insulin Sensitivity than Lipid Status. *J Clin Endocrinol Metab* **88**, 5444-5451, doi:10.1210/jc.2003-030791 (2003).

94 Zurlo, F. *et al.* Low ratio of fat to carbohydrate oxidation as predictor of weight gain: study of 24-h RQ. *Am J Physiol Endocrinol Metab* **259**, E650-657 (1990).

95 Boushel, R. *et al.* Patients with type 2 diabetes have normal mitochondrial function in skeletal muscle. *Diabetologia* **50**, 790-796, doi:10.1007/s00125-007-0594-3 (2007).

96 Petersen, K. F., Dufour, S., Befroy, D., Garcia, R. & Shulman, G. I. Impaired Mitochondrial Activity in the Insulin-Resistant Offspring of Patients with Type 2 Diabetes. *New England Journal of Medicine* **350**, 664-671, doi:doi:10.1056/NEJMoa031314 (2004).

97 Mogensen, M. *et al.* Mitochondrial respiration is decreased in skeletal muscle of patients with type 2 diabetes. *Diabetes* **56**, 1592-1599, doi:db06-0981 [pii] 10.2337/db06-0981 (2007).

98 Mootha, V. K. *et al.* PGC-1[alpha]-responsive genes involved in oxidative phosphorylation are coordinately downregulated in human diabetes. *Nat Genet* **34**, 267-273, doi:http://www.nature.com/ng/journal/v34/n3/suppinfo/ng1180_S1.html (2003).

99 Patti, M. E. *et al.* Coordinated reduction of genes of oxidative metabolism in humans with insulin resistance and diabetes: Potential role of PGC1 and NRF1. *Proc Natl Acad Sci U S A* **100**, 8466-8471, doi:10.1073/pnas.1032913100 1032913100 [pii] (2003).

100 Sreekumar, R., Halvatsiotis, P., Schimke, J. C. & Nair, K. S. Gene Expression Profile in Skeletal Muscle of Type 2 Diabetes and the Effect of Insulin Treatment. *Diabetes* **51**, 1913-1920, doi:10.2337/diabetes.51.6.1913 (2002).

101 Morino, K. *et al.* Reduced mitochondrial density and increased IRS-1 serine phosphorylation in muscle of insulin-resistant offspring of type 2 diabetic parents. *The Journal of Clinical Investigation* **115**, 3587-3593 (2005).

102 Nair, K. S. *et al.* Asian Indians Have Enhanced Skeletal Muscle Mitochondrial Capacity to Produce ATP in Association With Severe Insulin Resistance. *Diabetes* **57**, 1166-1175, doi:10.2337/db07-1556 (2008).

103 Frederiksen, C. *et al.* Transcriptional profiling of myotubes from patients with type 2 diabetes: no evidence for a primary defect in oxidative phosphorylation genes. *Diabetologia* **51**, 2068-2077, doi:10.1007/s00125-008-1122-9 (2008).

104 Crunkhorn, S. *et al.* Peroxisome Proliferator Activator Receptor Œ≥ Coactivator-1 Expression Is Reduced in Obesity. *Journal of Biological Chemistry* **282**, 15439-15450, doi:10.1074/jbc.M611214200 (2007).

105 Sparks, L. M. *et al.* A High-Fat Diet Coordinately Downregulates Genes Required for Mitochondrial Oxidative Phosphorylation in Skeletal Muscle. *Diabetes* **54**, 1926-1933, doi:10.2337/diabetes.54.7.1926 (2005).

106 Richardson, D. K. *et al.* Lipid Infusion Decreases the Expression of Nuclear Encoded Mitochondrial Genes and Increases the Expression of Extracellular Matrix Genes in Human Skeletal Muscle. *Journal of Biological Chemistry* **280**, 10290-10297, doi:10.1074/jbc.M408985200 (2005).

107 Garcia-Roves, P. *et al.* Raising plasma fatty acid concentration induces increased biogenesis of mitochondria in skeletal muscle. *Proceedings of the National Academy of Sciences* **104**, 10709-10713 (2007).

108 Hancock, C. R. *et al.* High-fat diets cause insulin resistance despite an increase in muscle mitochondria. *Proceedings of the National Academy of Sciences* **105**, 7815-7820 (2008).

109 Sreekumar, R. *et al.* Effects of caloric restriction on mitochondrial function and gene transcripts in rat muscle. *Am J Physiol Endocrinol Metab* **283**, E38-43, doi:10.1152/ajpendo.00387.2001 (2002).

110 Wisloff, U. *et al.* Cardiovascular Risk Factors Emerge After Artificial Selection for Low Aerobic Capacity. *Science* **307**, 418-420, doi:10.1126/science.1108177 (2005).

111 Parikh, H. *et al.* Molecular correlates for maximal oxygen uptake and type 1 fibers. *Am J Physiol Endocrinol Metab* **294**, E1152-1159, doi:10.1152/ajpendo.90255.2008 (2008).

112 Wright, D. C. *et al.* Exercise-induced Mitochondrial Biogenesis Begins before the Increase in Muscle PGC-1Œ± Expression. *Journal of Biological Chemistry* **282**, 194-199, doi:10.1074/jbc.M606116200 (2007).

113 Rönn, T. *et al.* Age influences DNA methylation and gene expression of <i>COX7A1</i> in human skeletal muscle. *Diabetologia* **51**, 1159-1168, doi:10.1007/s00125-008-1018-8 (2008).

114 Ling, C. *et al.* Multiple environmental and genetic factors influence skeletal muscle PGC-1Œ± and PGC-1Œ≤ gene expression in twins. *The Journal of Clinical Investigation* **114**, 1518-1526 (2004).

115 Ronn, T. *et al.* Genetic variation in ATP5O is associated with skeletal muscle ATP50 mRNA expression and glucose uptake in young twins. *PLoS ONE* **4**, e4793, doi:10.1371/journal.pone.0004793 (2009).

116 Ling, C. & Groop, L. Epigenetics: A Molecular Link Between Environmental Factors and Type 2 Diabetes. *Diabetes* **58**, 2718-2725, doi:10.2337/db09-1003 (2009).

117 Barrès, R. *et al.* Non-CpG Methylation of the PGC-1[alpha] Promoter through DNMT3B Controls Mitochondrial Density. *Cell Metabolism* **10**, 189-198 (2009).

118 Lerin, C. *et al.* GCN5 acetyltransferase complex controls glucose metabolism through transcriptional repression of PGC-1[alpha]. *Cell Metabolism* **3**, 429-438 (2006).

119 Lagouge, M. *et al.* Resveratrol Improves Mitochondrial Function and Protects against Metabolic Disease by Activating SIRT1 and PGC-1[alpha]. *Cell* **127**, 1109-1122 (2006).

120 Astrup, A. Thermogenesis in human brown adipose tissue and skeletal muscle induced by sympathomimetic stimulation. *Acta Endocrinol Suppl (Copenh)* **278**, 1-32 (1986).

121 Cannon, B. & Nedergaard, J. The biochemistry of an inefficient tissue: brown adipose tissue. *Essays Biochem* **20**, 110-164 (1985).

122 Cypess, A. M. *et al.* Identification and Importance of Brown Adipose Tissue in Adult Humans. *New England Journal of Medicine* **360**, 1509-1517, doi:doi:10.1056/NEJMoa0810780 (2009).

123 Weber, W. A. Brown Adipose Tissue and Nuclear Medicine Imaging. *J Nucl Med* **45**, 1101-1103 (2004).

124 Bouillaud, F., Ricquier, D., Thibault, J. & Weissenbach, J. Molecular approach to thermogenesis in brown adipose tissue: cDNA cloning of the mitochondrial uncoupling protein. *Proceedings of the National Academy of Sciences of the United States of America* **82**, 445-448 (1985).

125 Jacobsson, A., Stadler, U., Glotzer, M. A. & Kozak, L. P. Mitochondrial uncoupling protein from mouse brown fat. Molecular cloning, genetic mapping, and mRNA expression. *Journal of Biological Chemistry* **260**, 16250-16254 (1985).

126 Ricquier, D. & Bouillaud, F. The mitochondrial uncoupling protein: structural and genetic studies. *Prog Nucleic Acid Res Mol Biol* **56**, 83-108 (1997).

127 Kim, B. W., Choo, H. J., Lee, J. W., Kim, J. H. & Ko, Y. G. Extracellular ATP is generated by ATP synthase complex in adipocyte lipid rafts. *Exp Mol Med* **36**, 476-485, doi:200406301 [pii] (2004).

128 Luo, G.-F., Yu, T.-Y., Wen, X.-H., Li, Y. & Yang, G.-S. Alteration of mitochondrial oxidative capacity during porcine preadipocyte differentiation and in response to leptin. *Molecular and Cellular Biochemistry* **307**, 83-91, doi:10.1007/s11010-007-9587-2 (2008).

129 Wilson-Fritch, L. *et al.* Mitochondrial Biogenesis and Remodeling during Adipogenesis and in Response to the Insulin Sensitizer Rosiglitazone. *Mol. Cell. Biol.* **23**, 1085-1094, doi:10.1128/mcb.23.3.1085-1094.2003 (2003).

130 Owen, O. E., Kalhan, S. C. & Hanson, R. W. The Key Role of Anaplerosis and Cataplerosis for Citric Acid Cycle Function. *Journal of Biological Chemistry* **277**, 30409-30412, doi:10.1074/jbc.R200006200 (2002).

131 Koh, E. H. *et al.* Essential Role of Mitochondrial Function in Adiponectin Synthesis in Adipocytes. *Diabetes* **56**, 2973-2981, doi:10.2337/db07-0510 (2007).

132 Marette, A., Tulp, O. L. & Bukowiecki, L. J. Mechanism linking insulin resistance to defective thermogenesis in brown adipose tissue of obese diabetic SHR/N-cp rats. *Int J Obes* **15**, 823-831 (1991).

133 Nedergaard, J., Bengtsson, T. & Cannon, B. Unexpected evidence for active brown adipose tissue in adult humans. *Am J Physiol Endocrinol Metab* **293**, E444-452, doi:10.1152/ajpendo.00691.2006 (2007).

134 Saito, M. *et al.* High Incidence of Metabolically Active Brown Adipose Tissue in Healthy Adult Humans. *Diabetes* **58**, 1526-1531, doi:10.2337/db09-0530 (2009).

135 van Marken Lichtenbelt, W. D. *et al.* Cold-Activated Brown Adipose Tissue in Healthy Men. *New England Journal of Medicine* **360**, 1500-1508, doi:doi:10.1056/NEJMoa0808718 (2009).

136 Virtanen, K. A. *et al.* Functional Brown Adipose Tissue in Healthy Adults. *New England Journal of Medicine* **360**, 1518-1525, doi:doi:10.1056/NEJMoa0808949 (2009).

137 Zingaretti, M. C. *et al.* The presence of UCP1 demonstrates that metabolically active adipose tissue in the neck of adult humans truly represents brown adipose tissue. *FASEB J.* **23**, 3113-3120, doi:10.1096/fj.09-133546 (2009).

138 Cinti, S. Adipocyte differentiation and transdifferentiation: plasticity of the adipose organ. *J Endocrinol Invest* **25**, 823-835, doi:5808 [pii] (2002).

139 Deveaud, C., Beauvoit, B., Salin, B., Schaeffer, J. & Rigoulet, M. Regional differences in oxidative capacity of rat white adipose tissue are linked to the mitochondrial content of mature adipocytes. *Molecular and Cellular Biochemistry* **267**, 157-166, doi:10.1023/B:MCBI.0000049374.52989.9b (2004).

140 Bogacka, I., Xie, H., Bray, G. A. & Smith, S. R. Pioglitazone Induces Mitochondrial Biogenesis in Human Subcutaneous Adipose Tissue In Vivo. *Diabetes* **54**, 1392-1399, doi:10.2337/diabetes.54.5.1392 (2005).

141 Himms-Hagen, J. *et al.* Multilocular fat cells in WAT of CL-316243-treated rats derive directly from white adipocytes. *Am J Physiol Cell Physiol* **279**, C670-681 (2000).

142 Lončar, D. Convertible adipose tissue in mice. *Cell and Tissue Research* **266**, 149-161, doi:10.1007/bf00678721 (1991).

143 Orci, L. *et al.* Rapid transformation of white adipocytes into fat-oxidizing machines. *Proceedings of the National Academy of Sciences of the United States of America* **101**, 2058-2063 (2004).

144 Ström, K. *et al.* Attainment of Brown Adipocyte Features in White Adipocytes of Hormone-Sensitive Lipase Null Mice. *PLoS ONE* **3**, e1793 (2008).

145 Tiraby, C. *et al.* Acquirement of Brown Fat Cell Features by Human White Adipocytes. *Journal of Biological Chemistry* **278**, 33370-33376, doi:10.1074/jbc.M305235200 (2003).

146 Toh, S. Y. *et al.* Up-Regulation of Mitochondrial Activity and Acquirement of Brown Adipose Tissue-Like Property in the White Adipose Tissue of <italic>Fsp27</italic> Deficient Mice. *PLoS ONE* **3**, e2890 (2008).

147 Wilson-Fritch, L. *et al.* Mitochondrial remodeling in adipose tissue associated with obesity and treatment with rosiglitazone. *The Journal of Clinical Investigation* **114**, 1281-1289 (2004).

148 Petrovic, N. *et al.* Chronic peroxisome proliferator-activated receptor gamma (PPARgamma) activation of epididymally derived white adipocyte cultures reveals a population of thermogenically competent, UCP1-containing adipocytes molecularly distinct from classic brown adipocytes. *J Biol Chem* **285**, 7153-7164, doi:M109.053942 [pii] 10.1074/jbc.M109.053942 (2010).

149 de Ferranti, S. & Mozaffarian, D. The perfect storm: obesity, adipocyte dysfunction, and metabolic consequences. *Clin Chem* **54**, 945-955, doi:clinchem.2007.100156 [pii] 10.1373/clinchem.2007.100156 (2008).

150 Frayn, K. N., Langin, D. & Karpe, F. Fatty acid-induced mitochondrial uncoupling in adipocytes is not a promising target for treatment of insulin resistance unless adipocyte oxidative capacity is increased. *Diabetologia* **51**, 394-397, doi:10.1007/s00125-007-0901-z (2008).

151 Heilbronn, L., Smith, S. R. & Ravussin, E. Failure of fat cell proliferation, mitochondrial function and fat oxidation results in ectopic fat storage, insulin resistance and type II diabetes mellitus. *Int J Obes Relat Metab Disord* **28 Suppl 4**, S12-21, doi:0802853 [pii] 10.1038/sj.ijo.0802853 (2004).

152 Maasen, J. A. Mitochondria, body fat and type 2 diabetes: what is the connection? *Minerva Med* **99**, 241-251 (2008).

153 Maassen, J. A. *et al.* Mitochondrial diabetes and its lessons for common Type 2 diabetes. *Biochem. Soc. Trans.* **34**, 819-823, doi:10.1042/bst0340819 (2006).

154 Shi, X. *et al.* Paradoxical Effect of Mitochondrial Respiratory Chain Impairment on Insulin Signaling and Glucose Transport in Adipose Cells. *Journal of Biological Chemistry* **283**, 30658-30667, doi:10.1074/jbc.M800510200 (2008).

155 Choo, H. J. *et al.* Mitochondria are impaired in the adipocytes of type 2 diabetic mice. *Diabetologia* **49**, 784-791, doi:10.1007/s00125-006-0170-2 (2006).

156 Okamoto, Y. *et al.* Comparison of mitochondrial and macrophage content between subcutaneous and visceral fat in db/db mice. *Exp Mol Pathol* **83**, 73-83, doi:S0014-4800(07)00016-0 [pii] 10.1016/j.yexmp.2007.02.007 (2007).

157 Rong, J. X. *et al.* Adipose mitochondrial biogenesis is suppressed in db/db and high-fat diet-fed mice and improved by rosiglitazone. *Diabetes* **56**, 1751-1760, doi:db06-1135 [pii] 10.2337/db06-1135 (2007).

158 Sutherland, L. N., Capozzi, L. C., Turchinsky, N. J., Bell, R. C. & Wright, D. C. Time course of high-fat diet-induced reductions in adipose tissue mitochondrial proteins: potential mechanisms and the relationship to glucose intolerance. *Am J Physiol Endocrinol Metab* **295**, E1076-1083, doi:90408.2008 [pii] 10.1152/ajpendo.90408.2008 (2008).

159 Kaaman, M. *et al.* Strong association between mitochondrial DNA copy number and lipogenesis in human white adipose tissue. *Diabetologia* **50**, 2526-2533, doi:10.1007/s00125-007-0818-6 (2007).

160 Dahlman, I. *et al.* Downregulation of electron transport chain genes in visceral adipose tissue in type 2 diabetes independent of obesity and possibly involving tumor necrosis factor-alpha. *Diabetes* **55**, 1792-1799, doi:55/6/1792 [pii] 10.2337/db05-1421 (2006).

161 Boden, G. *et al.* Thiazolidinediones upregulate fatty acid uptake and oxidation in adipose tissue of diabetic patients. *Diabetes* **54**, 880-885, doi:54/3/880 [pii] (2005).

162 Bogacka, I., Ukropcova, B., McNeil, M., Gimble, J. M. & Smith, S. R. Structural and functional consequences of mitochondrial biogenesis in human adipocytes in vitro. *J Clin Endocrinol Metab* **90**, 6650-6656, doi:jc.2005-1024 [pii] 10.1210/jc.2005-1024 (2005).

163 Digby, J. E. *et al.* Thiazolidinedione exposure increases the expression of uncoupling protein 1 in cultured human preadipocytes. *Diabetes* **47**, 138-141 (1998).

164 Goetzman, E. S. The regulation of acyl-CoA dehydrogenases in adipose tissue by rosiglitazone. *Obesity (Silver Spring)* **17**, 196-198, doi:oby2008467 [pii] 10.1038/oby.2008.467 (2009).

165 Laplante, M. *et al.* Mechanisms of the depot specificity of peroxisome proliferator-activated receptor gamma action on adipose tissue metabolism. *Diabetes* **55**, 2771-2778, doi:55/10/2771 [pii] 10.2337/db06-0551 (2006).

166 Granneman, J. G., Li, P., Zhu, Z. & Lu, Y. Metabolic and cellular plasticity in white adipose tissue I: effects of beta3-adrenergic receptor activation. *Am J Physiol Endocrinol Metab* **289**, E608-616, doi:00009.2005 [pii] 10.1152/ajpendo.00009.2005 (2005).

167 Tedesco, L. *et al.* Cannabinoid type 1 receptor blockade promotes mitochondrial biogenesis through endothelial nitric oxide synthase expression in white adipocytes. *Diabetes* **57**, 2028-2036, doi:db07-1623 [pii] 10.2337/db07-1623 (2008).

168 Katic, M. *et al.* Mitochondrial gene expression and increased oxidative metabolism: role in increased lifespan of fat-specific insulin receptor knock-out mice. *Aging Cell* **6**, 827-839, doi:ACE346 [pii] 10.1111/j.1474-9726.2007.00346.x (2007).

169 Seale, P. *et al.* PRDM16 controls a brown fat/skeletal muscle switch. *Nature* **454**, 961-967, doi:nature07182 [pii] 10.1038/nature07182 (2008).

170 Seale, P. *et al.* Transcriptional control of brown fat determination by PRDM16. *Cell Metab* **6**, 38-54, doi:S1550-4131(07)00157-X [pii] 10.1016/j.cmet.2007.06.001 (2007).

171 Timmons, J. A. *et al.* Myogenic gene expression signature establishes that brown and white adipocytes originate from distinct cell lineages. *Proc Natl Acad Sci U S A* **104**, 4401-4406, doi:0610615104 [pii] 10.1073/pnas.0610615104 (2007).

172 Nishino, N. *et al.* FSP27 contributes to efficient energy storage in murine white adipocytes by promoting the formation of unilocular lipid droplets. *J Clin Invest* **118**, 2808-2821, doi:10.1172/JCI34090 (2008).

173 Semple, R. K. *et al.* Expression of the thermogenic nuclear hormone receptor coactivator PGC-1alpha is reduced in the adipose tissue of morbidly obese subjects. *Int J Obes Relat Metab Disord* **28**, 176-179, doi:10.1038/sj.ijo.0802482 0802482 [pii] (2004).

174 Kotronen, A., Seppala-Lindroos, A., Bergholm, R. & Yki-Jarvinen, H. Tissue specificity of insulin resistance in humans: fat in the liver rather than muscle is associated with features of the metabolic syndrome. *Diabetologia* **51**, 130-138, doi:10.1007/s00125-007-0867-x (2008).

175 Michael, M. D. *et al.* Loss of insulin signaling in hepatocytes leads to severe insulin resistance and progressive hepatic dysfunction. *Mol Cell* **6**, 87-97, doi:S1097-2765(05)00015-8 [pii] (2000).

176 Biddinger, S. B. *et al.* Hepatic insulin resistance is sufficient to produce dyslipidemia and susceptibility to atherosclerosis. *Cell Metab* **7**, 125-134, doi:S1550-4131(07)00368-3 [pii] 10.1016/j.cmet.2007.11.013 (2008).

177 Veltri, K. L., Espiritu, M. & Singh, G. Distinct genomic copy number in mitochondria of different mammalian organs. *J Cell Physiol* **143**, 160-164, doi:10.1002/jcp.1041430122 (1990).

178 Benard, G. *et al.* Physiological diversity of mitochondrial oxidative phosphorylation. *Am J Physiol Cell Physiol* **291**, C1172-1182, doi:00195.2006 [pii] 10.1152/ajpcell.00195.2006 (2006).

179 Agarwal, A. K. & Garg, A. Genetic disorders of adipose tissue development, differentiation, and death. *Annu Rev Genomics Hum Genet* **7**, 175-199, doi:10.1146/annurev.genom.7.080505.115715 (2006).

180 Hwang, J. H. *et al.* Increased intrahepatic triglyceride is associated with peripheral insulin resistance: in vivo MR imaging and spectroscopy studies. *Am J Physiol Endocrinol Metab* **293**, E1663-1669, doi:00590.2006 [pii] 10.1152/ajpendo.00590.2006 (2007).

181 Korenblat, K. M., Fabbrini, E., Mohammed, B. S. & Klein, S. Liver, muscle, and adipose tissue insulin action is directly related to intrahepatic triglyceride content in obese subjects. *Gastroenterology* **134**, 1369-1375, doi:S0016-5085(08)00181-9 [pii] 10.1053/j.gastro.2008.01.075 (2008).

182 Petersen, K. F. *et al.* Reversal of nonalcoholic hepatic steatosis, hepatic insulin resistance, and hyperglycemia by moderate weight reduction in patients with type 2 diabetes. *Diabetes* **54**, 603-608, doi:54/3/603 [pii] (2005).

183 Kim, J. K. *et al.* Tissue-specific overexpression of lipoprotein lipase causes tissue-specific insulin resistance. *Proc Natl Acad Sci U S A* **98**, 7522-7527, doi:10.1073/pnas.121164498 121164498 [pii] (2001).

184 Cheng, Z. *et al.* Foxo1 integrates insulin signaling with mitochondrial function in the liver. *Nat Med* **15**, 1307-1311, doi:nm.2049 [pii] 10.1038/nm.2049 (2009).

185 Cheung, P., Allis, C. D. & Sassone-Corsi, P. Signaling to chromatin through histone modifications. *Cell* **103**, 263-271, doi:S0092-8674(00)00118-5 [pii] (2000).

186 Jenuwein, T. & Allis, C. D. Translating the histone code. *Science* **293**, 1074-1080 (2001).

187 Li, B., Carey, M. & Workman, J. L. The role of chromatin during transcription. *Cell* **128**, 707-719, doi:S0092-8674(07)00109-2 [pii] 10.1016/j.cell.2007.01.015 (2007).

188 Zhang, L., Eugeni, E. E., Parthun, M. R. & Freitas, M. A. Identification of novel histone post-translational modifications by peptide mass fingerprinting. *Chromosoma* **112**, 77-86, doi:10.1007/s00412-003-0244-6 (2003).

189 Kouzarides, T. Histone methylation in transcriptional control. *Curr Opin Genet Dev* **12**, 198-209, doi:S0959437X02002873 [pii] (2002).

190 Tachibana, M., Sugimoto, K., Fukushima, T. & Shinkai, Y. Set domain-containing protein, G9a, is a novel lysine-preferring mammalian histone methyltransferase with hyperactivity and specific selectivity to lysines 9 and 27 of histone H3. *J Biol Chem* **276**, 25309-25317, doi:10.1074/jbc.M101914200 M101914200 [pii] (2001).

191 Brown, C. E., Lechner, T., Howe, L. & Workman, J. L. The many HATs of transcription coactivators. *Trends Biochem Sci* **25**, 15-19 (2000).

192 Haberland, M., Montgomery, R. L. & Olson, E. N. The many roles of histone deacetylases in development and physiology: implications for disease and therapy. *Nat Rev Genet* **10**, 32-42, doi:nrg2485 [pii] 10.1038/nrg2485 (2009).

193 McKinsey, T. A., Zhang, C. L., Lu, J. & Olson, E. N. Signal-dependent nuclear export of a histone deacetylase regulates muscle differentiation. *Nature* **408**, 106-111, doi:10.1038/35040593 (2000).

194 Lu, J., McKinsey, T. A., Nicol, R. L. & Olson, E. N. Signal-dependent activation of the MEF2 transcription factor by dissociation from histone deacetylases. *Proc Natl Acad Sci U S A* **97**, 4070-4075, doi:10.1073/pnas.080064097 080064097 [pii] (2000).

195 Passier, R. *et al.* CaM kinase signaling induces cardiac hypertrophy and activates the MEF2 transcription factor in vivo. *J Clin Invest* **105**, 1395-1406, doi:10.1172/JCI8551 (2000).

196 Vega, R. B. *et al.* Protein kinases C and D mediate agonist-dependent cardiac hypertrophy through nuclear export of histone deacetylase 5. *Mol Cell Biol* **24**, 8374-8385, doi:10.1128/MCB.24.19.8374-8385.2004 24/19/8374 [pii] (2004).

197 Lu, J., McKinsey, T. A., Zhang, C. L. & Olson, E. N. Regulation of skeletal myogenesis by association of the MEF2 transcription factor with class II histone deacetylases. *Mol Cell* **6**, 233-244, doi:S1097-2765(00)00025-3 [pii] (2000).

198 Youn, H. D., Grozinger, C. M. & Liu, J. O. Calcium regulates transcriptional repression of myocyte enhancer factor 2 by histone deacetylase 4. *J Biol Chem* **275**, 22563-22567, doi:10.1074/jbc.C000304200 C000304200 [pii] (2000).

199 Wang, A. H. *et al.* HDAC4, a human histone deacetylase related to yeast HDA1, is a transcriptional corepressor. *Mol Cell Biol* **19**, 7816-7827 (1999).

200 Miska, E. A. *et al.* HDAC4 deacetylase associates with and represses the MEF2 transcription factor. *EMBO J* **18**, 5099-5107, doi:10.1093/emboj/18.18.5099 (1999).

201 Sparrow, D. B. *et al.* MEF-2 function is modified by a novel co-repressor, MITR. *EMBO J* **18**, 5085-5098, doi:10.1093/emboj/18.18.5085 (1999).

202 Lahm, A. *et al.* Unraveling the hidden catalytic activity of vertebrate class IIa histone deacetylases. *Proc Natl Acad Sci U S A* **104**, 17335-17340, doi:0706487104 [pii] 10.1073/pnas.0706487104 (2007).

203 Fischle, W. *et al.* Enzymatic activity associated with class II HDACs is dependent on a multiprotein complex containing HDAC3 and SMRT/N-CoR. *Mol Cell* **9**, 45-57, doi:S1097276501004294 [pii] (2002).

204 Mai, A. & Altucci, L. Epi-drugs to fight cancer: from chemistry to cancer treatment, the road ahead. *Int J Biochem Cell Biol* **41**, 199-213, doi:S1357-2725(08)00336-1 [pii] 10.1016/j.biocel.2008.08.020 (2009).

205 Zhang, Y. & Talalay, P. Anticarcinogenic activities of organic isothiocyanates: chemistry and mechanisms. *Cancer Res* **54**, 1976s-1981s (1994).

206 Nian, H., Delage, B., Ho, E. & Dashwood, R. H. Modulation of histone deacetylase activity by dietary isothiocyanates and allyl sulfides: studies with sulforaphane and garlic organosulfur compounds. *Environ Mol Mutagen* **50**, 213-221, doi:10.1002/em.20454 (2009).

207 Myzak, M. C., Karplus, P. A., Chung, F. L. & Dashwood, R. H. A novel mechanism of chemoprotection by sulforaphane: inhibition of histone deacetylase. *Cancer Res* **64**, 5767-5774, doi:10.1158/0008-5472.CAN-04-1326 64/16/5767 [pii] (2004).

208 Myzak, M. C., Dashwood, W. M., Orner, G. A., Ho, E. & Dashwood, R. H. Sulforaphane inhibits histone deacetylase in vivo and suppresses tumorigenesis in Apc-minus mice. *FASEB J* **20**, 506-508, doi:05-4785fje [pii] 10.1096/fj.05-4785fje (2006).

209 Myzak, M. C., Hardin, K., Wang, R., Dashwood, R. H. & Ho, E. Sulforaphane inhibits histone deacetylase activity in BPH-1, LnCaP and PC-3 prostate epithelial cells. *Carcinogenesis* **27**, 811-819, doi:bgi265 [pii] 10.1093/carcin/bgi265 (2006).

210 Nian, H., Delage, B., Pinto, J. T. & Dashwood, R. H. Allyl mercaptan, a garlic-derived organosulfur compound, inhibits histone deacetylase and enhances Sp3 binding on the P21WAF1 promoter. *Carcinogenesis* **29**, 1816-1824, doi:bgn165 [pii] 10.1093/carcin/bgn165 (2008).

211 Cummings, J. H. & Englyst, H. N. Fermentation in the human large intestine and the available substrates. *Am J Clin Nutr* **45**, 1243-1255 (1987).

212 Gao, Z. *et al.* Butyrate improves insulin sensitivity and increases energy expenditure in mice. *Diabetes* **58**, 1509-1517, doi:db08-1637 [pii] 10.2337/db08-1637 (2009).

213 Yang, X. J. & Seto, E. Lysine acetylation: codified crosstalk with other posttranslational modifications. *Mol Cell* **31**, 449-461, doi:S1097-2765(08)00457-7 [pii] 10.1016/j.molcel.2008.07.002 (2008).

214 Imai, S., Armstrong, C. M., Kaeberlein, M. & Guarente, L. Transcriptional silencing and longevity protein Sir2 is an NAD-dependent histone deacetylase. *Nature* **403**, 795-800, doi:10.1038/35001622 (2000).

215 Yamamoto, H., Schoonjans, K. & Auwerx, J. Sirtuin functions in health and disease. *Mol Endocrinol* **21**, 1745-1755, doi:me.2007-0079 [pii] 10.1210/me.2007-0079 (2007).

216 Finkel, T., Deng, C. X. & Mostoslavsky, R. Recent progress in the biology and physiology of sirtuins. *Nature* **460**, 587-591, doi:nature08197 [pii] 10.1038/nature08197 (2009).

217 Rodgers, J. T. *et al.* Nutrient control of glucose homeostasis through a complex of PGC-1alpha and SIRT1. *Nature* **434**, 113-118, doi:nature03354 [pii] 10.1038/nature03354 (2005).

218 Rodgers, J. T. & Puigserver, P. Fasting-dependent glucose and lipid metabolic response through hepatic sirtuin 1. *Proc Natl Acad Sci U S A* **104**, 12861-12866, doi:0702509104 [pii] 10.1073/pnas.0702509104 (2007).

219 Howitz, K. T. *et al.* Small molecule activators of sirtuins extend Saccharomyces cerevisiae lifespan. *Nature* **425**, 191-196, doi:10.1038/nature01960 nature01960 [pii] (2003).

220 Baur, J. A. *et al.* Resveratrol improves health and survival of mice on a high-calorie diet. *Nature* **444**, 337-342, doi:nature05354 [pii] 10.1038/nature05354 (2006).

221 Canto, C. *et al.* AMPK regulates energy expenditure by modulating NAD+ metabolism and SIRT1 activity. *Nature* **458**, 1056-1060, doi:nature07813 [pii] 10.1038/nature07813 (2009).

222 Borra, M. T., Smith, B. C. & Denu, J. M. Mechanism of human SIRT1 activation by resveratrol. *J Biol Chem* **280**, 17187-17195, doi:M501250200 [pii] 10.1074/jbc.M501250200 (2005).

223 Kaeberlein, M. *et al.* Substrate-specific activation of sirtuins by resveratrol. *J Biol Chem* **280**, 17038-17045, doi:M500655200 [pii]

10.1074/jbc.M500655200 (2005).
224 Belandia, B., Orford, R. L., Hurst, H. C. & Parker, M. G. Targeting of SWI/SNF chromatin remodelling complexes to estrogen-responsive genes. *EMBO J* **21**, 4094-4103 (2002).
225 Potthoff, M. J. *et al.* Histone deacetylase degradation and MEF2 activation promote the formation of slow-twitch myofibers. *J Clin Invest* **117**, 2459-2467, doi:10.1172/JCI31960 (2007).
226 McGee, S. L., Fairlie, E., Garnham, A. P. & Hargreaves, M. Exercise-induced histone modifications in human skeletal muscle. *J Physiol* **587**, 5951-5958, doi:jphysiol.2009.181065 [pii]
10.1113/jphysiol.2009.181065 (2009).
227 Kelley, D. E., He, J., Menshikova, E. V. & Ritov, V. B. Dysfunction of Mitochondria in Human Skeletal Muscle in Type 2 Diabetes. *Diabetes* **51**, 2944-2950, doi:10.2337/diabetes.51.10.2944 (2002).
228 SIMONEAU, J.-A. â., VEERKAMP, J. H., TURCOTTE, L. P. & KELLEY, D. E. Markers of capacity to utilize fatty acids in human skeletal muscle: relation to insulin resistance and obesity and effects of weight loss. *The FASEB Journal* **13**, 2051-2060 (1999).
229 Yamauchi, T. *et al.* The mechanisms by which both heterozygous peroxisome proliferator-activated receptor gamma (PPARgamma) deficiency and PPARgamma agonist improve insulin resistance. *J Biol Chem* **276**, 41245-41254, doi:10.1074/jbc.M103241200 M103241200 [pii] (2001).